UNIVERSITA' DEGLI STUDI
DI MILANO – BICOCCA

SCUOLA DI DOTTORATO DI SCIENZE
Facoltà di Scienze Matematiche, Fisiche e Naturali
Corso di Dottorato di Ricerca in Scienze Chimiche XXII ciclo

Synthesis and biological characterization of new pharmacologically active molecules derived from natural compounds

Dott. Alessandro Palmioli

Tutor : Prof. Francesco Peri
Dipartimento di Biotecnologie e Bioscienze

Anno Accademico 2008-2009

Ma guardate l'idrogeno tacere nel mare
guardate l'ossigeno al suo fianco dormire:
soltanto una legge che io riesco a capire
ha potuto sposarli senza farli scoppiare.
Soltanto la legge che io riesco a capire.

Un Chimico,
Non al denaro, non all'amore nè al cielo
1971, Fabrizio De Andrè

Summary

Summary ..... **i**

1. Ras proteins, signalling and oncogenesis **1**

1.1. Biological function of Ras proteins *1*

1.1.1. Introduction 1

1.1.2. Ras upstream signalling 2

1.1.3. Ras downstream signalling 4

1.2. Mammalian Ras isoforms *7*

1.3. Structural features of Ras proteins *9*

1.3.1. Catalytic mechanism of intrinsic GTP hydrolysis 12

1.3.2. Interaction with GAP 15

1.3.3. Interaction with GEF 17

1.3.4. Interaction with effectors 18

1.3.5. Nucleotide binding site 18

1.3.6. Mg^{2+} binding site 19

1.4. Ras proteins and Oncogenesis *21*

1.4.1. Cancer 21

1.4.1. Oncogenic Ras in tumorigenesis and developmental disorders 22

2. Ras proteins as a target for new anti-cancer therapy development **25**

2.1. Strategy for interacting with Ras proteins *25*

2.1.1. Inhibition of Ras membrane localization 25

2.1.2 Inhibition of Ras expression 29

2.1.3 Interfering with Ras-effectors interaction 29

2.1.4 Restoration of mutant defective GTPase activity 31

2.2 Nucleotide exchange inhibition: a new class of Ras inhibitors *32*

3. Carbohydrates as a tool for the development of new drugs 39

3.1 "Glycorandomization" in drug discovery 42

3.1.1 Chemoenzymatic glycorandomization 43

3.1.2. Neoglycorandomization 44

4. Results and discussion 47

4.1. Objective and strategy 47

4.2. Structure-activity relationship in Ras inhibitors 49

4.2.1. Chemical synthesis 50

4.2.2. Biological evaluation 51

4.2.2.1. Biochemical assays on nucleotide exchange inhibition 51

4.2.2.2. *Ex vivo* experiments on human cancer cell viability. 52

4.2.3. Discussion 53

4.3. Different scaffold – pharmacophore combination in Ras Inhibitors 55

4.3.1. Docking calculation 56

4.3.2. Chemical synthesis 58

4.3.3. NMR binding studies 61

4.3.4. Biological evaluation 65

4.3.4.1. Biochemical assays on nucleotide exchange 65

4.3.4.2. *Ex vivo* experiments on human cancer cells 66

4.3.5. Discussion 68

4.4. Water-soluble Ras inhibitors by chemoselective ligation 71

4.4.1. Chemical synthesis 72

4.4.2. ITC and NMR/MD binding studies 74

4.4.3. Biological evaluation 79

4.4.3.1. Biochemical assay on nucleotide exchange 79

4.4.3.2. *Ex vivo* experiments on mammalian cells 80

4.4.4. Discussion 81

4.5. Conclusions and remarks 83

5. Materials and methods 85

5.1. Organic synthesis 85

5.1.1. General procedures 85

5.1.1.1. Dry solvents and reactions 85

5.1.1.2. Thin-layer chromatography (TLC) 85

5.1.1.3. Flash column chromatography 85

5.1.1.4. Mass spectrometry 86

5.1.1.5. NMR spectroscopy 86

5.1.1.6. Optical rotation 86

5.1.2. Synthesis of compounds 1-11 87

5.1.3. Synthesis of compounds 12-14 99

5.1.4. Synthesis of compounds 15-17 104

5.1.5. Synthesis of compounds 30-34 118

5.2. Biological procedures 125

5.2.1. Expression and isolation of proteins 125

5.2.2. Measurement of C-Cdc25^{Mm}-stimulated guanine nucleotide exchange on p21 h-Ras 125

5.2.1. Measurement of RasGRF1-stimulated guanine nucleotide exchange on p21 h-Ras 126

Papers 127

Communications 127

Bibliography 129

1. Ras proteins, signalling and oncogenesis

1.1. Biological function of Ras proteins

1.1.1. Introduction

Ras proteins are members of a large superfamily of low-molecular-weight guanine nucleotide-binding proteins that play an essential role in the control of cellular growth and differentiation. A common features of Ras proteins is that they act as molecular switch in signal transduction across membranes, in particular they take action in signal transfer induced by growth factors[1,2].

Ras proteins bind guanine nucleotides (GTP or GDP) with high affinity[3] and posses an intrinsic GTP hydrolysis (or GTPase) activity that shuttle them from an active GTP-bound to an inactive GDP-bound signalling state. Their capability to cycling between the active state and the inactive state makes Ras proteins molecular switches in different transduction pathways. In normal cells this "on-off" cycle is tightly controlled by GTPase activating proteins (GAPs) and guanine-nucleotide exchange factors (GEFs) as show in Figure 1.1. After GDP dissociation from Ras-GDP complex, since cellular GTP concentration is generally 10-fold higher than GDP, the re-bound nucleoside is usually GTP.

---

1. Bourne, H. R.; Sanders, D. A.; McCormick, F., The GTPase superfamily: a conserved switch for diverse cell functions. *Nature* **1990,** *348* (6297), 125-132.

2. Bourne, H. R.; Sanders, D. A.; McCormick, F., The GTPase superfamily: conserved structure and molecular mechanism. *Nature* **1991,** *349* (6305), 117-127.

3. Goody, R. S.; Frech, M.; Wittinghofer, A., Affinity of guanine nucleotide binding proteins for their ligands: facts and artefacts. *Trends in biochemical sciences* **1991,** *16* (9), 327.

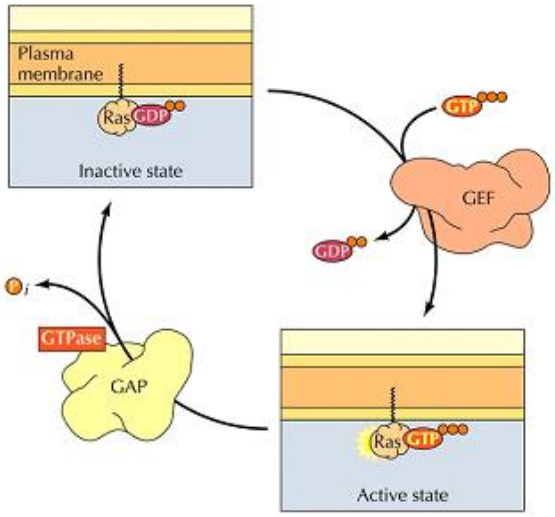

Figure 1.1: Cycling of the Ras proteins between the inactive form with bound GDP and the active form with bound GTP. Guanine nucleotide–exchange factor (GEF) facilitates dissociation of GDP from Ras. GTP then binds spontaneously, and GEF dissociates yielding the active Ras-GTP form. Hydrolysis of the bound GTP to regenerate the inactive Ras-GDP form is accelerated a hundredfold by GTPase-activating protein (GAP).

1.1.2. Ras upstream signalling

Ras proteins are activated by various extracellular stimuli, which are mediated by trans-membrane growth-factors receptor tyrosine kinases[4] (RTKs). In response to specific ligands (such as PDGF, EGF, IL2) these receptors dimerize and undergo to auto-phosphorilation by their tyrosine kinase activity. Phosphotyrosine residues in non-catalytical region of the receptors act as binding site for a variety of signalling adaptor proteins, such as growth-factor-receptors-bound proteins-2 (Grb2)[5]. This recruitment is primarily mediated by the interaction of the SH2 domain (src homology region 2) of the Grb2 with the tyrosine phosphorilated residues in the cytoplasmatic domain of activated receptors. Gbr2 also contains a SH3 (src

4. van Blesen, T.; Hawes, B. E.; Luttrell, D. K.; Krueger, K. M.; Touhara, K.; Porfflri, E.; Sakaue, M.; Luttrell, L. M.; Lefkowitz, R. J., Receptor-tyrosine-kinase-and G -mediated MAP kinase activation by a common signalling pathway. **1995**.

5. Lowenstein, E. J.; Daly, R. J.; Batzer, A. G.; Li, W.; Margolis, B.; Lammers, R.; Ullrich, A.; Skolnik, E. Y.; Bar-Sagi, D.; Schlessinger, J., The SH2 and SH3 domain-containing protein GRB2 links receptor tyrosine kinases to ras signaling. *Cell* **1992,** *70* (3), 431-442.

homology region 3) domain able to bind sequence rich in proline residues with high affinity. Through this domain, Gbr2 recruits **GEFs** proteins, which promote the nucleotide exchange GDP/GTP and so, Ras signalling activation (Figure 1.2).

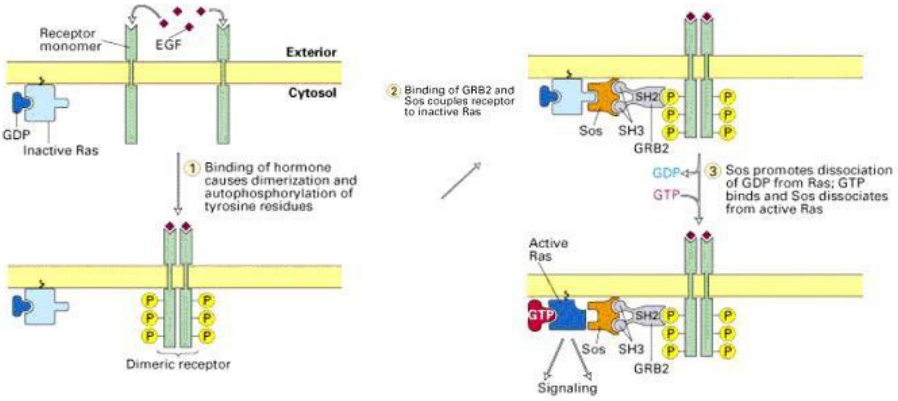

Figure 1.2: Activation of Ras proteins through tyrosine kinases receptors (RTKs)[6].

The first Ras-GEFs identified were a yeast cell-division-cycle 25 (Cdc25) protein that showed the ability to activate Ras proteins by stimulating its nucleotide-exchange activity[7]. Three main classes of Ras GEFs are currently known with a common Cdc25 homology catalytic domain: Sos, Ras-GRF and Ras-GRP. Among mammalian GEFs, the most characterized is Sos. According to the proposed model, Grb2 and Sos are thought to be pre-associated in the cytoplasm and be recruited by the active dimeric receptors to plasma membrane, where Ras proteins are localized. In addition to the Cdc25 homology domain, Sos contains a pleckstrine homology (PH) domain and an histone domain (HD) that contribute to membrane localization[8].

6. Lodish, H. F., *Molecular cell biology*. 6th ed.; W.H. Freeman: New York, 2008.

7. Robinson, L. C.; Gibbs, J. B.; Marshall, M. S.; Sigal, I. S.; Tatchell, K., CDC25: a component of the RAS-adenylate cyclase pathway in Saccharomyces cerevisiae. *Science* **1987,** *235* (4793), 1218-1221.

8. Sondermann, H.; Nagar, B.; Bar-Sagi, D.; Kuriyan, J., Computational docking and solution x-ray scattering predict a membrane-interacting role for the histone domain of the Ras activator son of sevenless. *Proceedings of the National Academy of Sciences* **2005,** *102* (46), 16632-16637.

Recent studies have demonstrated that the contact of the PH domain with membrane phospholipids induces conformational changes allowing to show an allosteric Ras-binding site. Structural studies suggested that Ras-GTP is an allosteric activator of Sos, while binding of Ras-GDP to this site reduces its activity[9].

Ras proteins are negatively regulated by GTPase activating proteins (GAPs). GAP proteins markedly stimulate intrinsic GTPase activity and ensure that Ras is rapidly inactivated after stimulation. At least six different members of GAP proteins exist that are active on Ras proteins[10]. $p120^{GAP}$ and neurofibromin-1 (NF1) are the two key Ras signal terminators. In contrast to GEFs, there are only a few details known with respect to pathways modulating GAPs activity.

1.1.3. Ras downstream signalling

Ras-GTP regulates complex signalling networks that modulate cell behaviour by binding and activating distinct classes of effectors proteins (Figure 1.3).

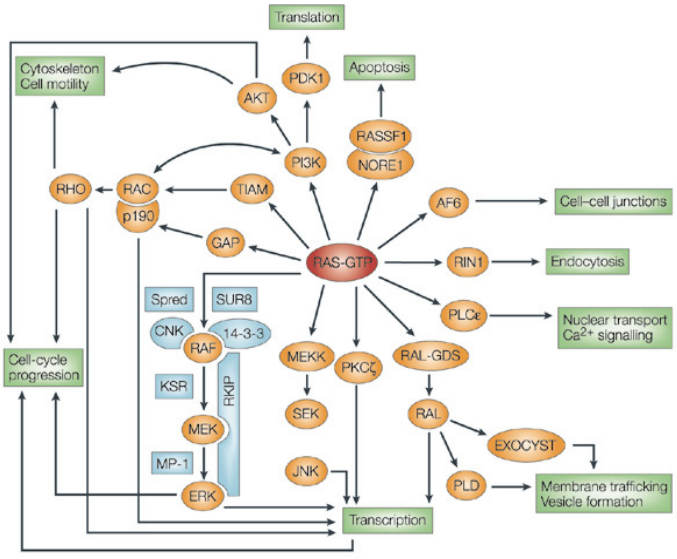

Figure 1.3: Signalling networks downstream Ras-GTP.

9. Sondermann, H.; Soisson, S. M.; Boykevisch, S.; Yang, S. S.; Bar-Sagi, D.; Kuriyan, J., Structural analysis of autoinhibition in the Ras activator Son of sevenless. *Cell* **2004,** *119* (3), 393-405.

10. Donovan, S.; Shannon, K. M.; Bollag, G., GTPase activating proteins: critical regulators of intracellular signaling. *BBA-Reviews on Cancer* **2002,** *1602* (1), 23-45.

The first and the best characterized mammalian Ras effectors is the protein serine/threonine kinase **Raf**[11]. There are three Raf serine/threonine kinases (c-Raf1, A-Raf and B-Raf) that activate the **MEK-ERK kinase cascade**. All Raf isoforms share a conserved region at N-terminus that encode for a Ras-binding domain (RBD) and two conserved regions at C-terminus that encode for serine/threonine kinase domain. Following Ras-GTP/Raf interaction, Raf undergoes conformational changes, phosphorylates and activates mitogen –activating proteins kinase kinase 1 and 2 (Mek1 and Mek2) that are capable of phophorylating and activating the extracellular signal-regulated kinase 1 and 2 (Erk1/Erk2). Erk1/2, finally, move to the nucleus and interact with various physiological targets, among which the transcriptional factors such as Myc, Jun and Fos. The final result is the expression of key cell-cycle regulatory proteins, such as **D-type cycline**, which enables the cell through the G1 phase of the cell cycle, and therefore promotes cell cycle progression[12].

Other Ras effectors are represented by phosphatidylinositol-3-kinases (**PI3K**). Ras-GTP can binds the catalytic subunit of type-I PI3Ks, resulting in translocation to the plasma membrane, activation and phosphorylation of phoshatidylinositol-4,5-bisphosphate (PIP2) to generate phoshatidylinositol-3,4,5-triphosphate (**PIP3**), a second messenger that binds a large number of proteins through the pleckstrine homology (PH) domain[13]. In this way, PI3K controls the activity of a large number of downstream kinases, such as **Pdk1** and **Akt,** that are essential for pro-survival cell signals[14]. In addition, PI3K can interact with **Rac**, a Rho-family GTPase protein that is involved in the regulation of actin expression[15], a cytoskeleton fundamental component, and in some transcription factors among which **NF-kB**.

---

11. Marais, R.; Light, Y.; Paterson, H. F.; Marshall, C. J., Ras recruits Raf-1 to the plasma membrane for activation by tyrosine phosphorylation. *Embo Journal* **1995,** 14, 3136-3136.

12. Yordy, J. S.; Muise-Helmericks, R. C., Signal transduction and the Ets family of transcription factors. *Oncogene* **2000,** *19* (55), 6503.

13. Rodriguez-Viciana, P.; Warne, P. H.; Dhand, R.; Vanhaesebroeck, B.; Gout, I.; Fry, M. J.; Waterfield, M. D.; Downward, J., Phosphatidylinositol-3-OH kinase direct target of Ras. **1994**.

14. Datta, S. R.; Brunet, A.; Greenberg, M. E., Cellular survival: a play in three Akts. *Genes & Development* **1999,** *13* (22), 2905-2927.

15. Hall, A., Rho GTPases and the actin cytoskeleton. *Science* **1998,** *279* (5350), 509.

A third well-studied effectors of Ras is a family of nucleotide-guanine exchange factors (**RalGEFs** such as RalGDS, Rgl/Rsb2, Rgl2/Rlf) for **Ral small GTPase proteins**[16]. The stimulation of Ral proteins has as consequence the activation of phospholipase D1 and Ralbp1, responsible, together with Akt/Pkb1, for the inhibition of the transcription factors **Forkhead**, implicated in the cellular cycle arrest and in apoptosis. Ral signalling has also been implicated in the regulation of endocytosis and exocytosis, actin organization and cell migration.

Phospholiphase Cε is a further Ras effectors that has been recently reported. PlCε binds directly to Ras-GTP, and the consequent hydrolysis of PIP2 to diacylglycerol and inositol-1,4,5 triphosphate serves to release calcium and activate protein kinase C[17,18]. A multiplicity of functions has been ascribed to PkC. PkC is involved in receptor desensitization, in modulating membrane structure events, in regulating transcription, in mediating immune responses, in regulating cell growth, and in learning and memory.

Several other Ras effectors have been described, which include a number of proteins with different roles in cell physiology. It appears evident that Ras proteins play a key role in different signal transduction pathways, and they are deeply implicated in critical cell events that influence cell-cycle progression. Since their critical role, it is quite clear that dysfunction in Ras signalling could have disastrous consequences in cell growth and development.

16. Kikuchi, A.; Demo, S. D.; Ye, Z. H.; Chen, Y. W.; Williams, L. T., ralGDS family members interact with the effector loop of ras p21. *Molecular and Cellular Biology* **1994,** *14* (11), 7483-7491.

17. Song, C.; Hu, C. D.; Masago, M.; Kariya, K.; Yamawaki-Kataoka, Y.; Shibatohge, M.; Wu, D.; Satoh, T.; Kataoka, T., Regulation of a novel human phospholipase C, PLC , through membrane targeting by Ras. *Journal of Biological Chemistry* **2001,** *276* (4), 2752-2757.

18. Kelley, G. G.; Reks, S. E.; Ondrako, J. M.; Smrcka, A. V., Phospholipase C : a novel Ras effector. *EMBO journal(Print)* **2001,** *20* (4), 743-754.

1.2. Mammalian Ras isoforms

Mammalian genomes encode three *RAS* genes that give rise to four highly homologous 21kD proteins: N-Ras, H-Ras, K-Ras4A and K-Ras4B (K-Ras isoforms result from alternative gene splicing). With the exception of K-Ras4B, which is constituted of 189 residues, the Ras proteins are composed by 188 amino acids (Figure 1.4).

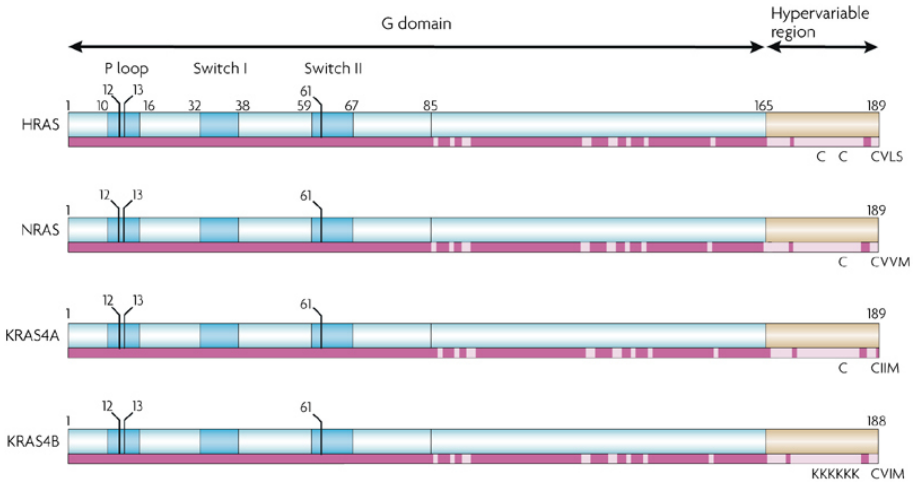

Figure 1.4: The four Ras isoforms[19]. H-RAS, N-RAS, K-RAS4A and K-RAS4B are highly homologous throughout the G domain (amino acids 1–165). The C-terminal hypervariable domain (amino acids 165–188/189) specifies membrane localization through post-translational modifications that include the farnesylation of each isoform on the C-terminal CAAX motif (CVLS, CVVM, CIIM and CVIM, respectively) and palmitoylation of key cysteines on HRAS, NRAS and KRAS4A; these cysteines are highlighted below each representation (C). Membrane localization of KRAS4B is facilitated by a stretch of lysines (KKKKKK) proximal to the CVIM motif. To highlight the degree of homology, a box at the bottom of each isoform representation shows the conserved residues in magenta and the variable residues in pink.

The N-terminal portion (residues 1-165) of Ras isoforms comprises a highly conserved G-domain that presents a common structure. Ras proteins diverge substantially at the C-terminal end, which is known as hypervariable region (HVR). This region contains conserved residues that specify post-translation modifications that are essential for the targeting of Ras proteins to the cytosolic leaflet of cellular

19. Schubbert, S.; Shannon, K.; Bollag, G., Hyperactive Ras in developmental disorders and cancer. *Nature Reviews Cancer* **2007,** *7* (4), 295-308.

membrane. It has been shown that the first 166 residues are necessary and sufficient for its biochemical proprieties and that the C-terminus is thus only necessary for localization in the plasma membrane and is not involved in any interaction[20].

All Ras proteins are farnesylated at a terminal **CAAX motif**[21], in which C is cysteine, A is usually an aliphatic aminoacid and X is any aminoacid. Although these CAAX-signal modifications appeared to be essential for the association of Ras with the plasma membrane, other studies identified the requirement for a second C-terminal signal recruitment and hence full Ras function. H-Ras, N-Ras and K-Ras4A are additionally modified by one or two palmitic acid chains just upstream of the CAAX motif that complemented farnesyl moiety to firmly anchor the proteins to the membrane. By contrast, K-Ras4B contains an alternative second signal that is composed of polybasic stretch of lysine residues which are believed to interact with negatively charged head groups of plasma membrane lipids[22]. K-Ras and N-Ras, moreover, can be geranylgeranylated when not farnesylated.

Not surprisingly, differences in post-translational modifications result in the distinct trafficking of proteins. In fact, while K-Ras4B rapidly appears at plasma membrane after processing in Endoplasmic Reticulum, where farnesylation takes place, the remaining Ras isoforms are further processed in the Golgi by palmitoyltransferase and then directed to plasma membrane by conventional vesicular transport. N-Ras and H-Ras also undergo to a palmitoylation-depalmitoylation cycle in which they move back and forth between the plasma membrane and Golgi through vesicle transport, so a significant portion of N-Ras and H-Ras reside in the Golgi. Different studies have shown that these proteins can signal on this organelle as well as on other endomembrane compartments, such as the endoplasmic reticulum. The differential subcellular location, as the variable expression levels, might be the

20. John, J.; Schlichting, I.; Schiltz, E.; Rosch, P.; Wittinghofer, A., C-terminal truncation of p21H preserves crucial kinetic and structural properties. *Journal of Biological Chemistry* **1989,** *264* (22), 13086-13092.

21. Casey, P. J.; Solski, P. A.; Der, C. J.; Buss, J. E., p21ras is modified by a farnesyl isoprenoid. *Proceedings of the National Academy of Sciences* **1989,** *86* (21), 8323-8327.

22. Hancock, J. F.; Paterson, H.; Marshall, C. J., A polybasic domain or palmitoylation is required for the addition of the CAAX motif to localize p21 to the plasma membrane. *Cell* **1990,** *63* (1), 133-139.

explanation of non-complete functional redundancy between Ras isoforms[23,24]. In fact, genetic studies in mice suggest that Ras proteins have both unique and overlapping roles in development. K-Ras is essential for mouse embryonic development; K-Ras-deficient mice die in after few days of gestation. By contrast, mice deficient in H-Ras and N-Ras, both alone or in combination, develop normally and are viable and fertile[25].

1.3. Structural features of Ras proteins

The overall Ras structure is constituted by a hydrophobic core of **six stranded β-sheets** and **five α-helices** that are interconnected by a series of ten loops (Figure 1.5). This fold is characteristic of guanine-nucleotide binding proteins, including the large family of heterotrimeric G proteins. It is called the G-domain fold and contains five G motifs which are involved in the binding of guanine-nucleotides and in the coordination of a Mg^{2+} cation, important cofactor for GTPase activity[26].

According to this model, Ras proteins present a conserved motive rich in glycine that is directly involved in binding the charged phosphate groups. This motive is characterized by the sequence ^{10}GxxxxGKS/T and it is called **P-Loop**. Through its totally conserved Lys16, it forms a ring like structure that wraps tightly around the β-phosphate of GTP/GDP.

23. Omerovic, J.; Prior, A., Compartmentalized signalling: Ras proteins and signalling nanoclusters. *FEBS Journal* **2009,** *276* (7), 1817-1825.

24. Omerovic, J.; Laude, A. J.; Prior, I. A., Ras proteins: paradigms for compartmentalised and isoform-specific signalling. *Cellular and Molecular Life Sciences (CMLS)* **2007,** *64* (19-20), 2575-2589.

25. Esteban, L. M.; Vicario-Abejon, C.; Fernandez-Salguero, P.; Fernandez-Medarde, A.; Swaminathan, N.; Yienger, K.; Lopez, E.; Malumbres, M.; McKay, R.; Ward, J. M., Targeted genomic disruption of H-ras and N-ras, individually or in combination, reveals the dispensability of both loci for mouse growth and development. *Molecular and cellular biology* **2001,** *21* (5), 1444-1452.

26. Vetter, I. R.; Wittinghofer, A., The guanine nucleotide-binding switch in three dimensions. *Science* **2001,** *294* (5545), 1299-1304.

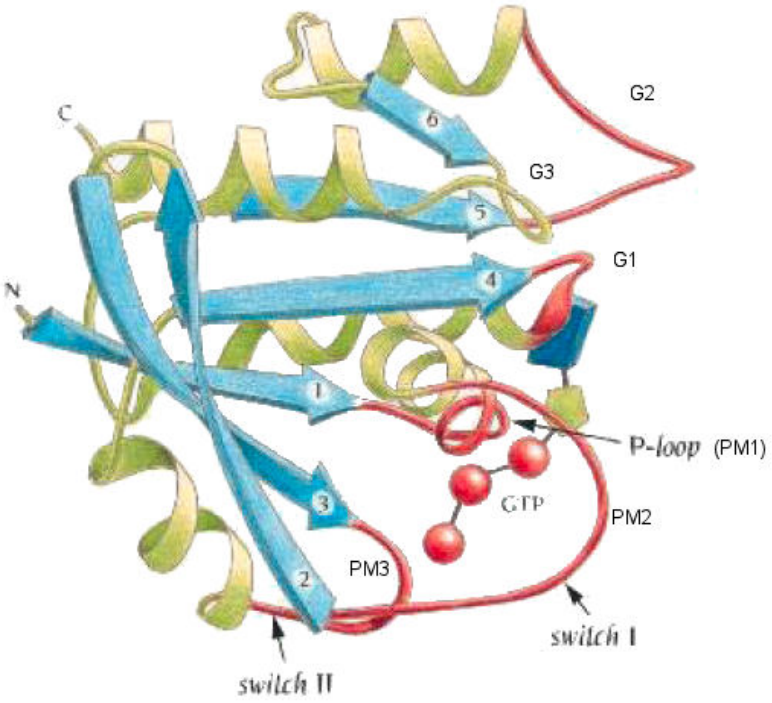

Figure 1.5 : Three-dimensional structure of p21 H-Ras-GTP.

Crystallographic structure of inactive Ras-GDP (2.0 Å, Protein Data Bank code 4q21) and active Ras-GppNHp (1.35 Å, PDB code 5p21) are determined. The structural difference between the active state and inactive state conformations reside mainly in two highly dynamic regions, termed Switch I (residue 32-40) and Switch II (residue 60-76). Switch I comprises loop 2 and β-sheets 3, while Switch II comprises loop 4 and α-helices 2. These regions present a conserved residue of threonine at position 35 and a conserved residue of glycine at position 60 that directly bind the γ-phosphate of GTP (Figures 1.6 and 1.7).

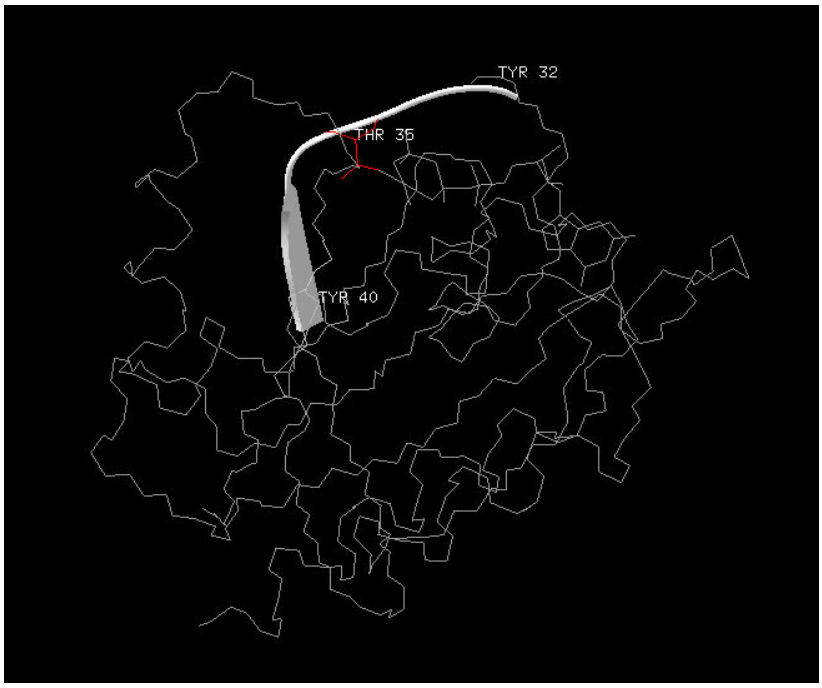

Figure 1.6 : Switch I region (residue 32 – 40)

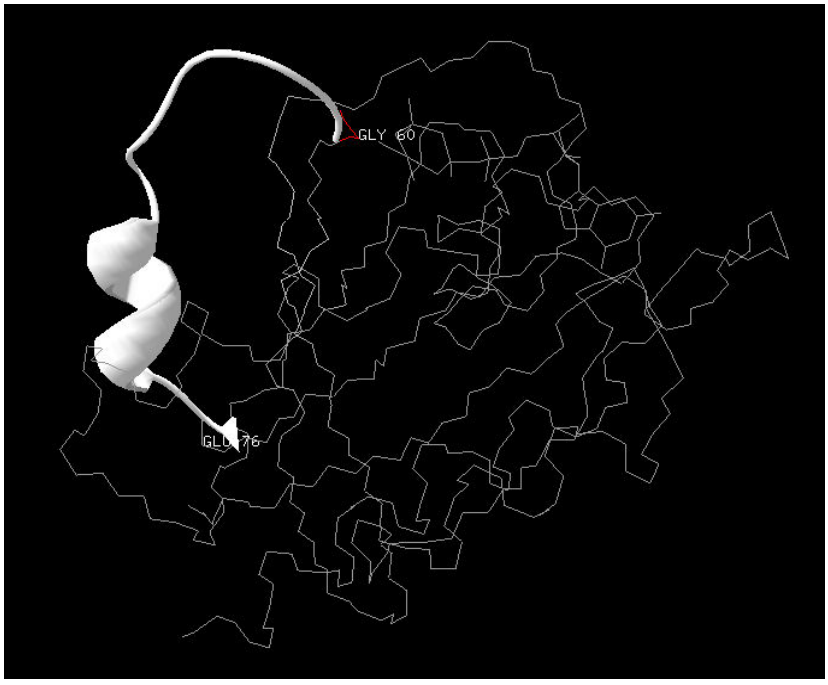

Figure 1.7: Switch II region (residue 60 – 76)

The binding of GTP alters the conformation of Switch I, primarily through the inward reorientation of the side chain of **Thr35**, thereby enabling its interaction with γ-phosphate as well as the Mg^{2+} ion. Similarly, the γ-phosphate induces significant changes in the orientation of the Switch II region thought interactions with **Gly60** (Figure 1.8). Interesting, both regions Switch I and Switch II are involved in the binding with regulating GAP and GEF proteins, as well as effectors proteins.

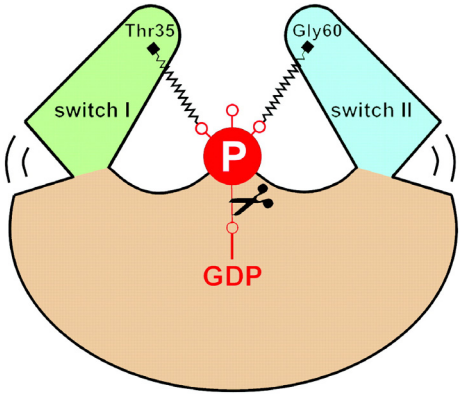

Figure 1.8: Schematic diagram of Switch mechanism. Release of the γ-phosphate after GTP hydrolysis allows the switch regions to relax into a different conformation.

1.3.1. Catalytic mechanism of intrinsic GTP hydrolysis

The mechanism of Ras GTP-hydrolysis is the key step of Ras signalling inactivation but despite the biological importance and despite structural and kinetics studies, the question remains controversial. The reaction consists in the hydrolysis of the phosphoanhydridic bond between phosphate β and γ of GTP. Likewise others proteins with GTPase activity, Ras requires the presence of divalent cations. Mg^{2+} is its enzymatic cofactors and is able to coordinate the negative charge of the terminal phosphoric groups of GTP or GDP.

The reaction that takes place is the following (Scheme 1.1):

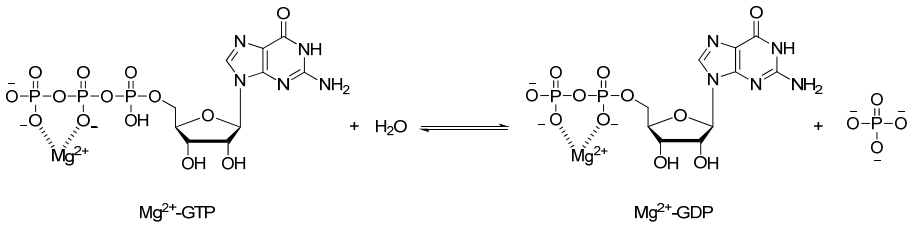

Scheme 1.1: Hydrolysis reaction of GTP catalysed by Ras proteins.

Crystallographic studies on Ras-GppNHp allowed the identification of a molecule of water that was found close to γ-phosphate and is considered the attacking nucleophile[27]; the major unresolved problem is the nature of the general base activating the catalytic water molecule. The first idea was that a residue of glutamine in position 61, found close to the γ-phosphate, might be fill this role (Scheme 1.2).

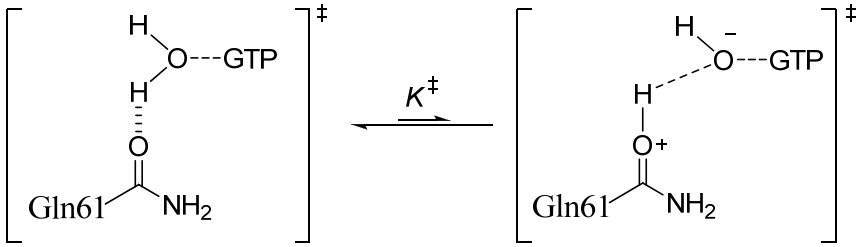

Scheme 1.2: Transition state hypotized with Gln61 as general base. On the basis of pKa, the value of $K^{\ddagger}$ was estimated about 10^{-16}.

Although this hypothesis is supported by different experimental evidences, more recent mechanistic proposal suggests that the γ-phosphate might act itself as a base. In this model the residue **Gln61** stabilizes the transition state according to its capability of acting as donor and acceptor of hydrogen bonds (Scheme 1.3).

27. Pai, E. F.; Krengel, U.; Petsko, G. A.; Goody, R. S.; Kabsch, W.; Wittinghofer, A., Refined crystal structure of the triphosphate conformation of H-ras p21 at 1.35 A resolution: implications for the mechanism of GTP hydrolysis. *EMBO J* **1990,** *9* (8), 2351-2359.

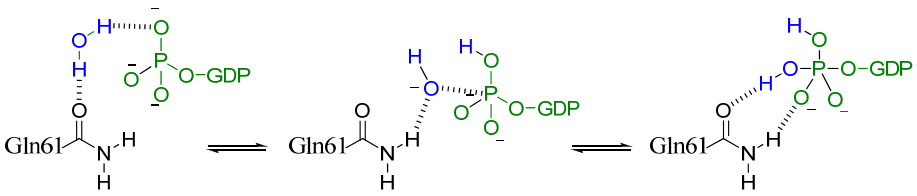

Scheme 1.3: Proposed substrate assisted mechanism for the intrinsic GTPase reaction of Ras, where γ-phosphate group itself activates the attacking nucleophilic water molecule.

In addition, the backbone amide of **Gly13** is positioned to donate a hydrogen bond to the β-γ bridge oxygen of GTP and to β-phosphate oxygen when GDP is bound. Other interactions such as β-nonbrindging oxygen with Lys16 and Mg^{2+} may be strengthened in the transition state. Also **Tyr35** seems to contribute positioning the water molecule with respect to the γ-phosphate group and lowering the entropic barrier for reaction. All these interactions can contribute to the modest catalysis of Ras[28,29] (Figure 1.9)

28. Maegley, K. A.; Admiraal, S. J.; Herschlag, D., Ras-catalyzed hydrolysis of GTP: a new perspective from model studies. *Proceedings of the National Academy of Sciences* **1996,** *93* (16), 8160-8166.

29. Wittinghofer, A.; Waldmann, H., Ras - A molecular switch involved in tumor formation. *Angew Chem Int Edit* **2000,** *39* (23), 4193-4214.

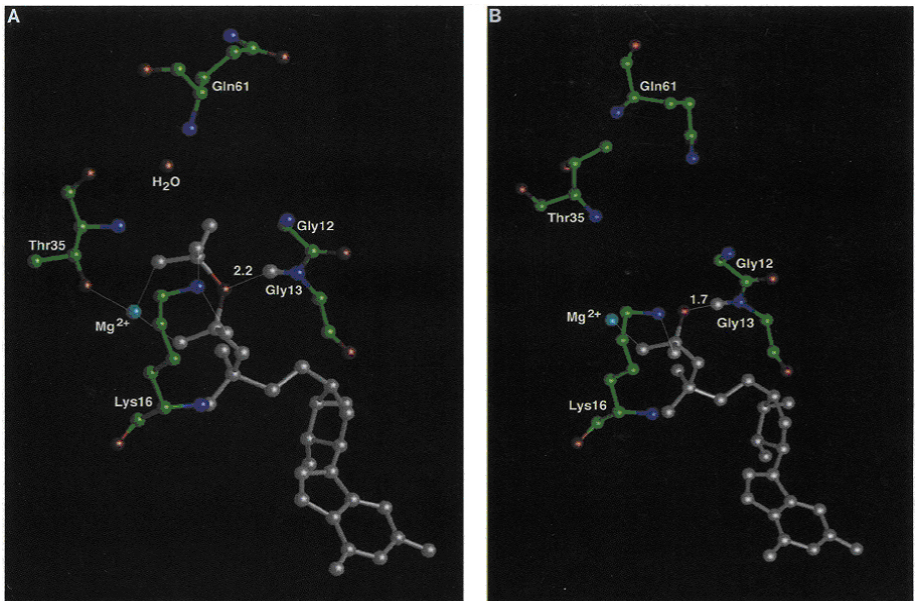

Figure 1.9 : Crystallographic structure of Ras active site with GppNHp (analogous of GTP) (panel A) **and with GDP** (panel B)**.**

1.3.2. Interaction with GAP

Although Ras proteins have a measurable intrinsic GTPase activity (GTP hydrolysis rate constant 0.028 min^{-1})[30], this activity is considered physiologically less important than the GAP-mediated reaction. Two model of GAP-mediated hydrolysis have been proposed. According to the first, RasGTP-GAP interaction causes conformational changes that stabilize the catalytically-active state of Ras and enhances his intrinsic GTPase activity. The second, instead, proposes that Ras needed the presence of chemical groups of GAP, which therefore is directly involved in catalytic reaction. The issue is finally solved by the determination of the structure of the complex between RasGDP and $p120^{GAP}$ in presence of aluminium fluoride (AlF_3), which mimics the transition state of the GTPase reaction[31]. It has

30. Neal, S. E.; Eccleston, J. F.; Hall, A.; Webb, M. R., Kinetic analysis of the hydrolysis of GTP by p21N-ras. The basal GTPase mechanism. *Journal of Biological Chemistry* **1988,** *263* (36), 19718-19722.

31. Scheffzek, K.; Ahmadian, M. R.; Kabsch, W.; Wiesmuller, L.; Lautwein, A.; Schmitz, F.; Wittinghofer, A., The Ras-RasGAP complex: structural basis for GTPase activation and its loss in oncogenic Ras mutants. *Science* **1997,** *277* (5324), 333.

been shown that an arginine residue from the conserved Phe-Leu-Arg (FLR) motif of GAP, called "finger loop", penetrates the active site of Ras and contacts the aluminium fluoride. During the hydrolysis reaction a partial negative charge develops in the phosphoryl groups of transition state, here mimicked from AlF_3. The positively charged guanidinium group of Arg789 neutralizes this negative charge and thereby stabilizes the transition state of the reaction. This structure also shows the involvement of the Gln61 though a double hydrogen bond to transition state and the attacking water, as previously described (Figure 1.10).

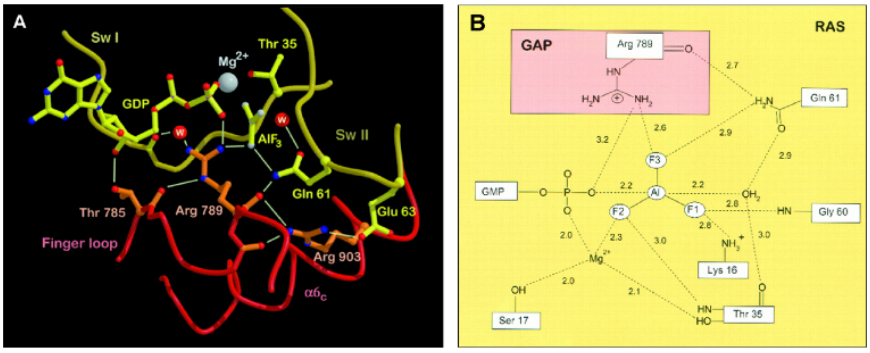

Figure 1.10: Structural (A) **and schematic** (B) **view of active site, with the important elements of catalysis.**

This study also reports the residues of Ras directly interact with GAP, principally located at the Switch I and Switch II regions and in P-loop region (Figure 1.11).

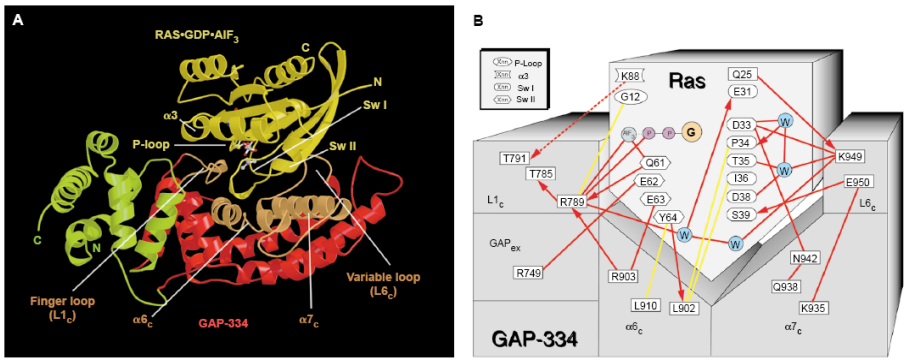

Figure 1.11 : Structural (A) **and schematic** (B) **representation of complex RasGDP-AlF_3** (in yellow) **and $p120^{GAP}$.** Contact region is represented in light brown.

1.3.3. Interaction with GEF

The structure of the intermediary binary complex of Ras with Sos (Figure 1.12A), a mammalian GEF, has been determined[32]. Ras and Sos form a tightly complex that induces the release of the bound nucleotide. The most important interactions of Ras with Sos involve Switch I and Switch II regions, and, more relevant for the nucleotide exchange mechanism, P-loop and Mg^{2+} binding site. The Switch I region is completely flipped out of its normal position such that residues, such as Phe28 and Thr35, which contact guanine base and phosphate groups, are removed from their binding site position. In addition, Switch I displacement triggers the insertion of helical hairpins close to Mg^{2+} binding site and P-loop, thus creating structural changes. Almost all residues of Switch II are involved in the interaction with Sos. These interactions cause a pushing toward the nucleotide binding-site that leads to the occupation of Mg^{2+} binding site by Ala59 and a complete rearrangement of P-loop due to tightly interaction between Lys16 and Glu62 (Figure 1.12B).

These structural perturbations break the network of direct and water-mediated interactions between Switch regions, nucleotide and Mg^{2+} ion, causing an enhancement in the nucleotide ejection rate. The re-binding nucleotide is preferentially GTP, which is more abundant in the cytosol.

32. Boriack-Sjodin, P. A.; Margarit, S. M.; Bar-Sagi, D.; Kuriyan, J., The structural basis of the activation of Ras by Sos. *Nature* **1998,** *394* (6691), 337.

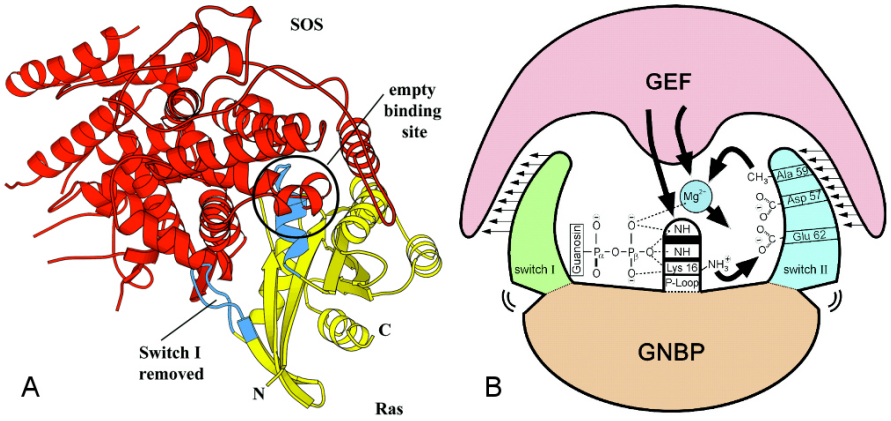

Figure 1.12: Ribbon representation of binary Ras-Sos complex (A) **and schematic diagram of GEF action** (B)**.**

1.3.4. Interaction with effectors

Once activated, RasGTP is able to interact with their effectors because of the conformational changes that take place. Common characteristic structure of Ras effectors is a Ras binding domain (**RBD**), composed of 10/20 amino acids, and with a common topology, that is, ubiquitin folding (ββααββα). The interaction with Ras involves only the Switch I region (residues 32-40) and not the Switch II region; the D38A mutation, for example, prevents all Ras-effector interactions[33].

GTP hydrolysis causes a reduction of Ras affinity for its effectors, probably due to conformational changes that involve the Switch I region.

1.3.5. Nucleotide binding site

The network of interactions at the nucleotide binding site of the Ras bound to the triphosphate analogous GppNHp is shown in Scheme 1.4.

33. Herrmann, C., Ras-effector interactions: after one decade. *Current Opinion in Structural Biology* **2003,** *13* (1), 122-129.

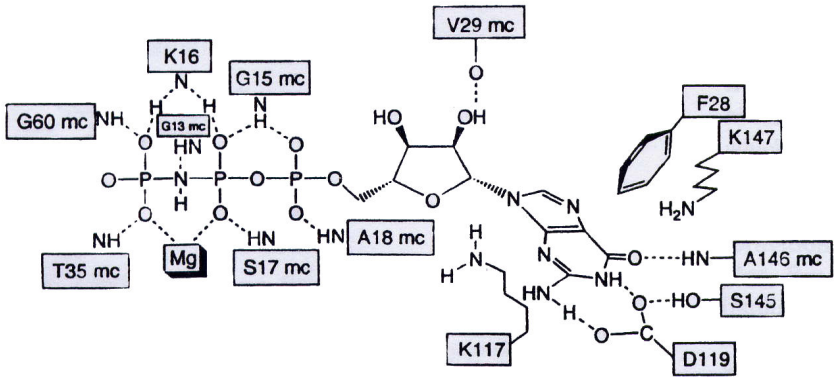

Scheme 1.4: Interaction of GppNHp in Ras nucleotide binding site. mc=peptide main chain

The guanine base of the nucleotide is located in a hydrophobic pocket where contacts the aromatic portion of phenylalanine residue **F28** and the side chains of lysine residues **K117** and **K147**. The aspartate residue **D119** is involved in a double hydrogen bond to the guanine base. It is the major element responsible for the high specificity of the protein for guanine nucleotides. Alanine **A146**, that interacts with the nitrogen atom of the main chain with O6 of the base, also contributes to the specificity of the binding to guanine base. Residue 116, 117, 119 and 146 are highly conserved in proteins that bind guanyl nucleotides[34].

1.3.6. Mg^{2+} binding site

Like all the proteins that are involved in phosphate group transfer, Ras proteins need divalent cations such as Mg^{2+}, whose presence increases protein affinity for nucleotides. The ion is coordinated by six oxygen atoms (both Ras-GTP as Ras-GDP) forming a perfect double trigonal pyramid, as shown in the Figure 1.13. Two of these oxygen atoms belong to β and γ phosphate groups; two other oxygen atoms belong to Ser17 and Thr35 side chains, highly conserved in all proteins that bind guanyl nucleotides. The two octahedron apical positions are represented by the

34. Rensland, H.; John, J.; Linke, R.; Simon, I.; Schlichting, I.; Wittinghofer, A.; Goody, R. S., Substrate and Product Structural Requirements for Binding of Nucleotides to H-ras p21: The Mechanism of Discrimination between Guanosine and Adenosine Nucleotides. *Biochemistry* **2002,** *34* (2), 593-599.

oxygen atoms of two water molecules: one is coordinated by α phosphate; the other one is coordinated by Asp57 residue. Mutagenesis experiments have shown that S17A and D57A mutations cause a decrease in Ras affinity for the nucleotide, underlying the importance of the cation for the interaction with GTP or GDP[35].

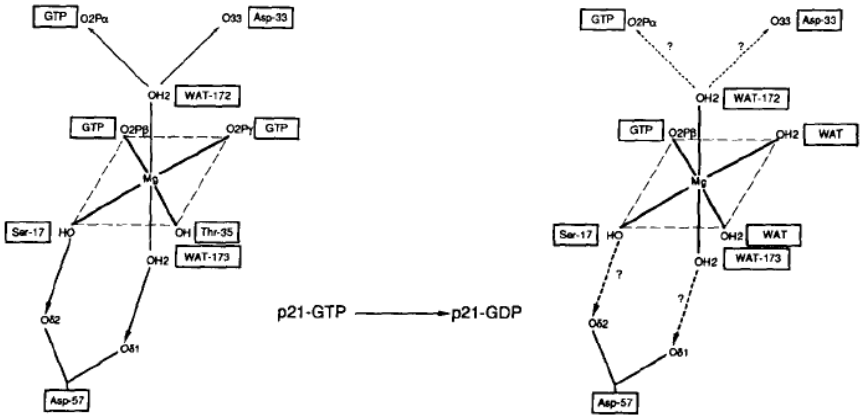

Figure 1.13: Mg^{2+} coordination on p21-GppNHp and GDP complex, as determined by crystallographic studies.

35. John, J.; Rensland, H.; Schlichting, I.; Vetter, I.; Borasio, G. D.; Goody, R. S.; Wittinghofer, A., Kinetic and structural analysis of the Mg(2+)-binding site of the guanine nucleotide-binding protein p21H-ras. *J. Biol. Chem.* **1993,** *268* (2), 923-929.

1.4. Ras proteins and Oncogenesis

1.4.1. Cancer

Cellular growth and development are tightly regulated in normal cells to ensure tissue integrity. Any occurrences that lead to uncontrolled growth could be have disastrous consequence for the organism. Cancer is a class of diseases characterized by the uncontrolled and irreversible proliferation of abnormal cells, which bring to formation of a malignant neoplasia.

Common features of malignant tumoral cells are the uncontrolled growth, invasion of neighbouring tissues and sometimes metastasis. Thus, malignant tumours can invade other organs and tissues, becoming life-threatening.

In general, all cancers are caused by abnormality in genetic material of the transformed cells that transmits this aberrant genetic patrimony to its progeny. Different factors can promote transformation, and they can be both endogenous, such as hormones, and exogenous such us viruses, ionizing radiation or chemical mutagens. In general, transformation of normal cells in tumoral ones is a multi-step process and demands a number of key-events that include the acquisition of cell self-sufficiency to growth signals. This factor is probably a consequence of the stimulation to proliferation by autocrin growths, of the over-expression of growth factor receptors, of the over-expression or the activation of cytoplasmatic components of signalling pathways.

Genetic changes can occurs at different levels, from single nucleotide point mutation to gain or loss entire chromosomes. There are two broad categories of genes which are affected by these mutations:

- **Oncogenes**: they are tumour-inducing genes and generally have a dominant character. First, they were discovered as genes brought by retroviruses that cause the transformation of target cells. Normally quiescent cellular counterparts of oncogenes are called **proto-oncogenes**. In general, proto-oncogenes promote cell growth and differentiation in a variety of ways, such as production of growth factors or the involvement in signalling transduction pathway. Mutations in proto-oncogenes, that modify their

expression or function, transform it in oncogenes and then have as result promotion of tumours formation.

- **Tumour suppressor genes**: they are genes that normally impose some restriction to cellular cycle and cell growth. In general, they encode proteins that function to suppress cell growth or protect the genome from damage that could lead to uncontrolled growth. Loss of restriction is obviously tumorigenic, because it has as result the impossibility to correct check cell progression into the cycle.

1.4.1. Oncogenic Ras in tumorigenesis and developmental disorders

Ras proteins, as described in paragraph 1.1.3, are molecular switches involved in signal transduction in response of external stimuli. Their activation is tightly regulated and they are able to activate different effectors enzymes, regulating various cellular events, like cell cycle progression, survival and differentiation. The *ras* genes were originally found in retroviruses that trigger sarcoma-type tumours in rats[36] (ras = rat sarcoma), and then cellular homologous were identified in human genome[37]. Therefore *ras* genes are fully considered proto-oncogenes. As a consequence of mutations, ras oncogenes could encode for oncogenic variant of Ras proteins that show constitutively activation and thus abnormal cellular signalling.

In many cases, Ras somatic mutations associated with tumoral transformation take place in three residues: **glycine G12**, **glycine G13** and **glutamine Q61**. These changes impair the intrinsic GTPase activity and confer resistance to GAPs, thereby generating permanently active Ras molecules with severe consequence for the cell. It has been demonstrated that the presence of any side chain at position G12 and partially at position G13 prevents the interaction with GAP Arg789 residue in the

36. Harvey, J. J.; Harvey, An unidentified virus which causes the rapid production of tumours in mice. *Nature* **1964,** *204* (4963), 1104.

37. Chang, E. H.; Gonda, M. A.; Ellis, R. W.; Scolnick, E. M.; Lowy, D. R., Human genome contains four genes homologous to transforming genes of Harvey and Kirsten murine sarcoma viruses. *Proceedings of the National Academy of Sciences of the United States of America* **1982,** *79* (16), 4848-4852.

catalytic site. Interesting, the G12P mutant, where glycine is substituted by a proline, shows resistance to GAPs, but also an increased intrinsic GTPase activity and, thus, it does not transform cells[38]. Gln61 has a central function in GTP hydrolysis in that it contacts and coordinates the hydrolytic water molecule and the O-atom of the γ-phosphate of GTP and thus stabilizes the transition state. Amino acids with other side chains apparently cannot fulfil this function, as shown by the oncogenic effect of Gln61 mutants in which Gln61 is replaced by other amino acids (other than Glu).
Activating Ras mutations occur in about 30 % of human cancers. Specific *Ras* genes are mutated in different malignancies: K-Ras mutation are prevalent in pancreatic, colorectal, endometrial, biliary tract, lung and cervical cancer; K-Ras and N-Ras mutation are found in myeloid malignancies; N-Ras and H-Ras mutations predominate in melanoma and bladder cancer, respectively (Table 1.1).

Cancer type	*HRAS*	*KRAS*	*NRAS*
Biliary tract	0%	33%	1%
Bladder	11%	4%	3%
Breast	0%	4%	0%
Cervix	9%	9%	1%
Colon	0%	32%	3%
Endometrial	1%	15%	0%
Kidney	0%	1%	0%
Liver	0%	8%	10%
Lung	1%	19%	1%
Melanoma	6%	2%	18%
Myeloid leukaemia	0%	5%	14%
Ovarian	0%	17%	4%
Pancreas	0%	60%	2%
Thyroid	5%	4%	7%

Table 1.1: Ras mutation in human cancer.

38. Franken, S. M.; Scheidig, A. J.; Krengel, U.; Rensland, H.; Lautwein, A.; Geyer, M.; Scheffzek, K.; Goody, R. S.; Kalbitzer, H. R., Three-dimensional structures and properties of a transforming and a nontransforming glycine-12 mutant of p21H-ras. *Biochemistry* **1993,** *32* (33), 8411-8420.

Although somatic point mutations in human *Ras* genes are already know for many years, germline mutations in Ras as well as in other Ras-signalling pathway components have been detected only recently. These mutations are involved in a set of rare developmental diseases that have been summarize under the term "Neuro-Cardio-Facial-Cutaneous" (NCFC) syndrome[39]. These include Neurofibromatosis type I, Noonan syndrome, Leopard syndrome and Costello syndrome. In general, patients with these diseases are characterized by facial dimorphisms, heart defects and short stature. In addition, skin and genital malformations, mental retardation and predisposition to certain malignancies have been described.

Principally H-Ras and K-Ras are involved in these syndromes. For instance, the germline mutation G12S, K117R and A146T in *H-Ras* genes have been reported in Costello syndrome, whereas the germline mutations V14I, T58I and D153 in *K-Ras* were found in patient with Noonan syndrome[18]. All these mutants displayed impaired GTPase activity and reduced responsiveness to GAPs, but overall these functions are less impaired than for oncogenic mutant.

39. Bentires-Alj, M.; Kontaridis, M. I.; Neel, B. G., Stops along the RAS pathway in human genetic disease. *Nature medicine* **2006,** *12* (3), 283-285.

2. Ras proteins as a target for new anti-cancer therapy development

After more than 30 years of intense research, Ras proteins are the most studied target in cancer biology. It is estimated that more 30% of all human tumour present mutations in *RAS* genes. The oncogenic Ras proteins present point mutations that lead to the accumulation of Ras in the active signalling state, which contribute to tumour formation. Therefore, modulation of Ras activity represents a promising approach for the development of new anticancer therapies[40,41].

2.1. Strategy for interacting with Ras proteins

With the aid of deep structural and biochemical knowledge, different approaches have been pursued in order to inhibiting the aberrant signalling mediated by Ras proteins. The most important strategies consist in:

- inhibition of Ras membrane localization;
- blocking of Ras expression;
- antagonizing of the interaction with downstream effectors proteins;
- restoration or stimulation of mutant defective GTPase activity.

2.1.1. Inhibition of Ras membrane localization

Ras proteins must be localized at the plasma membrane in order to perform their biological function in both the normal and the oncogenic variants. The anchorage to the membrane requires a post-translational processing that involves an enzyme

40. Friday, B. B.; Adjei, A. A., K-ras as a target for cancer therapy. *Biochimica et biophysica acta* **2005,** *1756* (2), 127-44.

41. Kloog, Y.; Cox, A. D., RAS inhibitors: potential for cancer therapeutics. *Molecular Medicine Today* **2000,** *6* (10), 398-402.

farnesyltrasferase (FTasi), which transfers a farnesyl moiety at C-terminal extremity. Since this process is indispensable for Ras localization, it has become one of the most important targets to inhibit Ras functionality.

Several strategies have been developed to inhibit the farnesylation of Ras, the most common being the design of compounds that mimic the C-terminal CAAX motif of Ras and compete for binding to farnesyltrasferase. Another strategy has been the design of farnesyldiphosphate (FDP) analogous, that compete with the natural substrate of the enzyme. The third approach comprises the design of molecules that share proprieties of both farnesyldiphosphate and CAAX motif in order to mimic the transition state in the farnesylation process; these compounds are known as bisubstrate analogues (Scheme 2.1).

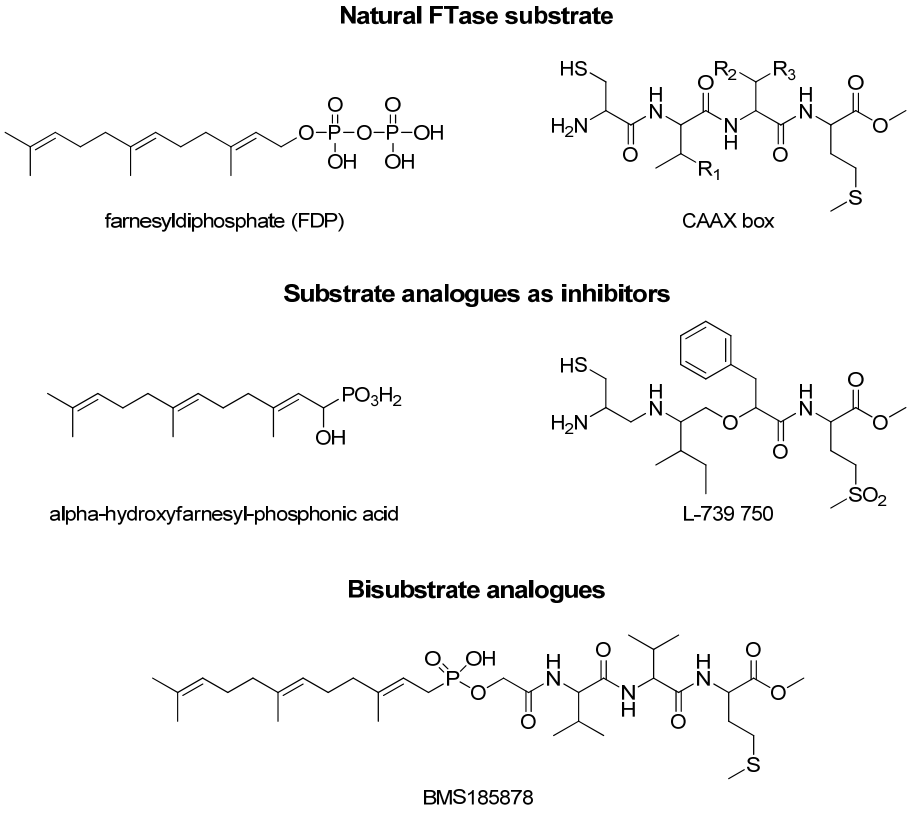

Scheme 2.1: Natural substrates and analogues inhibitors of FTase.

A large number of highly effective farnesyltrasferase inhibitors (FTIs), both from natural sources, such as limonene or manumycin A, and of synthetic origin such as **SCH66336** (Sarasar) or **R115777** (Zanestra), have been discovered[42].

These compounds efficiently inhibit the farnesylation of H-Ras in cells culture and promote the reversion of mammalian carcinomas in transgenic rats that express activated H-Ras proteins. Moreover, they present very low toxicity, so these results are promising in the perspective to use them in the treatment of different human cancers. Unfortunately, their early potential has not been repeated in human patients. In fact, with exception of H-Ras, that is only farnesylated, K-Ras and N-Ras, more frequently mutated in human tumours, can, in alternative, be geranylgeranylated by the enzyme geranylgeranyltrasferase (GGTase), overcoming the farnesyltransferase inhibition. The attempt to employ a combination of FTIs and GGTIs failed because of the high toxicity of the mixture[43]. It is possible that the lack of toxicity of FTIs is due to the fact that they fail to inhibit effectively the function of all endogenous Ras proteins, which are known to be essential for normal cell growth. Recently, the FTI ability to cause growth arrest in G2/M phase in some circumstances and to induce apoptosis in others, without passing through the inhibition of Ras processing, has been demonstrated[44].

Ras anchorage to the cytoplasmic membrane is also targeted by another class of molecule that mimics Ras farnesylcysteine (S-prenyl analogues). Among these, farnesylthiosalisylic acid (FTS) is the most studied (Scheme 2.2).

---

42. Cox, A. D.; Der, C. J., Farnesyltransferase inhibitors: promises and realities. *Current Opinion in Pharmacology* **2002,** *2* (4), 388-393.

43. Lobell, R. B.; Omer, C. A.; Abrams, M. T.; Bhimnathwala, H. G.; Brucker, M. J.; Buser, C. A.; Davide, J. P.; deSolms, S. J.; Dinsmore, C. J.; Ellis-Hutchings, M. S.; Kral, A. M.; Liu, D.; Lumma, W. C.; Machotka, S. V.; Rands, E.; Williams, T. M.; Graham, S. L.; Hartman, G. D.; Oliff, A. I.; Heimbrook, D. C.; Kohl, N. E., Evaluation of Farnesyl:Protein Transferase and Geranylgeranyl:Protein Transferase Inhibitor Combinations in Preclinical Models. *Cancer Res* **2001,** *61* (24), 8758-8768.

44. Prendergast, G. C., Actin'up: RhoB in cancer and apoptosis. *Nature Reviews Cancer* **2001,** *1* (2), 162-168.

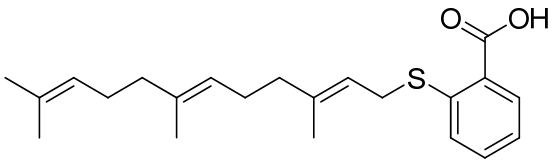

Scheme 2.2: structure of S-trans, trans-farnesylthiosalisylic acid (FTS)

FTS acts *in vitro* as inhibitor of Ras S-prenylcysteine methylation, and *in vivo* it inhibits the growth of human cells expressing oncogenic variants of H-Ras, reverting their transformed morphology in a dose dependent manner and at a concentration lower (0.1-10 μM) than those required for methylation inhibition. The lack of cytotoxicity at these concentration values suggests moreover that such compound is not able to prevent the correct process of isoprenylation in the normal cells[45]. In addition, it has been demonstrated that this compound blocks the growth of human melanoma cells[46]. FTS seems to be able to compete with Ras for anchorage sites to the membrane, and to promote Ras dislodging from the membrane, making it therefore susceptible to proteolytic degradation and carrying to a reduction of its total level inside the cell. On the basis of its mechanism of action, FTS is capable of acting as antagonist of whichever Ras isoforms, provided that farnesylated[47,48]. Very recent studies have been demonstrated that FTS also may consider as potential drug

45. Marom, M.; Haklai, R.; Ben-Baruch, G.; Marciano, D.; Egozi, Y.; Kloog, Y., Selective inhibition of Ras-dependent cell growth by farnesylthiosalisylic acid. *Journal of Biological Chemistry* **1995,** *270* (38), 22263.

46. Jansen, B.; Schlagbauer-Wadl, H.; Kahr, H.; Heere-Ress, E.; Mayer, B. X.; Eichler, H. G.; Pehamberger, H.; Gana-Weisz, M.; Ben-David, E.; Kloog, Y.; Wolff, K., Novel Ras antagonist blocks human melanoma growth. *Proceedings of the National Academy of Sciences of the United States of America* **1999,** *96* (24), 14019-14024.

47. Haklai, R.; Weisz, M. G.; Elad, G.; Paz, A.; Marciano, D.; Egozi, Y.; Ben-Baruch, G.; Kloog, Y., Dislodgment and Accelerated Degradation of Ras. *Biochemistry* **1998,** *37* (5), 1306-1314.

48. Gana-Weisz, M.; Halaschek-Wiener, J.; Jansen, B.; Elad, G.; Haklai, R.; Kloog, Y., The Ras Inhibitor S-trans,trans-Farnesylthiosalicylic Acid Chemosensitizes Human Tumor Cells Without Causing Resistance. *Clin Cancer Res* **2002,** *8* (2), 555-565.

in the treatment of Neurofibromatosis Type I (NF1), reducing the level of active Ras from the membrane[49].

2.1.2 Inhibition of Ras expression

A different approach to the therapeutic targeting of the Ras proteins is to decrease their expression level. The inhibition has been achieved by using short antisense synthetic oligonucleotides that are specific for sequences in Ras mRNAs. Binding to the complementary RNA, these oligonucleotides interfere with protein expression in different way: one is promoting the degradation of the mRNA by directing RNaseH to the RNA-DNA duplex; another is interfering with mRNA translation by steric hindrance[50]. Early trials in nude mouse models showed promising data in reducing the growth of K-Ras-transformed lung tumour cells. Different compounds are now in clinical trial phase, but several difficulties related to the use of this compounds as anti-cancers therapies exist, depending on toxicity phenomena, high levels of specificity and effectively delivery[51].

2.1.3 Interfering with Ras-effectors interaction

Aberrant Ras functions might also been disrupted by interfering with the interaction of Ras with its downstream effectors proteins. Although Ras proteins interact with various effectors proteins, they share a common fold, called Ras-binding domain (RBD domain), responsible for the binding to a specific region of Ras [par. 1.3.4]. Accordingly, it appears possible to develop selective inhibitors of this interaction. The first results come from a synthetic peptide that mimics the Ras-binding domain,

---

49. Barkan, B.; Starinsky, S.; Friedman, E.; Stein, R.; Kloog, Y., The Ras Inhibitor Farnesylthiosalicylic Acid as a Potential Therapy for Neurofibromatosis Type 1. Ibid.**2006,** *12* (18), 5533-5542.

50. Crooke, S. T., Potential roles of antisense technology in cancer chemotherapy. *Oncogene* **2000,** *19* (56), 6651.

51. Ross, P. J.; George, M.; Cunningham, D.; DiStefano, F.; Andreyev, H. J. N.; Workman, P.; Clarke, P. A., Inhibition of Kirsten-ras Expression in Human Colorectal Cancer Using Rationally Selected Kirsten-ras Antisense Oligonucleotides1. *Molecular Cancer Therapeutics* **2001,** *1* (1), 29-41.

preventing the interaction between c-Raf1 and Ras, and thus inhibiting the Ras-induced proliferation of NIH3T3 cells[52]. Inhibition of Ras-Raf interaction can be provided also by small molecules. A successful candidate is the non-steroidal anti-inflammatory drug (NSAID) **sulindac sulphide** that has been used in treatment of patient with the Inherited Cancer Disposition Familial Adenomatous Polyposis and seems to target Ras-Raf interaction. Although its low affinity for the complex, it constitutes a promising lead compound[53]. Recent studies show a mini library of sulindac-derived compounds able to inhibit Ras-induced cell transformation by blocking Ras-Raf interaction with increasing potency[54] (Scheme 2.3).

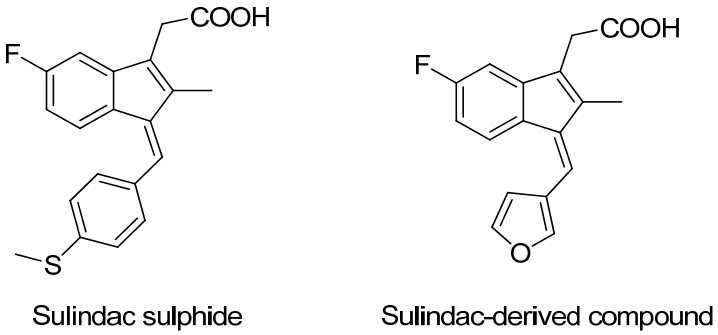

Scheme 2.3: Structure of sulindac sulphide and of sulindac-derived compound. Sulindac sulphide show an IC_{50} in the inhibition of Ras-Raf interaction of 210 μM, whereas the IC_{50} of the derived compound is 30μM.

52. Clark, G. J.; Drugan, J. K.; Terrell, R. S.; Bradham, C.; Der, C. J.; Bell, R. M.; Campbell, S., Peptides containing a consensus Ras binding sequence from Raf-1 and theGTPase activating protein NF1 inhibit Ras function. *Proceedings of the National Academy of Sciences of the United States of America* **1996,** *93* (4), 1577-1581.

53. Herrmann, C.; Block, C.; Geisen, C.; Haas, K.; Weber, C.; Winde, G.; Möröy, T.; Müller, O., Sulindac sulfide inhibits Ras signaling. *Oncogene* **1998,** *17* (14), 1769.

54. Herbert, W.; Ioanna-Maria, K.; Mercedes, C.; Eleni, G.; Christian, H.; Christoph, B.; Hartmut, O.; Oliver, M., Sulindac-Derived Ras Pathway Inhibitors Target the Ras-Raf Interaction and Downstream Effectors in the Ras Pathway13. *Angewandte Chemie International Edition* **2004,** *43* (4), 454-458.

2.1.4 Restoration of mutant defective GTPase activity

The major problem of oncogenic Ras variants is their inability to hydrolyze GTP. As a consequence, they remain constitutively in the active state, responsible for the tumoral transformation. A valid strategy to switch off the signal of these variants consists in the design of compounds capable of restoring Ras GTPase activity. Such molecules take advantage of the phenomenon named "substrate-assisted catalysis": the substrate is able to supply those catalytic functional groups lost as a result of the mutation, thus restoring the defective catalytic activity of the protein. Prototype of this compound family is the **GTP-diaminobenzophenone-phosphoroamidate** (**DABP-GTP**) (Scheme 2.4). DABP-GTP is a GTP analogue that furnishes the amino group, essential for catalysis, lost because of Ras mutations in Gln-61 residue and, in this way, restores Ras GTPase activity.

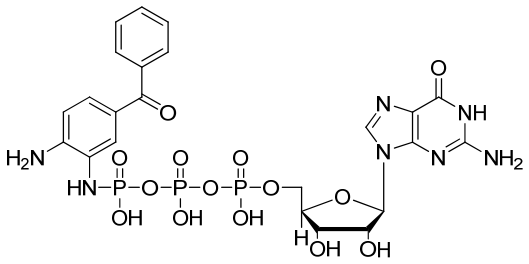

Scheme 2.4: Structure of DABP-GTP.

DABP-GTP can acts as substrate also for the wild-type Ras proteins, but it is hydrolyzed more efficiently by the mutants; for this reason, it is extremely selective for Ras oncogenic forms, and, therefore, the signalling of the Ras proteins wild-type would not be altered by this type of inhibitors. Clearly, such GTP analogues themselves are not good lead compounds, since the high affinity for Ras and the high concentration of GTP in the cells makes this approach unfeasible. Nevertheless, the search for small compounds homing in Ras active site and carrying chemical groups as indicated by the GAP and DABP-GTP studies, makes this approach a valid one[55].

55. Ahmadian, M. R.; Zor, T.; Vogt, D.; Kabsch, W.; Selinger, Z.; Wittinghofer, A.; Scheffzek, K., Guanosine triphosphatase stimulation of oncogenic Ras mutants. *Proceedings of the National Academy of Sciences of the United States of America* **1999,** *96* (12), 7065-7070.

2.2 Nucleotide exchange inhibition: a new class of Ras inhibitors

The GDP/GTP nucleotide exchange is a key activation step regulating Ras function. For this reason, it can represent a valid target for the development of new anti-tumour drugs.

Few years ago, the Schering-Plough Research Institute laboratories, obtained a small library of compounds able to bind Ras and interfere with protein activation, preventing nucleotide exchange. These molecules have a common structural base, as show in Scheme 2.5, and differ for the substituent group R on the sulphonamidic nitrogen.

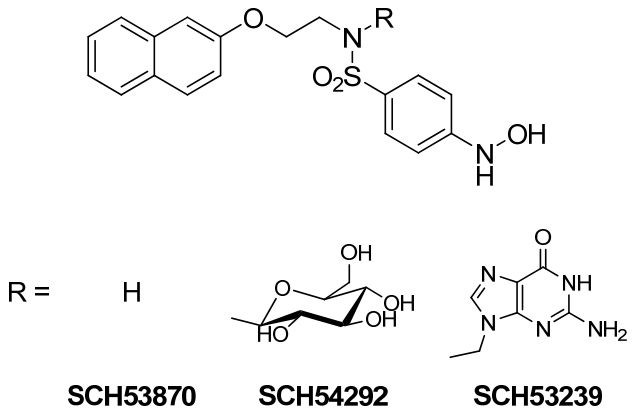

Scheme 2.5: Structure of Schering-Plough inhibitors.

Originally these molecules were designed to compete with GDP for the binding to the nucleotide binding site. Indeed, they present an IC_{50} value of 0.5 μM (SCH53870 and SCH53239) and of 0.7 μM (SCH54292) in nucleotide exchange *in vitro* assay on Ras, but do not compete with GDP[56].

56. Taveras, A. G.; Remiszewski, S. W.; et al., Ras oncoprotein inhibitors: the discovery of potent, ras nucleotide exchange inhibitors and the structural determination of a drug-protein complex. *Bioorganic & medicinal chemistry* **1997,** *5* (1), 125-33.

In order to clarify the nature of the interaction between such compounds and the Ras-GDP complex, NMR and mass spectrometry analysis, in addition to computation calculations, were performed. Electron Spray Ionization (ESI) mass analysis showed, in the case of SCH53870 and SCH54292, a peak corresponding to the mass of ternary complex Ras-GDP-inhibitor, without the presence of the mass of the dimeric species Ras-inhibitor. These results confirmed the 1:1 stoichiometry of complex (Ras-GDP:Inhibitor) and the non-covalent nature of the bond. A further investigation about the binding site of these compounds was made by carrying out covalent modifications of the protein followed by LC-ESI MS peptide mapping. Under appropriate conditions, succinic anhydride reacts specifically with the amino groups of exposed lysine residues on the surface of a protein. It is reasonable that Lys involved in inhibitor binding, or being adjacent to the binding site, may be sterically hindered by the bound drug and thereby protected from succinylation. According to this procedure, mass analysis of peptide fragments obtained after enzymatic digestion showed that SCH53870 and SCH54292 bind Ras close to Lys101, localized next to Switch II region. The inhibitors binding site is therefore distinguishes from the nucleotide binding site[57]. The binding site investigation has been deepened with the aid of NMR spectroscopy, in particular with two-dimensional NOESY and ^{1}H-^{15}N HSQC experiments. It was verified that Ras protein can exist in two alternative conformations in slow exchange respect to the NMR time scale, when Mg^{2+} ion concentration is low. These conformation changes involve residues in the GDP binding pocket, in the Switch I and Switch II regions. The protein open conformation seems to facilitate fast GDP exchange and enhance inhibitor binding. Two dimensional NOESY and ^{1}H-^{15}N HSQC analysis of Ras-GDP-SCH54292 complex, in addition with a computational analysis, using the Monte Carlo method, provided a model of these interactions (Figure 2.1). According to this model, the binding site of SCH54292 is in the vicinity of the critical switch II region, which, like Switch I region, changes conformation depending on the nature

57. Ganguly, A. K.; Pramanik, B. N.; Huang, E. C.; Liberles, S.; Heimark, L.; Liu, Y. H.; Tsarbopoulos, A.; Doll, R. J.; Taveras, A. G.; Remiszewski, S.; Snow, M. E.; Wang, Y. S.; Vibulbhan, B.; Cesarz, D.; Brown, J. E.; del Rosario, J.; James, L.; Kirschmeier, P.; Girijavallabhan, V., Detection and structural characterization of ras oncoprotein-inhibitors complexes by electrospray mass spectrometry. *Bioorganic & medicinal chemistry* **1997,** *5* (5), 817-820.

of the bound nucleotide. This structure places the naphthyl group of SCH54292 in a hydrophobic pocket formed by Met72, Gln99, Ile100 and Val103 of the protein. The phenyl group is in the proximity of Gln61, Gly60, Tyr96 and Lys16, and the hydroxylamine moiety extends into a pocket near the Mg^{2+}, probably coordinating the ion and phosphate groups of GDP, whereas the sugar moiety point out of the binding pocket and is not involved in significant interaction with the protein[58].

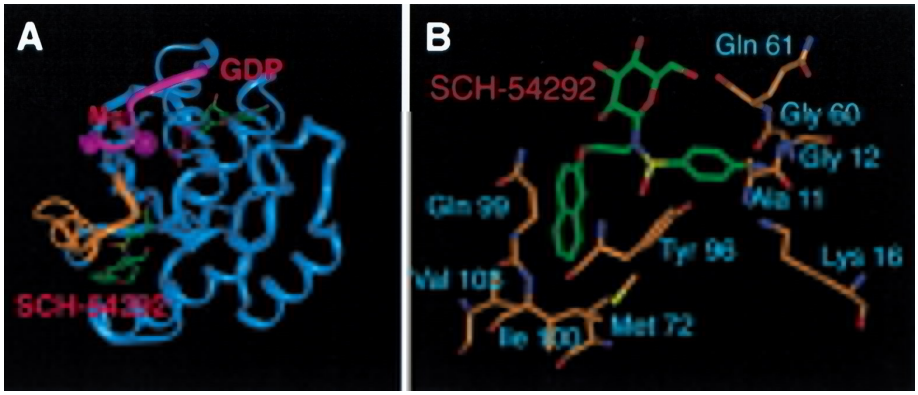

Figure 2.1: Interaction of SCH54292 with the complex Ras-GDP. (A) Structure of ternary complex constituited by Ras (blue), GDP (green and purple) , SCH54292(green) and magnesium (purple). Switch I is represented in magenta, Switch II in orange. (B) Detail of interaction between SCH54292 (green) and Ras protein (brown).

In this context, the group of Prof. Peri is involved for several years in the research of molecules capable of interfering with Ras signalling, through the inhibition of the protein nucleotide exchange. In particular, a library of synthetic compounds was projected and synthesized in order to clarify the structure-activity relationship of this family of inhibitors. These compounds share common pharmacophoric groups, a phenylhydroxylamine moiety and one or two aromatic groups, that are believed to be responsible for their biological activity. In the first generation of molecules, these structural elements were supported on a linear spacer, resulting in a structure very

58. Ganguly, A. K.; Wang, Y. S.; Pramanik, B. N.; Doll, R. J.; Snow, M. E.; Taveras, A. G.; Remiszewski, S.; Cesarz, D.; Del Rosario, J.; Vibulbhan, B., Interaction of a novel GDP exchange inhibitor with the Ras protein. *Biochemistry* **1998,** *37* (45), 15631-15637.

similar to Schering-Plough compounds[59]. In the second generation of compounds, the pharmacophoric groups were supported on a bicyclic scaffold derived from the natural monosaccharide D-arabinose.

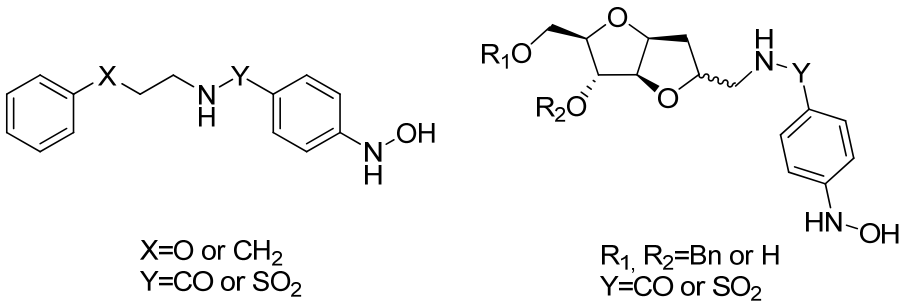

Scheme 2.6 : Structure of linear and bicyclic nucleotide exchange inhibitors.

These compounds presented the ability to inhibit the GEF-mediated nucleotide exchange on $p21^{H\text{-}Ras}$ in *in vitro* biochemical assay with a potency in the micromolar range. The same molecules also inhibited growth and proliferation of K-Ras transformed NIH3T3 mammalian cells[60]. Further investigations about the interaction of these compounds and Ras have been provided by NMR experiments and computational studies. NMR binding studies (STD and trNOE experiments[61]) showed that both the phenylhydroxylamine and the *O*-benzyl moiety directly interact with Ras and these interaction seems to be the driving force of the binding. On the contrary, the protons on the bicyclic scaffold do not interact directly with the protein. The observation that compounds lacking both the *O*-benzyl groups are totally inactive, supported the hypothesis that the phenylhydroxylamino group must be accompanied by another aromatic moiety to have binding and biological activity. According to our computation studies, these compounds seem to bind Ras in the

59. Colombo, S.; Peri, F.; Tisi, R.; Nicotra, F.; Martegani, E. In *Design and characterization of a new class of inhibitors of Ras activation*, Diederich, M., Ed. New York Acad Sciences: 2004; pp 52-61.

60. Peri, F.; Airoldi, C.; Colombo, S.; Martegani, E.; van Neuren, A. S.; Stein, M.; Marinzi, C.; Nicotra, F., Design, synthesis and biological evaluation of sugar-derived Ras inhibitors. *Chembiochem* **2005,** *6* (10), 1839-1848.

61. Bernd Meyer; Thomas Peters, NMR Spectroscopy Techniques for Screening and Identifying Ligand Binding to Protein Receptors. *Angewandte Chemie International Edition* **2003,** *42* (8), 864-890.

same pocket previously identified by the Schering-Plough researchers, located close to the Switch II region (Figure 2.2). In particular, a benzyl moiety is placed in a hydrophobic cavity of Ras and interacts with residue Val9, Met72, Gln99 and Ile100, whereas the phenylhydroxylamine group interacts with Mg^{2+} ion and with Thr58 residue[62].

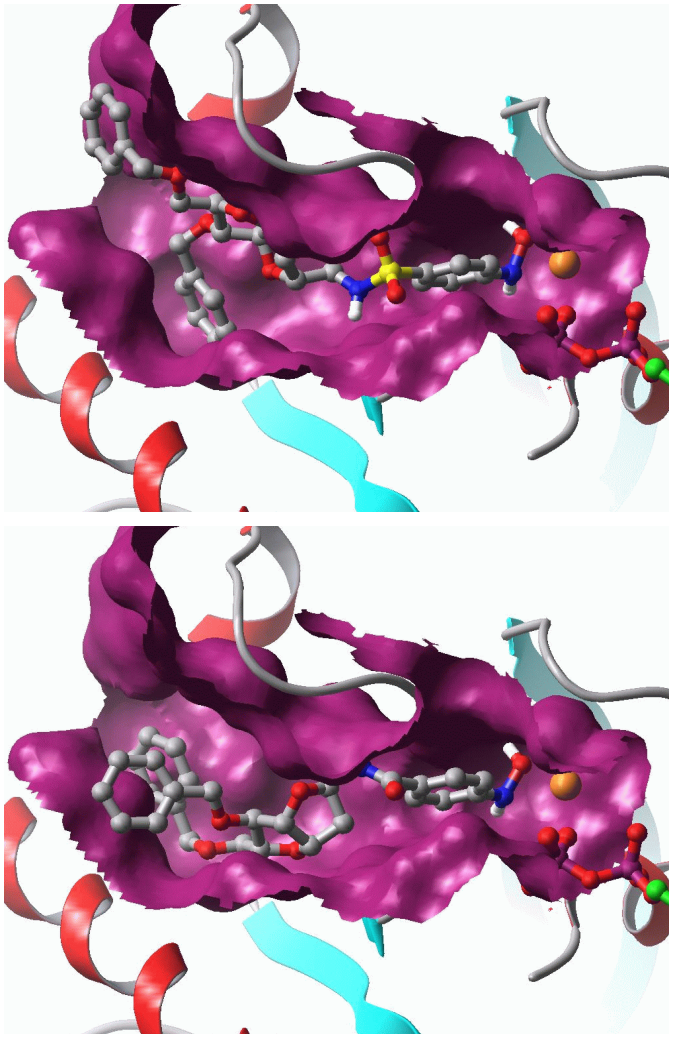

Figure 2.2: Docking of bicyclic compounds into the binding cavity of Ras.

62. Peri, F.; Airoldi, C.; Colombo, S.; Mari, S.; Jimenez-Barbero, J.; Martegani, E.; Nicotra, F., Sugar-derived Ras inhibitors: Group epitope mapping by NMR spectroscopy and biological evaluation. *Eur J Org Chem* **2006,** (16), 3707-3720.

In addition, two compounds based on scaffold derived from monosaccharide D-glucose have been presented (Scheme 2.7). The design of these compounds was guided by the necessity to increase the water solubility of such inhibitors. They bear a thiophenyl groups on the C1 position and the phenylhydroxylamine group on the position C6 of the unprotected glucose.

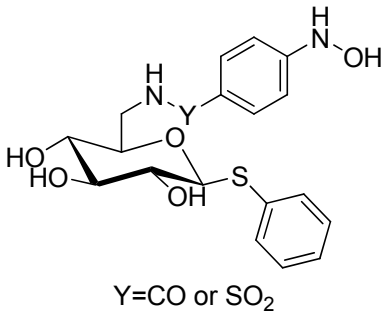

Scheme 2.7: Structure of glucose-derived nucleotide exchange inhibitors.

Interesting, both glucose and arabinose-derived compounds, interfered with the interaction of GEF molecules with Ras, as shown in Surface Plasmon Resonance (SPR) studies. These data reinforced the hypothesis that these inhibitors bind to a site close to Switch II region[63].

However, despite these promising results, all Ras inhibitors described present some important drawback. First, they had a very poor solubility in aqueous medium, essential propriety for drug-development and to further study their inhibition mechanism. Moreover they were unstable in any organic solvent as well as in water/DMSO mixtures at room temperature, according to the oxidative degradation of hydroxylamine to the corresponding nitroso and azooxy derivatives described in literature[64,65]

63. Airoldi, C.; Palmioli, A.; D'Urzo, A.; Colombo, S.; Vanoni, M.; Martegani, E.; Peri, F., Glucose-derived Ras pathway inhibitors: Evidence of Ras-ligand binding and Ras-GEF (Cdc25) 14 interaction inhibition. *Chembiochem* **2007,** *8* (12), 1376-1379.

64. Kazanis, S.; McClelland, R. A., Electrophilic intermediate in the reaction of glutathione and nitroso arenes. *Journal of the American Chemical Society* **2002,** *114* (8), 3052-3059.

65. Wang, C. Y.; Zheng, D.; Hughes, J. B., Stability of hydroxylamino-and amino-intermediates from reduction of 2, 4, 6-trinitrotoluene, 2, 4-dinitrotoluene, and 2, 6-dinitrotoluene. *Biotechnology Letters* **2000,** *22* (1), 15-19.

3. Carbohydrates as a tool for the development of new drugs

The challenge of drug discovery process is to design and synthesize molecules with high affinity and specificity for pharmacologically important targets. The major difficulty is to place pharmacophoric groups in just the right spatial arrangement to elicit the desired biological response. The process of drug design and development is based on the concept that bioactive molecules are composed of binding components, otherwise called pharmacophoric groups, which interact directly with the target and are responsible for the biological activity, and a non binding components, which orient pharmacophoric groups for binding thus acting as scaffold. The ideal scaffold may present a low molecular weight and a chemical stable nonbinding core with a number of functional groups with orthogonal reactivity. The core must be rigid to allow a controlled three-dimensional presentation of the pharmacophores. The spatial presentation of the functional groups has to be adjustable to generate the disposition required for tightest binding, and the resulting molecule will require reasonable biological stability. Additional functional groups are desirable to modulate pharmacokinetic (PK) parameters such as solubility and permeability.

Carbohydrates are a perfect tool in this context. In fact, they present a rigid core with a number of functional (hydroxyl or amino) groups in defined spatial orientations and they provide a series of scaffolds in which all possible isomers either occurs naturally or are available by the inversion of individual positions. For instance, looking at the simple hexapyranose in Figure 3.1, there are five possible substitution sites related to five stereocentres, each with two possible orientations (axial or equatorial). The possibilities of spatial presentation of substituent increase dramatically, by simple considering different substitution patterns.

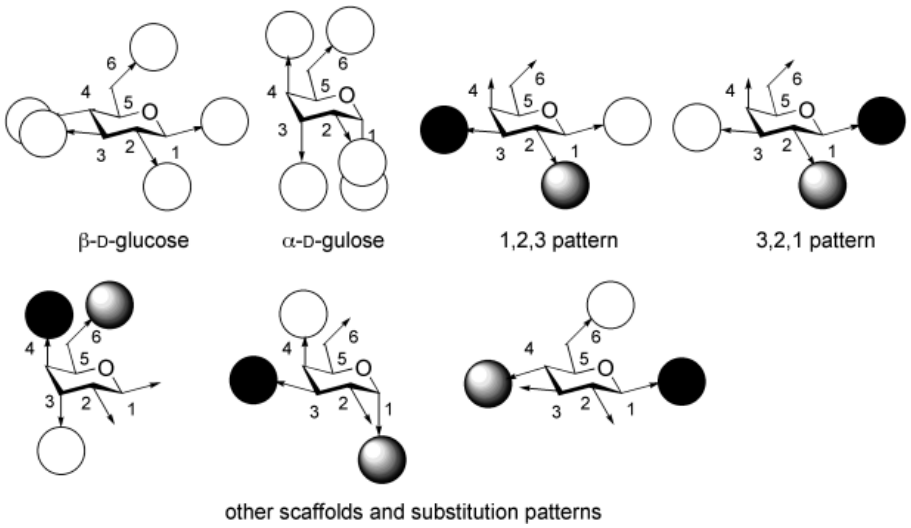

Figure 3.1: The various orientation on carbohydrate scaffold.

In addition, substituted carbohydrate derivatives are generally quite stable and the PK parameters are mostly dictated by the nature of the substituent presented. Finally, they are a relatively cheaper natural source of chemical materials[66, 67].
Several reports on the use of carbohydrates as scaffold are present in literature[68] and there are different carbohydrate-based drugs on the market or in different stages of development. An interesting and pioneer example of the use of monosaccharide as a scaffold for the synthesis of bioactive compounds is represented by the work of Hirschmann and co-workers that describe the synthesis of somatostatin mimics (Figure 3.2) derived from D-glucose[69].

66. Meutermans, W.; Le, G. T.; Becker, B., Carbohydrates as scaffolds in drug discovery. *Chemmedchem* **2006,** *1* (11), 1164-1194.

67. Peri, F.; Cipolla, L.; Forni, E.; Nicotra, F., Carbohydrate-based scaffolds for the generation of sortiments of bioactive compounds. *Monatshefte für Chemie/Chemical Monthly* **2002,** *133* (4), 369-382.

68. Gruner, S. A. W.; Locardi, E.; Lohof, E.; Kessler, H., Carbohydrate-Based Mimetics in Drug Design: Sugar Amino Acids and Carbohydrate Scaffoldsâ€ *Chemical Reviews* **2002,** *102* (2), 491-514.

69. Hirschmann, R.; Nicolaou, K. C.; Pietranico, S.; Salvino, J.; Leahy, E. M.; Sprengeler, P. A.; Furst, G.; Strader, C. D.; Smith, A. B., Nonpeptidal peptidomimetics with .beta.-D-glucose scaffolding. A partial somatostatin agonist bearing a close structural relationship to a potent, selective substance P antagonist. *Journal of the American Chemical Society* **2002,** *114* (23), 9217-9218.

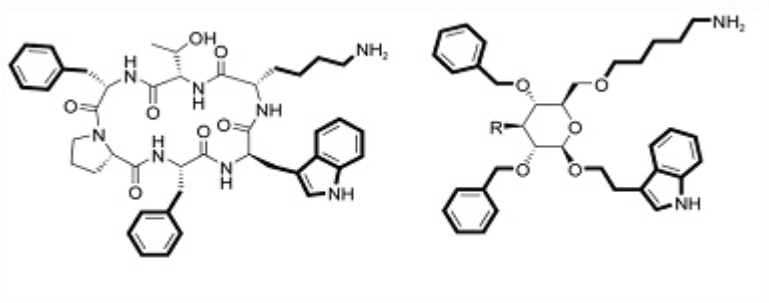

Figure 3.2: Pepidomimetic and carbohydrate-based mimic of somatostatin. In bold are highlight the pharmacophoric groups.

The conformational rigidity of natural carbohydrates can be also increased by chemical modifications, in order to obtain better scaffolding qualities. One possible way to reduce molecular flexibility is the introduction of a second and even a third ring to the sugar backbone. Several polycyclic scaffold have been developed by Prof. Nicotra and co-workers, using an original strategy based on a iodocyclization procedure. Starting from a polybenzylated sugars with an anomeric appendage with a C=C double bond, a cyclic iodoether was obtained by treatment with iodine. The mechanism of this iodocyclization consists in the attack of the intermediate iodinium ion by the benzyloxy group in γ-position, respect to the double bond, with loss of the benzyl group (Scheme 3.1).

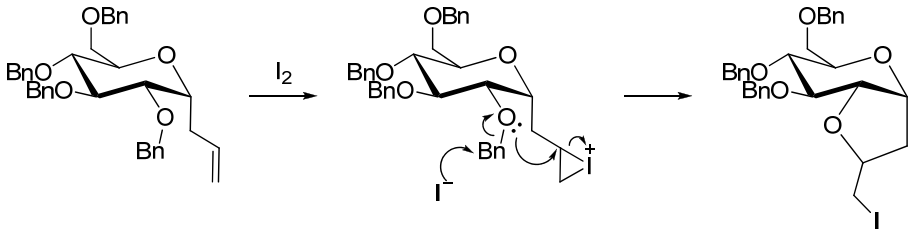

Scheme 3.1: Mechanism of iodocyclization.

With this simple procedure, several original bicyclic and tricyclic carbohydrate-based scaffolds (Scheme 3.2), with conformationally constrained structures, have

been developed from different natural monosaccharide, such as glucose, arabinose and fructose[70, 71].

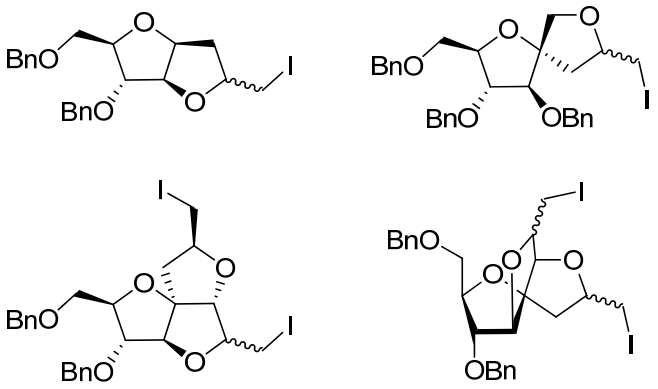

Scheme 3.2: Some original polycyclic carbohydrate-based scaffold.

An application of these studies is represented by a sugar-derived amino acid obtained by the iodocyclization of D-arabinofuranose. The obtained bicyclic structure is conformationally constrained and has been incorporated in a cyclic RGD peptide as β-turn mimetic[72].

3.1 "Glycorandomization" in drug discovery

The employment of sugar moieties in drug development is not limited to a passive role as scaffold supporting pharmacophore groups, but they can also actively influence pharmacology and pharmacokinetic properties. In fact, sugars appended to

70. Velter, I.; La Ferla, B.; Nicotra, F., Carbohydrate-Based Molecular Scaffolding. *Journal of Carbohydrate Chemistry* **2006,** *25* (2), 97-138.

71. Forni, E.; Cipolla, L.; Caneva, E.; La Ferla, B.; Peri, F.; Nicotra, F., Polycyclic scaffolds from fructose. *Tetrahedron Letters* **2002,** *43* (7), 1355-1357.

72. Peri, F.; Bassetti, R.; Caneva, E.; Gioia, L. d.; Ferla, B. L.; Presta, M.; Tanghetti, E.; Nicotra, F., Arabinose-derived bicyclic amino acids: synthesis, conformational analysis and construction of an alpha, beta 3-selective RGD peptide. *Journal of the Chemical Society, Perkin Transactions 1* **2002,** (5), 638-644.

natural pharmaceutically important products are known to influence drug solubility, target recognition, toxicity, and mechanism of action. Recently, Thorson and co-workers have published several papers describing the generation of "glycorandomized" libraries of bioactive natural compounds, which differ only in their glycosyl substituents, that, nevertheless, drastically alter their biological activity[73, 74, 75]. However, studies devoted to systematically understand and exploit the role of carbohydrates in drug discovery are often limited by the availability of practical synthetic tools. Two complementary strategies for rapid glycorandomization have been described: (1) the "chemoenzymatic glycorandomization", a biocatalytic approach that relies on the substrate promiscuity of enzymes to activate and attach sugars to natural products, and (2) the "neoglycorandomization", a chemical approach based on a one-step sugar ligation reaction[76].

3.1.1 Chemoenzymatic glycorandomization

Chemoenzymatic glycorandomization employs the intrinsic or engineered substrates promiscuity of anomeric kinases and nucleotidylyltransferase (Ntf) to provide nucleotide diphosphosugar (NDP sugar) donor libraries to inherently promiscuous natural products glycosyltrasferases (GlyT), thereby providing a rapid library of glycoconjugate compounds. A further chemical diversification can be provided by downstream chemoselective modifications. The main advantages of this approach are twofold. First, an efficient *in vitro* multienzyme, single vessel reaction is anticipated to simplify greatly glycorandomized library production in comparison to

73. Griffith, B. R.; Langenhan, J. M.; Thorson, J. S., `Sweetening' natural products via glycorandomization. *Current Opinion in Biotechnology* **2005,** *16* (6), 622-630.

74. Ahmed, A.; Peters, N. R.; Fitzgerald, M. K.; Watson, J. A.; Hoffmann, F. M.; Thorson, J. S., Colchicine Glycorandomization Influences Cytotoxicity and Mechanism of Action. *Journal of the American Chemical Society* **2006,** *128* (44), 14224-14225.

75. Griffith, B. R.; Krepel, C.; Fu, X.; Blanchard, S.; Ahmed, A.; Edmiston, C. E.; Thorson, J. S., Model for Antibiotic Optimization via Neoglycosylation: Synthesis of Liponeoglycopeptides Active against VRE. Ibid.**2007,** *129* (26), 8150-8155.

76. Langenhan, J. M.; Griffith, B. R.; Thorson, J. S., Neoglycorandomization and Chemoenzymatic Glycorandomization: Two Complementary Tools for Natural Product Diversification. *Journal of Natural Products* **2005,** *68* (11), 1696-1711.

traditional glycosylation strategies. Second, enzymatic processes are amenable to *in vivo* applications that should facilitate the process and significantly enhance the ability to scale production. An example of the utility of chemoenzymatic approaches to diversify complex natural product architectures has been reported for the production of a Vancomycin analogues library[77, 78].

3.1.2. Neoglycorandomization

The method of neoglycorandomization is based on the chemoselective formation of a neoglycosidic bond between a reducing sugar and a *N*,*O*-substituted hydroxylamine. In sharp contrast to traditional chemical glycosylation reactions, which rely upon tedious sugar donor protection and activation schemes, the neoglycosylation reaction utilizes unprotected and non-activated reducing sugars under mild aqueous conditions. Early examples of this chemoselective reaction revealed that, unlike primary alkoxyamines which provide open-chain oxime isomers, secondary alkoxyamines react to form closed-ring neoglycosides (Figure 3.3). Presumably, such secondary alkoxyamines react with reducing sugar to form an intermediate oxy-imminium species, which undergoes ring closure with O-5[79, 80].

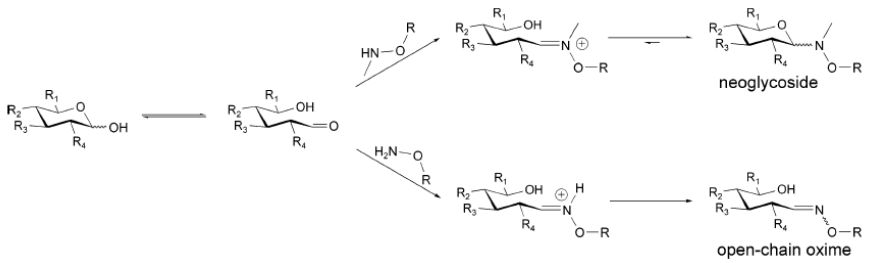

Figure 3.3: Reaction of primary and secondary alkoxyamines with reducing sugars.

77. Fu, X.; Albermann, C.; Zhang, C.; Thorson, J. S., Diversifying Vancomycin via Chemoenzymatic Strategies. *Organic Letters* **2005,** *7* (8), 1513-1515.

78. Thorson, J. S., *Glycorandomization and production of novel vancomycin analogs*. US Patent References 7259141: 2004.

79. Peri, F.; Dumy, P.; Mutter, M., Chemo- and stereoselective glycosylation of hydroxylamino derivatives: A versatile approach to glycoconjugates. *Tetrahedron* **1998,** *54* (40), 12269-12278.

80. Peri, F.; Nicotra, F., Chemoselective Ligation in Glycochemistry. *ChemInform* **2004,** *35* (27).

The stereochemistry of the neoglycoside product depends on the identity of the sugar, and an equilibration between the product isomers is sometimes observed. In the case of glucose and *N*-acetylglucosamine, the β-pyranose configuration is stereoselectively obtained. In the case of galctose derivatives a mixture of α + β (7:1) pyranosidic forms is observed, whereas for mannose derivatives a mixture of α + β pyranosidic and α + β furanosidic configuration is observed. The preference for the β-anomer in the case of glucose, galactose, and *N*-acetylglucosamine can be explained in terms of stabilization of the β conformation of the oxyiminium intermediate (Figure 3.3) through the reverse anomeric effect that is particularly relevant when a positively charged nitrogen atom is linked to the anomeric position[81].

In addition, very recently, it has been demonstrated that neoglycoconjugates are stable for many days in neutral aqueous condition. The hydrolysis rate increases in acidic condition and suggests that caution should be employed when using these conjugates below pH 6.0[82].

The neoglycosylation reaction is largely employed in the synthesis of neoglycopeptides, neooligosaccharides, and, obviously, in the development of neoglycorandomized libraries. The most representative example can be found in the synthesis of a large library of digitoxin derivatives, as a model platform to examine the general utilities of neoglycorandomization[83].

---

81. Peri, F.; Jiménez-Barbero, J.; García-Aparicio, V.; Tvaroscaronka, I.; Nicotra, F., Synthesis and Conformational Analysis of Novel N(OCH3)-linked Disaccharide Analogues. *Chemistry - A European Journal* **2004,** *10* (6), 1433-1444.

82. Gudmundsdottir, A. V.; Paul, C. E.; Nitz, M., Stability studies of hydrazide and hydroxylamine-based glycoconjugates in aqueous solution. *Carbohydrate Research* **2009,** *344* (3), 278-284.

83. Langenhan, J. M.; Peters, N. l. R.; Guzei, I. A.; Hoffmann, F. M.; Thorson, J. S., Enhancing the anticancer properties of cardiac glycosides by neoglycorandomization. *Proceedings of the National Academy of Sciences of the United States of America* **2005,** *102* (35), 12305-12310.

4. Results and discussion

4.1. Objective and strategy

The role of Ras proteins in oncogenesis is well established, therefore the inhibition of oncogenic variants of these proteins represents an interesting and promising research field for the development of new anticancer therapies. Several approaches have been explored to attend this issue. One of the most interesting strategy consists on interfere with the protein activation, that is a key event not only for the explication of the biological functions, but also for Ras-induced cell transformation.

The objective of this thesis has been the development of new molecules able to prevent the activation of Ras proteins, inhibiting the GEF-catalyzed nucleotide exchange.

Inspired by the work of the Schering-Plough researchers, that pioneered this class of inhibitors[56-58], our group is involved in this research area from few years and has developed several inhibitors able to inactivate Ras proteins. These molecules have in common two pharmacophoric groups represented by a phenylhydroxylamine group and by another aromatic moiety, and bind Ras in the proximity of Switch II region[59-62]. However, these molecules present chemical and metabolically instability and have poor solubility in water. Both these factors hamper a subsequent development of these lead compounds in drugs.

The design of new molecules was aimed to address two main point: first, to replace the phenylhydroxylamine group with safer and more stable group, second, to improve the water solubility.

In order to obtain new efficient inhibitors we adopted the rational drug designed strategy supported by NMR and computational docking studies. In addition, in order to modulate the solubility and the pharmacokinetic proprieties of our molecules, we synthesized new compounds in which the pharmacophoric groups are linked to a carbohydrate entity through a chemoselective glycosylation approach. Finally the biological activity and the nature of the interaction between such inhibitors and the human H-Ras proteins were deeply investigate, providing important information for a further development of anti-cancer drugs.

It is important to underline that, given the multidisciplinary approach of the project, this work comprises various activities among which chemical synthesis, computational studies, NMR binding experiments, biochemical assay, etc... The work described in this PhD thesis has therefore been developed in collaboration with other research groups.

4.2. Structure-activity relationship in Ras inhibitors

The aim of the first part of the work was to look for a pharmacophoric group able to substitute the phenyl hydroxylamine moiety. We synthesized a small panel of molecules (Scheme 4.1) showing a structure very similar to the Schering-Plough inhibitors, in which phenyl hydroxylamine group was replaced by another aromatic group. That moiety should be able to form hydrogen bond and polar interaction with Ras similarly to phenylhydroxylamine. The compound **1** was already prepared by our group and was used in this context as positive control of inhibition[59].

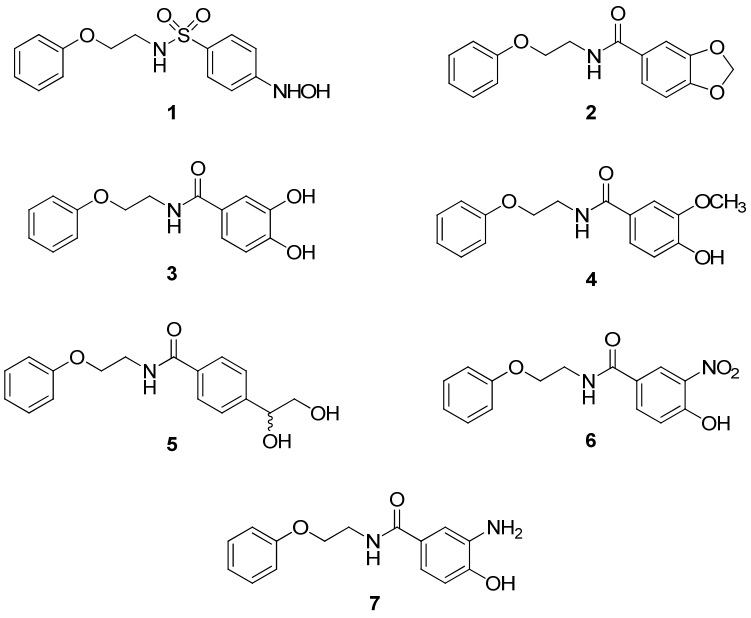

Scheme 4.1: Structure of molecules 1-7.

We investigated the structure-activity relationship in this panel of compounds by the analysis of their ability to prevent the guanine nucleotide exchange on purified p21 h-Ras and to inhibit the growth of the K-Ras mutated human colorectal cancer cells HCT-116.

4.2.1. Chemical synthesis

Compounds **1-7** were synthetically derived from the amine precursors **8** as show in Scheme 4.2.

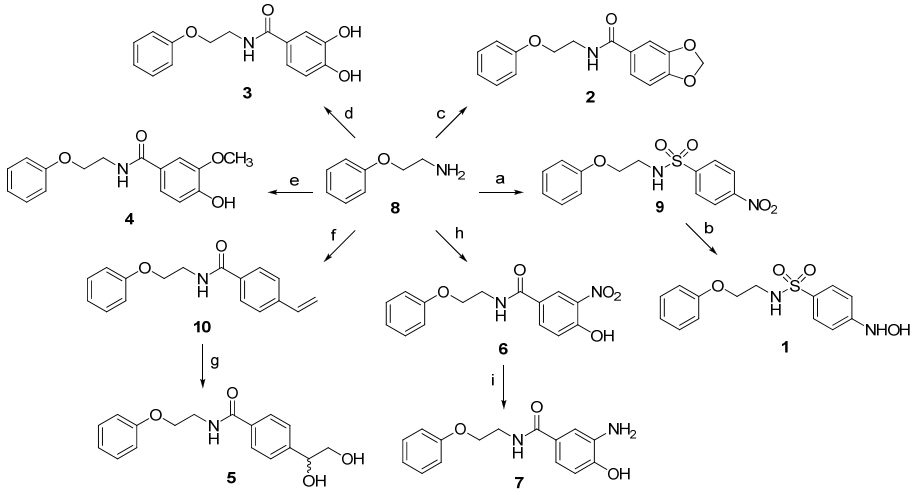

Scheme 4.2. Reagents and conditions: a) p-nitrobenzensulfonyl chloride, Et_3N, DMF, r.t., 3h, 82%; b) hydrazine hydrate, Pd/C, MeOH, THF, 0°C, 1h, 80%; c) 3,4-(Methylenedioxy)benzoic acid, HOBt, DIC, DIPEA, DMF, r.t., 3h, 50%; d) 3,4-dihydoxybenzoic acid, HOBt, DIC, DIPEA, DMF, r.t., overnight, 37%; e) 3-methoxy 4-hydroxybenzoic acid, HOBT, DIC, DIPEA, DMF, r.t., overnight, 63%; f) 4-vinyl benzoic acid, HOBt, DIC, DIPEA, DMF, r.t., overnight, 55%; g) OsO_4, 4-methylmorpholine *N*-oxide, MeCN, water, r.t., 2h, 81%; h) 3-nitro-4-hydroxy benzoic acid, HOBt, DIC, DIPEA, DMF, r.t., 3h, 45%; i) H_2, Pd/C, MeOH, r.t., 1h, 86%.

Treatment of 2-phenyloxy-ethylamine **8** with p-nitrobenzensulfonyl chloride in presence of triethylamine (Et_3N) in dimethylformamide (DMF) provided p-nitrosulfonamide **9**. The nitro group was reduced to hydroxylamine by treatment with hydrazine hydrate in presence of palladium over charcoal in methanol (MeOH) and tetrahydrofuran (THF) affording compound **1**. Condensation of amine **8** with 3,4-(methylenedioxy)benzoic acid, 3,4-dihydoxybenzoic acid and 3-methoxy-4-hydroxybenzoic acid in presence of *N*-hydroxybenzotriazole (HOBt), diisocarbodiimmide (DIC) and diisopropylamine (DIPEA) in DMF afforded respectively compounds **2**, **3** and **4**. Treatment of amine **8** with 4-vinyl benzoic acid in presence of HOBt, DIC and DIPEA in DMF provided compound **10**. The vinyl

moiety of **10** was oxidized to vicinal diol by using osmium tetroxide in presence of 4-methylmorpholine-*N*-oxide, affording compound **5**. Compound **6** was obtained by condensation of amine **8** with 3-nitro-4-hydroxybenzoic acid in presence of HOBt, DIC and DIPEA in DMF. Compound **7** was obtained by catalytic hydrogenation of nitro group of compound **6**.

4.2.2. Biological evaluation

4.2.2.1. Biochemical assays on nucleotide exchange inhibition

Molecules **1-7** were first tested for their ability to inhibit the C-Cdc25^{Mm}-stimulated nucleotide exchange on purified p21 h-Ras. For this purpose, a modified version of Lenzen's method was used[84]. The C-Cdc25^{Mm}-stimulated guanine nucleotide exchange was monitored using 2' (3')-*O*-(*N*-methylantraniloyl)-GTP (mant-GTP) as fluorescent non-hydrolysable analogous of GTP. p21 h-Ras was incubated with mant-GTP in presence and in absence of 100 μM of the compounds **1-7.** The exchange reaction starts when C-Cdc25^{Mm} is added. Molecule **1** was tested using as positive control and showed a strong inhibition of the exchange reaction (about 50 %), in agreement with preliminary data previously published[59]. Compounds **6** and **7** resulted to be completely, inactive, whereas compound **2-5** were able to inhibit the exchange reaction although with a reduced effect (about 10-25 %) respect of the reference compound **1** (Figure 4.1).

84. Lenzen, C.; Cool, R.; Wittinghofer, A., Analysis of intrinsic and CDC25-stimulated guanine nucleotide exchange of p21ras-nucleotide complexes by fluorescence measurements. *Methods in enzymology* **1995,** *255*, 95.

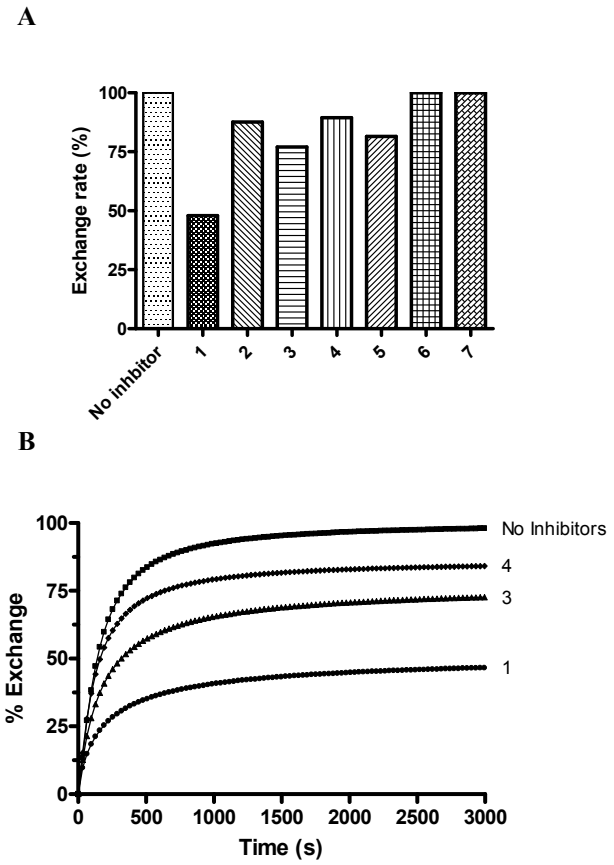

Figure 4.1: C-Cdc25-stimulated nucleotide exchange on p21-hRas. (A) Effect of compounds **1**-**7**. (B) Stimulated exchange reaction in presence of 100 μM of compound **1**, **3**, **4**.

4.2.2.2. *Ex vivo* experiments on human cancer cell viability.

We evaluated the action of compounds **1-7** on K-Ras mutated colorectal human cancer cells. The HCT-116 colorectal cancer cell line contains two alleles of the K-Ras gene, one of which is wild type (wt), while the other displays a heterozygous G38A single point mutation leading to an aminoacid change from Glycine to Aspartic acid (G13D). This results in constitutive activation of the corresponding encoded K-Ras protein. The cells were incubated with the compounds and then cell viability was measured, using an ATP-based assay. Compounds **1** and **3** showed a

relevant cell toxicity (viability < 20%) at the concentration of 100 μM as reported in Figure 4.2; at the same concentration, compound **4** presented a slight toxic effect (viability > 60%) was shown, whereas compound **2, 5, 6** and **7** were totally inactive.

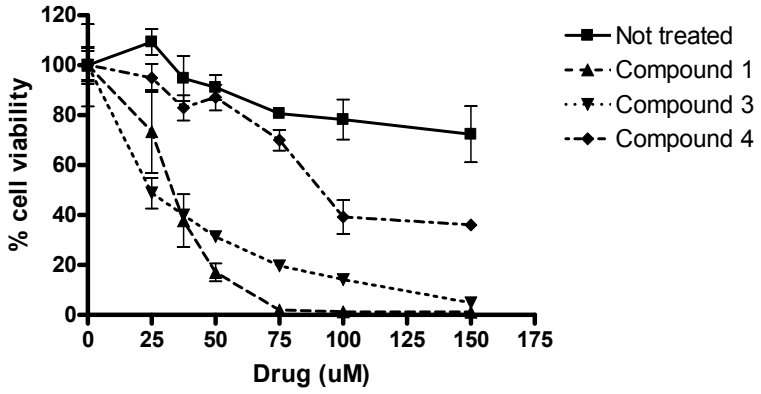

Figure 4.2: Effect of compounds 1, 3, and 4 on HCT-116 colorectal cancer cells. Results represent the average of at least three independent experiments, while error bars indicate standard error of the mean (SEM).

4.2.3. Discussion

Reference compound **1**, which presents a phenylhydroxylamine moiety, resulted able to inhibit nucleotide exchange reaction in biochemical assay and presented *ex vivo* cytotoxicity on human cancer cells. The biological activity was partially retained only in compound **3** where the phenylhydroxylamine moiety was replaced by a catechol group. A possible explanation is that catechol group is able to establish efficient interaction with Ras residues, as well as phenylhydroxylamine moiety. Compound **4** showed to be a weaker inhibitor probably because the presence of the O-methyl group disfavours the binding with Ras. The importance of these results dwells in the fact that they show that phenylhydroxylamine moiety can be replaced by a more stable catechol group in this class of Ras inhibitors. Moreover, the hydroxyl groups of the catechol moiety increase the solubility in water of these molecules.

4.3. Different scaffold – pharmacophore combination in Ras Inhibitors

The second step of this work was a structure-activity relationship study on a panel of nine compounds (Scheme 4.3) in which two pharmacophoric groups, catechol and methoxyphenol group, previously identified, and the well-known phenyl hydroxylamine group were supported on three different scaffolds: linear (ethylene amide), bicyclic (derived from D-arabinose) and cyclic pyranose (from D-glucose).

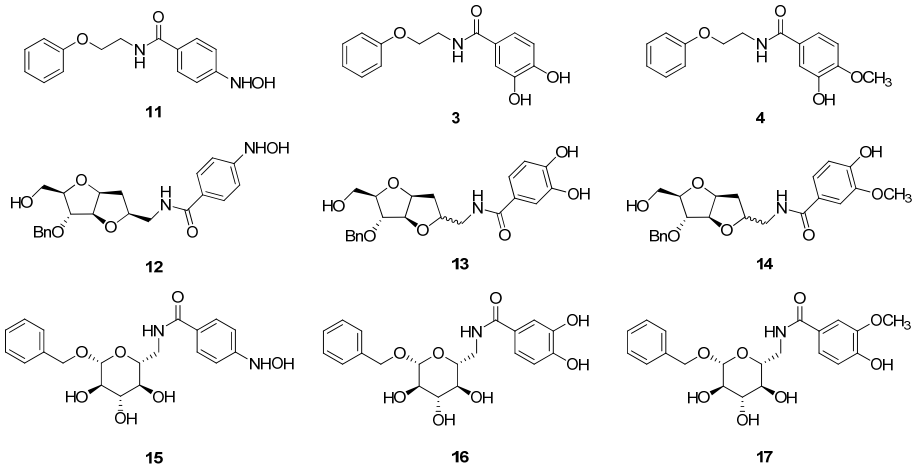

Scheme 4.3: Chemical structure of compounds 3-4 and 11-17.

The choice of the scaffolds was based on previous structure-activity studies showing that an arabinose-derived bicyclic scaffold and a cyclic thioglucoside were suitable for the generation of Ras ligands[61-62]. The phenyl hydroxylamine group was replaced by a catechol group (compounds **3**, **13** and **16)** or a methoxyphenol group (compounds **4, 14** and **17**) on the basis of previously studies that demonstrated that catechol proved as effective as toxic phenylhydroxylamine group in Ras inhibition [par. 4.2]. Our goal was the characterization of the role, and the relevance, of the

scaffold and of the pharmacophore groups in the modulation of the biological activity in Ras inhibitors[85].

4.3.1. Docking calculation

The rational design of the new molecules was leaded by previous structure-activity data and a novel detailed docking analysis, carried out using Autodock 4.0 software[86]. The binding energies for the best poses obtained by docking calculations are reported in Table 4.1. Molecules **11**, **3** and **4**, presenting a linear scaffold, and compounds **15**, **16** and **17**, showing a glucopyranose core, are characterized by similar binding energies, irrespective of the presence of phenyl hydroxylamine or catechol moieties, whereas compounds **12**, **13** and **14**, featuring the arabinose-derived scaffold, are characterized by significantly more favourable binding energies. Docking analysis also clearly showed that the stereoisomer with C-2 (S) configuration in the arabinose-derived bicyclic scaffold has a more favourable binding constant that the corresponding (R) isomer.

Ligand	11	3	4	12	13(S)	13(R)	14	15	16	17
Binding Energy (kcal/mol)	-6.00	-6.27	-6.44	-8.19	-7.95	-6.39	-7.47	-6.05	-6.59	-6.18

Table 4.1: Computed binding energy of putative inhibitors.

A detailed description of the binding contacts between putative inhibitors and Ras has been also established. High-scoring poses obtained by docking calculations correspond to structures in which the ligands bind the protein in a cleft in the vicinity of the Switch II region, in good agreement with previous data[60]. For all compounds, it is evident that the interaction of the two aromatic groups is the

85. Palmioli, A.; Sacco, E.; Airoldi, C.; Di Nicolantonio, F.; D'Urzo, A.; Shirasawa, S.; Sasazuki, T.; Di Domizio, A.; De Gioia, L.; Martegani, E.; Bardelli, A.; Peri, F.; Vanoni, M., Selective cytotoxicity of a bicyclic Ras inhibitor in cancer cells expressing K-RasG13D. *Biochemical and Biophysical Research Communications* **2009,** *386* (4), 593-597.

86. Morris, G.; Goodsell, D.; Halliday, R.; Huey, R.; Hart, W.; Belew, R.; Olson, A., Automated docking using a Lamarckian genetic algorithm and an empirical binding free energy function. *Journal of Computational Chemistry* **1998,** *19* (14), 1639-1662.

driving force for Ras binding. In particular, the phenyl hydroxylamine and the catechol groups are involved in hydrophobic interactions with the aromatic ring of Tyr96, and form hydrogen bonds with the hydroxyl group of Tyr96 and some amino acids of the Switch II region, such as Gly60, Gln61 and Glu62. Generally, the benzyloxy and phenyloxy groups are involved in a higher number of binding interactions than phenylhydroxylamine or catechol groups. In Figure 4.3 the structure of complex and the detailed map of the contact between compound **11** and RasGDP are reported.

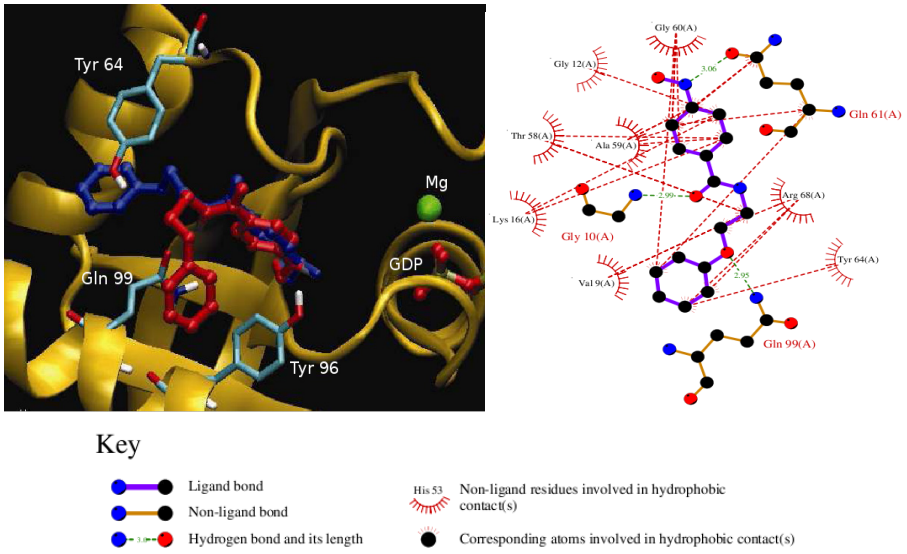

Figure 4.3: Structure of highest-ranking complexes between compound 11 and Ras-GDP. The best poses can be divided in two main families characterized by different orientations of the phenyloxy or benzyloxy groups. In the first one (blue colour) these groups strongly interacts with Tyr64, whereas in the second set of structures (red colour) they have hydrophobic contacts with Tyr96.

4.3.2. Chemical synthesis

Compounds **11, 3** and **4** were synthesized as shown in the Scheme 4.4:

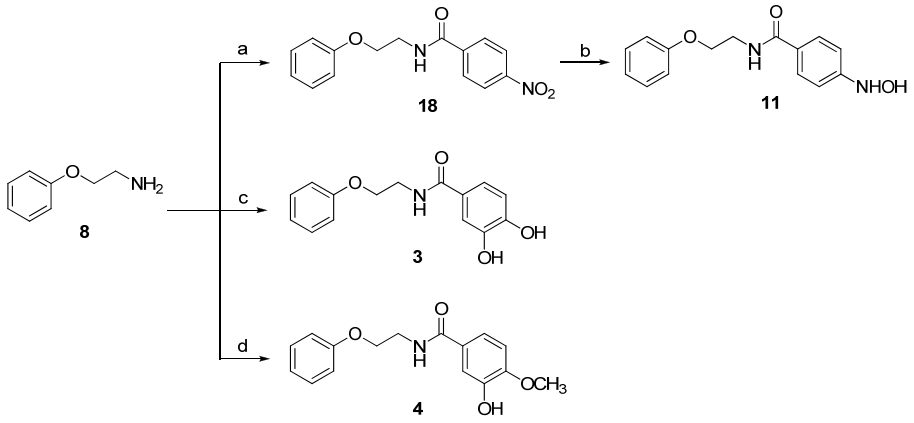

Scheme 4.4. Reagent and conditions: a) 4-nitrobenzoic acid, HOBt, DIC, DIPEA, DMF, overnight, r.t., 89%; b) hydrazine hydrate, Pd/C, THF, MeOH, 1 hour, 0°C, 90%; c) 3,4-dihydoxybenzoic acid, HOBt, DIC, DIPEA, DMF, overnight, r.t., 15%; d) 3-methoxy 4-hydroxybenzoic acid, HOBT, DIC, DIPEA, DMF, overnight, r.t., 63%.

2-Phenyloxy-(ethyl) amine **8**[59] was reacted with 4-nitrobenzoic acid in presence of DIC, HOBt and DIPEA in DMF to give compound **18**, whose nitro group was partially reduced in presence of hydrazine hydrate and Pd/C to give compound **11**. Compound **3** and **4** were synthesized as previously described in paragraph 4.2.1.

Compound **13** and **14** were synthesized as shown in the Scheme 4.5:

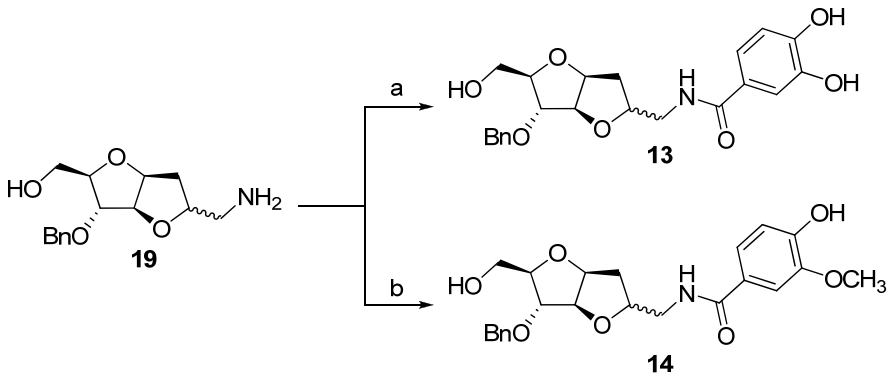

Scheme 4.5: Reagent and conditions: a) 3,4-dihydoxybenzoic acid, HOBt, DIC, DIPEA, DMF, overnight, r.t., 30%; b) 3-methoxy-4-hydroxybenzoic acid, HOBT, DIC, DIPEA, DMF, overnight, r.t., 57%.

Compound **12** and bicyclic arabinose-derived scaffold amine **19** were synthesized according to procedure previously reported[61]. Compounds **13** and **14** were obtained by condensation of amine **19** with 3,4-dihydroxy benzoic acid and with 3-methoxy-4-hydroxy benzoic acid according to condensation conditions described above. Compound **13** and **14** were obtained as mixture of diastereoisomers at C-2 (ratio R/S 3:1) that were not possible to separate by flash chromatography.

Compounds **15, 16** and **17** were prepared starting from natural ***D*-glucose** following the synthetic pathway reported in Scheme 4.6:

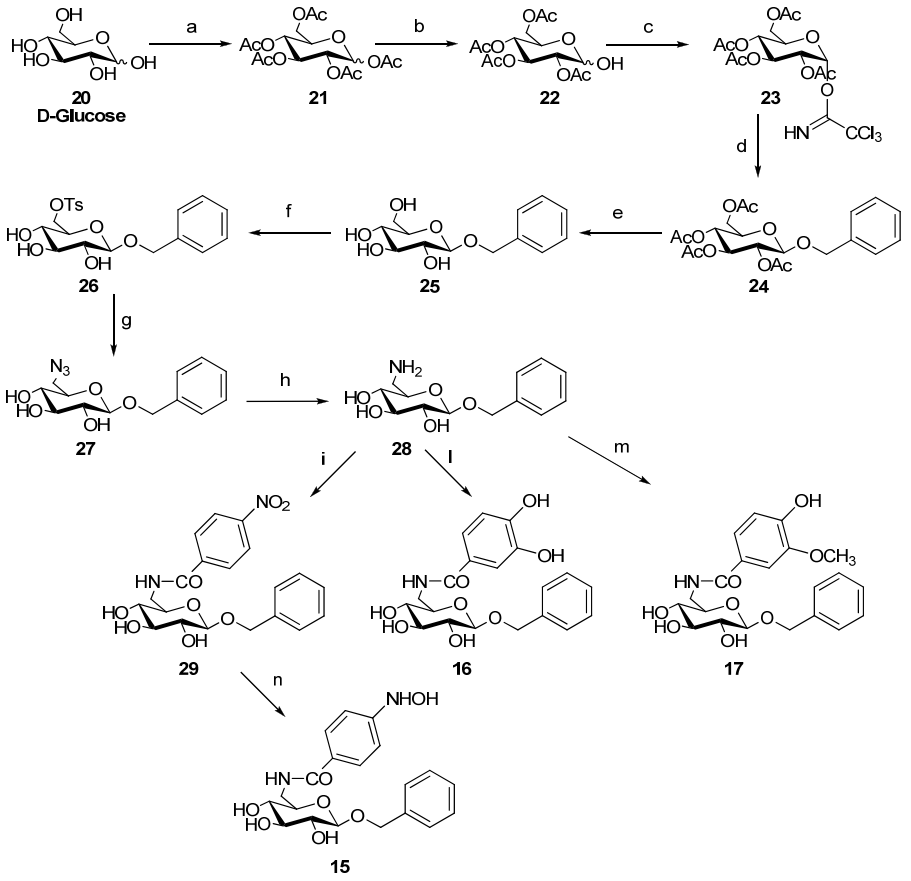

Scheme 4.6. Reagents and conditions: a) Ac_2O, DMAP, Py, r.t., 2 h, quant. yield; b) $AcONH_3NH_2$, DMF, r.t., 1 h, 80%; c) Cl_3CCN, DBU, CH_2Cl_2, r.t., 1h 30 min; d) $PhCH_2OH$, TMSOTf, CH_2Cl_2, 0 °C, 3 h, 80%; e) NaOMe, MeOH, r.t., 2 h, quant. yield; f) tosyl chloride, Py, r.t., 5 h ,63%; g) NaN_3, TBAI, DMF, 60 °C, 24 h, 98%; h) Ph_3P, H_2O, THF, 60 °C, 3 h, 96%; i) p-nitrobenzoic acid, DIC, HOBt, DIPEA, DMF, r.t., 24 h, 78%; l) 3,4-dihydroxybenzoic acid, DIC, HOBt, DIPEA, DMF, r.t., 24 h, 25%; m) 3-methoxy 4-hydroxy benzoic acid, DIC, HOBt, DIPEA, DMF, r.t., 24 h, 64%; n) NH_2NH_2, Pd/C, THF, 0 °C, 2h, 88%.

The selective activation of tetraacetylglucose **22** anomeric position as trichloroacetimidate derivative **23**, followed by treatment with benzyl alcohol in presence of trimethylsilyl trifluoromethanesulphonate (TMSOTf), gave compound

24 as product of glycosylation reaction. Treatment of compound **24** with sodium methoxide yielded the benzyl-β-D-glucopyranoside **25.** Primary hydroxyl group on position C6 was selectively activated to nucleophilic substitution by tosylation, yielding compound **26**. Nucleophilic displacement of tosyl group with ammonium azide afforded compound **27**, which was converted into the corresponding ammine **28** by hydrolysis. Treatment of amine **28** with 3,4-dihydroxy benzoic acid, 3-methoxy 4-hydroxy benzoic acid and 4-nitro benzoic acid in presence of DIC, HOBt and DIPEA in DMF gave respectively the compound **16**, 1**7** and **29.** Compound **15** was then obtained by partial reduction of the nitro group of **29** in presence of hydrazine hydrate and Pd/C.

4.3.3. NMR binding studies

The ability of compounds **11-17** and **3-4** to binding human $p21^{h\text{-}Ras}$ was tested by solution NMR experiments. Saturation-Transfer Difference (STD) and transfer-Nuclear Overhauser Effect SpectrometrY (trNOESY) experiments are very helpful tools in order to detect ligand binding to receptors[61]. Moreover, STD data allow identifying which region of the ligand directly interacts to the protein target (binding epitope mapping)[87]. STD spectra recorded on compounds **3-4** and **11-17** are reported in Figure 4.4 and the resulting epitope mapping with an estimation of STD intensity is reported in Figure 4.5.

87. Mayer, M.; Meyer, B., Group Epitope Mapping by Saturation Transfer Difference NMR To Identify Segments of a Ligand in Direct Contact with a Protein Receptor. *Journal of the American Chemical Society* **2001,** *123* (25), 6108-6117.

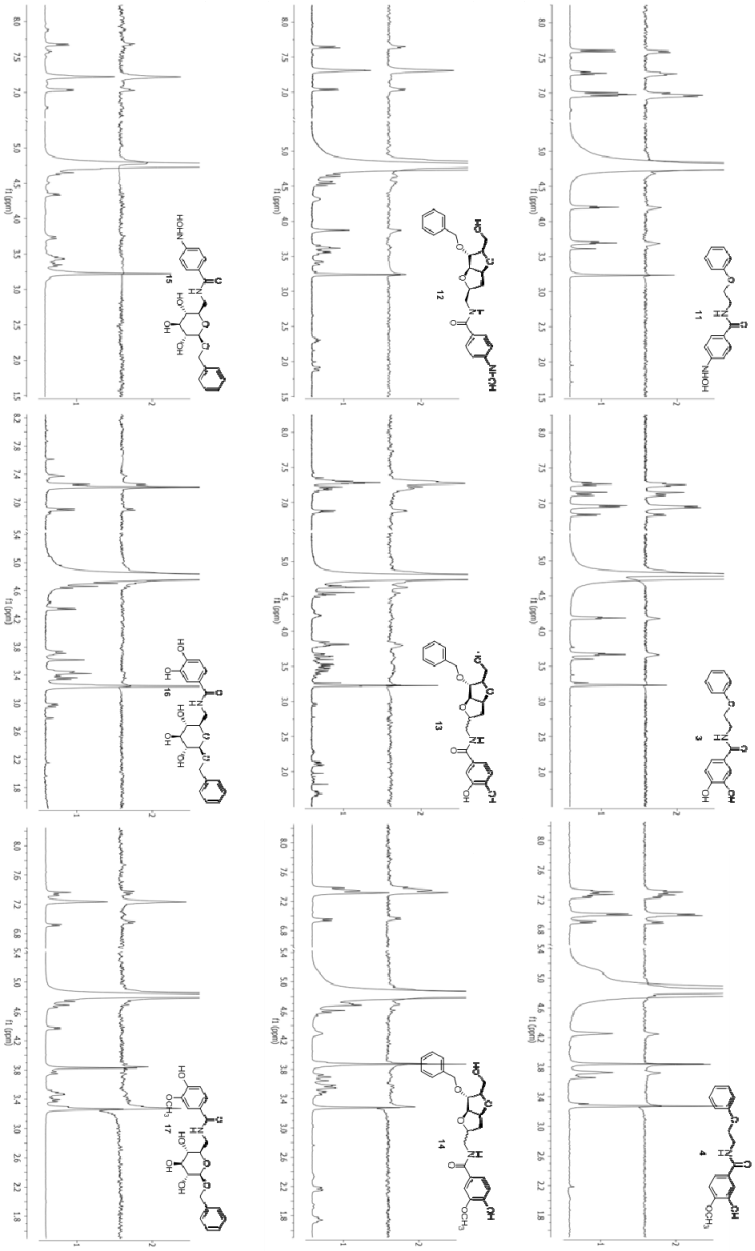

Figure 4.4: ^{1}H NMR (lower trace), **and STD spectra** (upper trace) **of 3-4 and 11-17 with Ras-GDP complex.** Ligand/protein ratio 30:1, number of scans (ns) =1360, on-resonance frequency=0.0 ppm, off-resonance frequency=40 ppm, total saturation time=2 s, T_2 filter=1.5 ms. Spectra were recorded on the same sample, dissolved in a d_{11}–Tris buffer (pH 7.3, containing CD_3OD (9%), NaCl (100 mM), $MgCl_2$ (5 mM) and GDP (10 µM)). Total sample volume 550 µL.

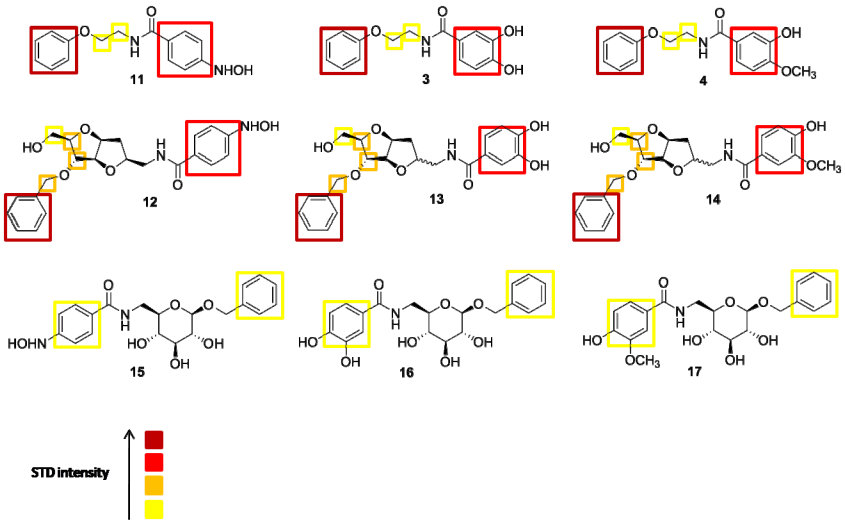

Figure 4.5: STD intensities and mapping of the groups interacting with Ras-GDP in compounds 3-4 and 11-17.

A semi-quantitative analysis based on STD signal intensities at different saturation times indicates that in all molecules the aromatic groups have strong interaction with Ras-GDP, according to what observed by docking analysis. Interestingly, and still in agreement with docking analysis, the phenyloxy or benzyloxy groups of compounds **11-17** seem to interact stronger with protein then the phenylhydroxylamine, the catechol or the methoxyphenol group. The substitution of the phenylhydroxylamine with the catechol or the methoxyphenol does not affect the binding significantly; on the other hand, scaffold nature seems to affect considerably the binding affinity. Compounds **3-4** and **11-14** gave rise to STD spectra with very good signal/noise ratios for all protein saturation times (with the only exception of sat. time = 0.3 s), while STD signal intensities were poorer for molecules **15-17**. In addition, a deeper inspection of STD spectra reveals the selective saturation of the ethylene linker protons in **11**, **3** and **4**, weak signals of the protons on C-4 and C-5 of the bicyclic core appear in spectra of **12-14**, while no signal corresponding to glucose scaffold of **15-17** are detected. In trNOESY experiments, evidences of binding were obtained only for compounds **11-14** and **3-4** that changed the sign and type of cross-peaks upon addition of Ras. Conversely, compounds **15-17** did not show any trNOESY signal, confirming that glucose-derived compounds bind Ras much weaker.

In Figure 4.6 is reported the 2DNOESY spectrum of compound **3** alone and the trNOESY spectrum of the complex of compound **3** with Ras-GDP.

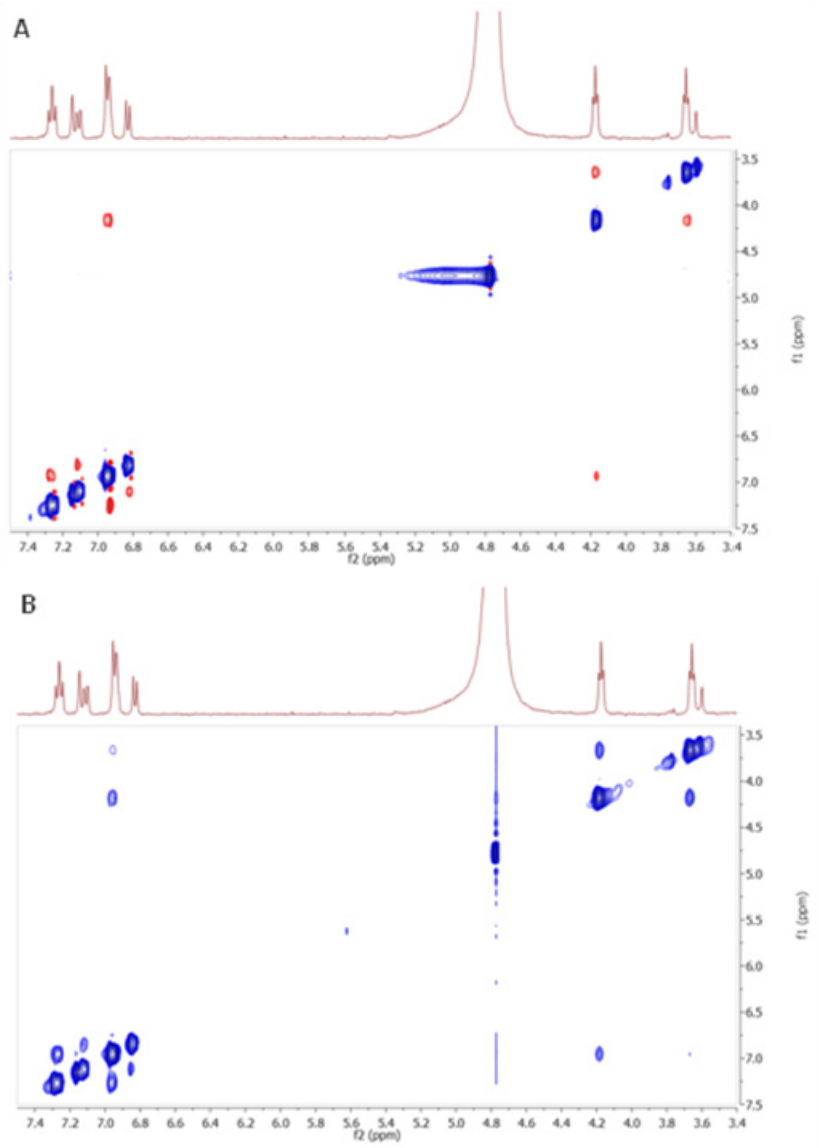

Figure 4.6: 2DNOESY spectrum of 3 (A)**, and trNOESY spectrum of 3 with Ras-GDP complex** (B)**:** ligand/protein ratio 30:1, number of scans in f2=64, number of increments in f1=128. Each sample was dissolved in a d_{11}–Tris buffer (pH 7.3, CD_3OD (9%), NaCl (100 mM), $MgCl_2$ (5 mM), GDP (10 μM)). Total sample volume was 550 mL.

4.3.4. Biological evaluation

4.3.4.1. Biochemical assays on nucleotide exchange

In order to correlate the binding data with the biochemical activities, the inhibitory effect of compounds containing the catechol group (**3**, **13** and **16**) or the hydroxylamine group (**11**, **12** and **15**) on the GEF-stimulated exchange of Ras-bound GDP was tested. In this case, the catalytic domain of Ras-specific GEF RasGrf1 was used to promote the exchange of bound GDP for mant-GDP, as described by Lenzen and coworkers[84]. The initial rate of the reaction was determined and was used to construct a dose-response curve that allowed to calculate the maximal inhibition (I_{max}) within the tested dosages and to estimate an IC_{50} value. The ratio between these two values summarizes in a single number the potency (P) of each compound, so that $P = I_{max}/IC_{50}$. In Figure 4.7, inhibition potency values have been reported in the z axis for the compounds that have been defined in the horizontal plane as a combination of scaffolds and functional group types. They indicate that compounds **15** and **16** (glucopyranose scaffold) have a very low potency, regardless of pharmacophore (phenylhydroxylamine or catechol). For compounds with either a linear or a bicyclic scaffold, catechol proved to be slightly better pharmacophore, the more active compound being compound **13**.

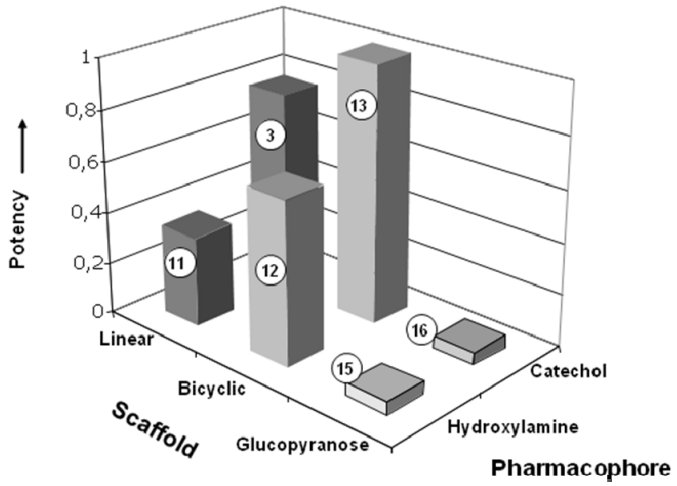

Figure 4.7: Inhibitor potency on nucleotide exchange of compounds 3 and 11-16.

4.3.4.2. *Ex vivo* experiments on human cancer cells

We tested the activity of catechol (**3**, **13** and **16**) and methoxyphenol-containing (**4**, **14** and **17**) lead compounds and that of reference compound **12** with an hydroxylamine groups on K-Ras mutated colorectal cancer cells, HCT-116 and DLD-1, using an ATP-based viability assay, as described in par. 4.2.2.2. In addition, by plasmid mediated homologous recombination, Shirasawa and co-workers[88] generated HCT-116 clones in which the k-ras D13 allele had been selectively deleted. These derivative cells, such as the HKe-3 clone, still retain one k-ras allele encoding for the wild type protein. With the same gene targeting strategy, HCT-116 clones were obtained carrying only the k-ras D13 allele, but in which the wt allele had been knocked-out (HK2-6). We tested the activity of compounds **3**, **12**, **13** and **16** on parental HCT-116 and DLD-1 (Figure 4.8) and on both HKe-3 and HK2-6 clones (Fig.4.9); the IC_{50} values for each compound, derived from dose-response curves, are reported in Table 4.2.

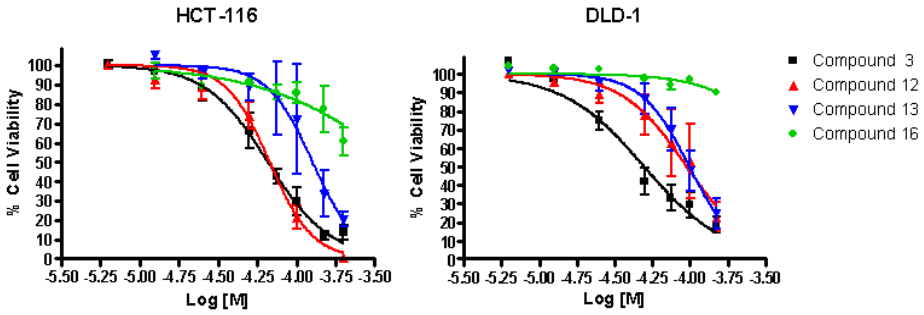

Figure 4.8: Effect of lead compounds on human colorectal cancer cells HCT-116 and DLD-1. Results represent the average of at least three independent experiments, while error bars indicate standard error of the mean (SEM).

88. Shirasawa, S.; Furuse, M.; Yokoyama, N.; Sasazuki, T., Altered growth of human colon cancer cell lines disrupted at activated Ki-ras. *Science* **1993,** *260* (5104), 85-88.

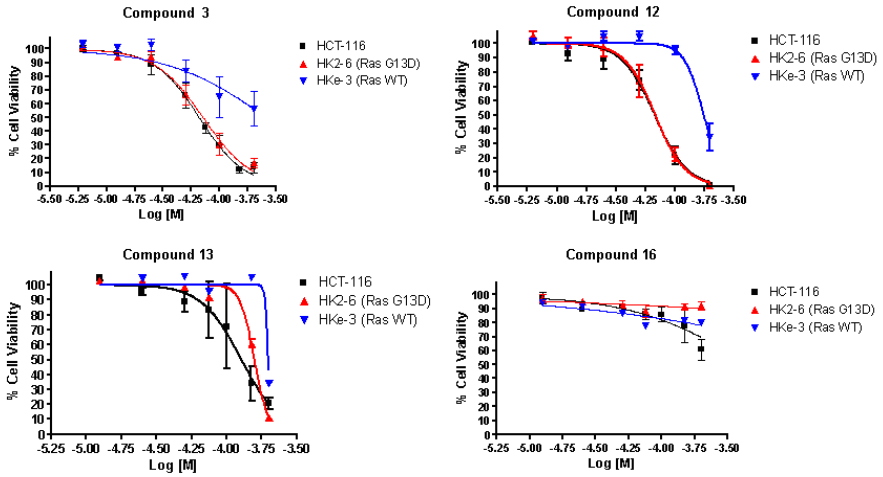

Figure 4.9: Effect of lead compounds on human colorectal cancer parental cell lines HCT-116 (wt/G13D) and on its derivative clones HK2-6 (-/G13D) and HKe (wt/-). Results represent the average of at least three independent experiments, while error bars indicate standard error of the mean (SEM).

Compound	DLD-1	HCT-116	HKe-3	HK2-6
3	50 ± 8	66 ± 7	205 ± 12	71 ± 11
12	96 ± 24	68 ± 8	177 ± 16	68 ± 9
13	99 ± 14	127 ± 40	197 ± 18	158 ± 4
16	>200	> 200	>200	> 200

Table 4.2: IC_{50} value of indicate compounds. Result indicate average IC_{50} values ± SEM (expressed as μM concentration)

Compounds **3**, **12** and **13** showed a selective toxicity effect on cells containing the G13D oncogenic mutant (both HCT-116 parental and HK2-6 clone) while resulted to be selectively less effective on the HK-3e clone that expresses only wt Ras. Once again, compound **16** and **17** with a glucose scaffold was inactive (non-toxic) on all cell types; compounds **4** and **14** containing a methoxyphenol group presented a slight effect only at high concentration level (>100 μM) as show in Figure 4.10.

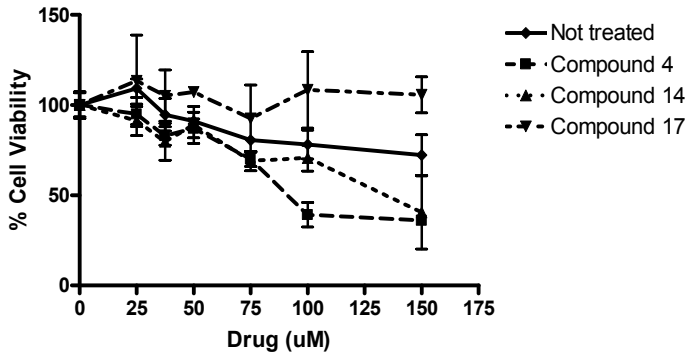

Figure 4.10: Effect of compounds 4, 14 and 17 containing a methoxy phenol pharmacophore on HCT-116 cells. Results represent the average of at least three independent experiments, while error bars indicate standard error of the mean (SEM).

4.3.5. Discussion

The data reported here allow important considerations on the structure-activity relationship in this class of Ras inhibitors. NMR binding experiments, according to computational docking calculations, confirm the determinant role of the aromatic moieties in the binding of the ligands to Ras. Also the scaffold seems to play a relevant role in the binding affinity: only in the case of compounds **12, 13** and **14** (with arabinose-derived bicyclic core) and compound **11**, **2** and **3** (with linear linker) the scaffold participated actively to the binding. Compounds **15**, **16** and **17,** in which the pharmacophoric groups are supported on a glucopyranose-derived scaffold, show a poor binding affinity; probably this scaffold, more flexible respect to the bicyclic one, placed the pharmacophore in a non-efficient spatial arrangement. The grading of the binding affinity was consistent with biochemical assays run on purified wild type Ras and with cytotoxicity studies on human cancer cells. Interesting, compounds **3**, **12** and **13** show a mild selective cytotoxicity effect on 50-100 μM concentration on cells expressing oncogenic Ras^{G13D} (both parental HCT-116 and HK-2 derivative clone). To our knowledge, no other small molecules are known with selective action on Ras mutants. Moreover these data provides further evidence that the substitution of the phenyl hydroxylamine group with a more stable catechol group allows to retain part of the biological activity; on the other hand, the

methoxy phenol group (present in compounds **4**, **14** and **17**) was confirmed as less effective pharmacophore. Unfortunately, once again, all these molecules present a poor water solubility that compromises any other deeper investigation of the binding site and of the mechanism of action.

4.4. Water-soluble Ras inhibitors by chemoselective ligation

In order to try to increase Ras inhibitors water solubility, we design new compounds (Scheme 4.7) in which the pharmacophoric portion, previously identified, was bound to a sugar moiety with a chemoselective glycosylation approach. In this manner, it was been possible to synthesized a small library of active compounds in which different sugar moieties could be served to modulate the pharmacokinetic properties of the drugs such as solubility or cellular uptake.

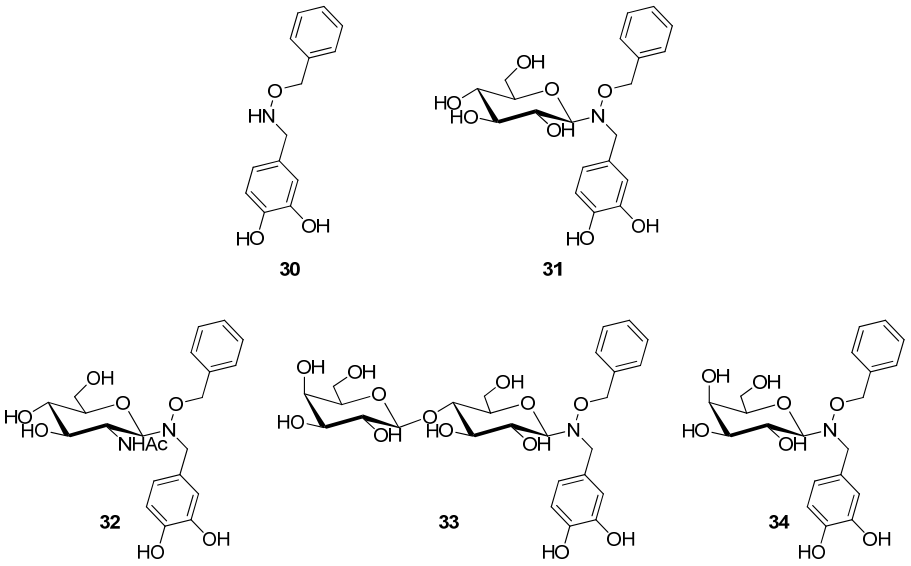

Scheme 4.7: Structure of compounds 30-34.

For this purpose, *O*-benzyl-*N*-(3,4-dihydroxy)benzyl hydroxylamine (compound **30**), representing the pharmacophoric portion, was *N*-glycosylated with *D*-glucose (compound **31**), *N*-acetyl-D-glucosamine (compound **32**), lactose (compound **33**) or D-galactose (compound **34**).

Compound **31** was fully characterized by the point of view of the binding and biological activity[89], whereas compounds **30** and **32-34** are still under investigation.

4.4.1. Chemical synthesis

Compound **30** was synthesized according to the following synthetic pathway:

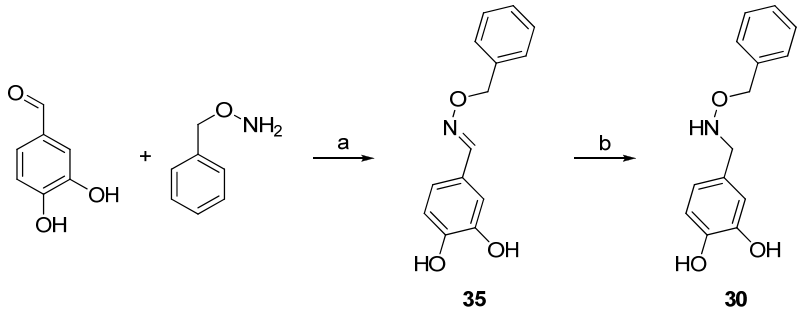

Scheme 4.8. Reagent and conditions: a) Pyridine, r.t., overnight, quant. yield. b) NaCNBH3, glacial acetic acid, r.t., overnight, 80%.

Commercially available 3,4-dihydroxybenzaldeide was reacted with *O*-benzylhydroxylamine in pyridine, afforded compound **35** in a quantitative yield**.** Reduction of the oxime **35** in presence of $NaCNBH_3$ in glacial acetic acid, afforded compound **30**.

The chemoselective glycosylation between *N*,*O*-disubstitutedhydroxylamine **30** and the unprotected reducing saccharides D-glucose, *N*-acetyl-D-glucosamine, lactose and D-galactose was performed in a equal amount mixture of aqueous buffer acetate (pH 4.6), glacial acetic acid and dimethylformamide stirred at 50°C overnight, affording respectively compounds **31**, **32**, **33** and **34** (Scheme 4.9). The *N*-glycoside product was obtained stereoselectively, at least in the case of D-glucose, *N*-acetyl-D-glucosamine and lactose, with the β-anomeric configuration. In the case of D-galactose, instead, an equilibrium mixture of predominant β-anomer with minor α-anomer was observed, as described in literature[81].

89. Palmioli, A.; Sacco, E.; Abraham, S.; Thomas, C. J.; Domizio, A. D.; Gioia, L. D.; Gaponenko, V.; Vanoni, M.; Peri, F., First experimental identification of Ras-inhibitor binding interface using a water-soluble Ras ligand. *Bioorganic & Medicinal Chemistry Letters* **2009,** *19* (15), 4217-4222.

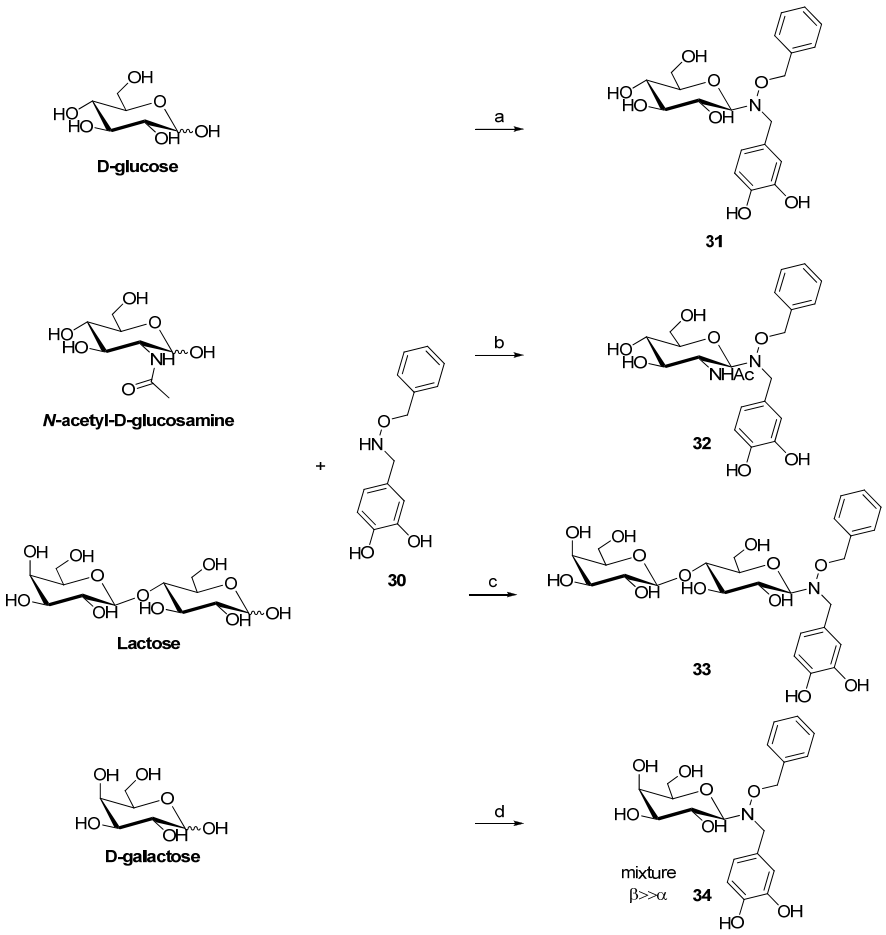

Scheme 4.9. Reaction and conditions: a) aqueous acetate buffer (pH 4.6)/AcOH/DMF, 50°C, overnight, 65%. b) aqueous acetate buffer (pH 4.6)/AcOH/DMF, 50°C, overnight, 46%. c) aqueous acetate buffer (pH 4.6)/AcOH/DMF, 50°C, overnight, 52%. d) aqueous acetate buffer (pH 4.6)/AcOH/DMF, 50°C, overnight, 90%.

All these compounds were clearly soluble in water or Tris buffer at a concentration of several mM. The stability of compound **31** in aqueous condition was investigated. For this purpose a sample of **31,** at the concentration of 10 mM in D_2O, was monitored by ^{1}H-NMR spectroscopy. As shown in Figure 4.11, compound **31** resulted to be stable at neutral pH for months[82].

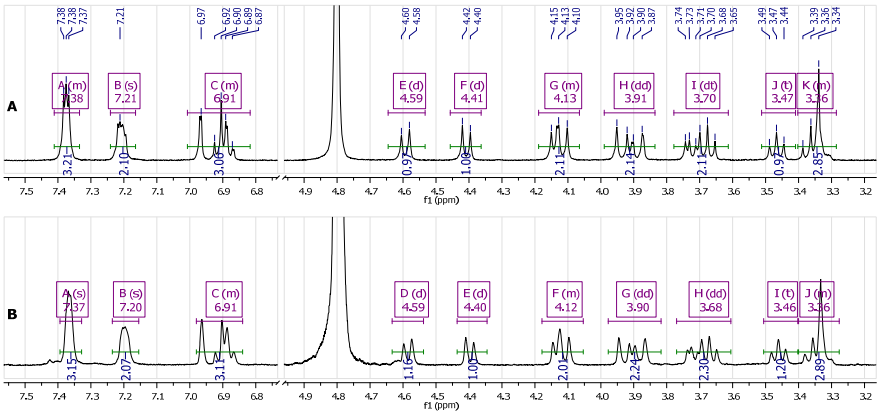

Figure 4.11: ^{1}H-NMR spectra of compound 31 (A) and after 5 months (B). The sample was dissolved in 550 µL of D_2O (10 mM).

4.4.2. ITC and NMR/MD binding studies

The binding affinity of compound **31** towards wild type H-Ras (1-166) and its oncogenic mutants Ras^{G13D} and Ras^{Q61L} was first investigated by Isothermal Titration Calorimetric (ITC) studies. This molecule was able to bind wild type H-Ras with an affinity of 37 µM and with an enthalpy of binding of -1964±40 cal/mol, exhibiting exothermic heats in ITC profile (Table 4.3 and Figure 4.12). It was also able to bind the oncogenic mutants Ras^{G13D} in the same µM range, whereas it showed reduced binding affinity for Ras^{Q61L}. Interesting, the stoichiometry of the interactions was equimolar (1:1).

	Ras variant	Affinity[a]	Enthalpy[b]
Compound 31	wt	37.2	-1964 (40.8)
	G13D	34.3	-2176 (20.4)
	Q61L	66.8	-1376 (38.3)

Table 4.3: Binding affinity and enthalpy of compound 31 and wild type Ras and oncogenic mutants Ras^{G13D} and Ras^{Q61L}. [a] µM; [b] ± error calculated on the basis of three independent experiments.

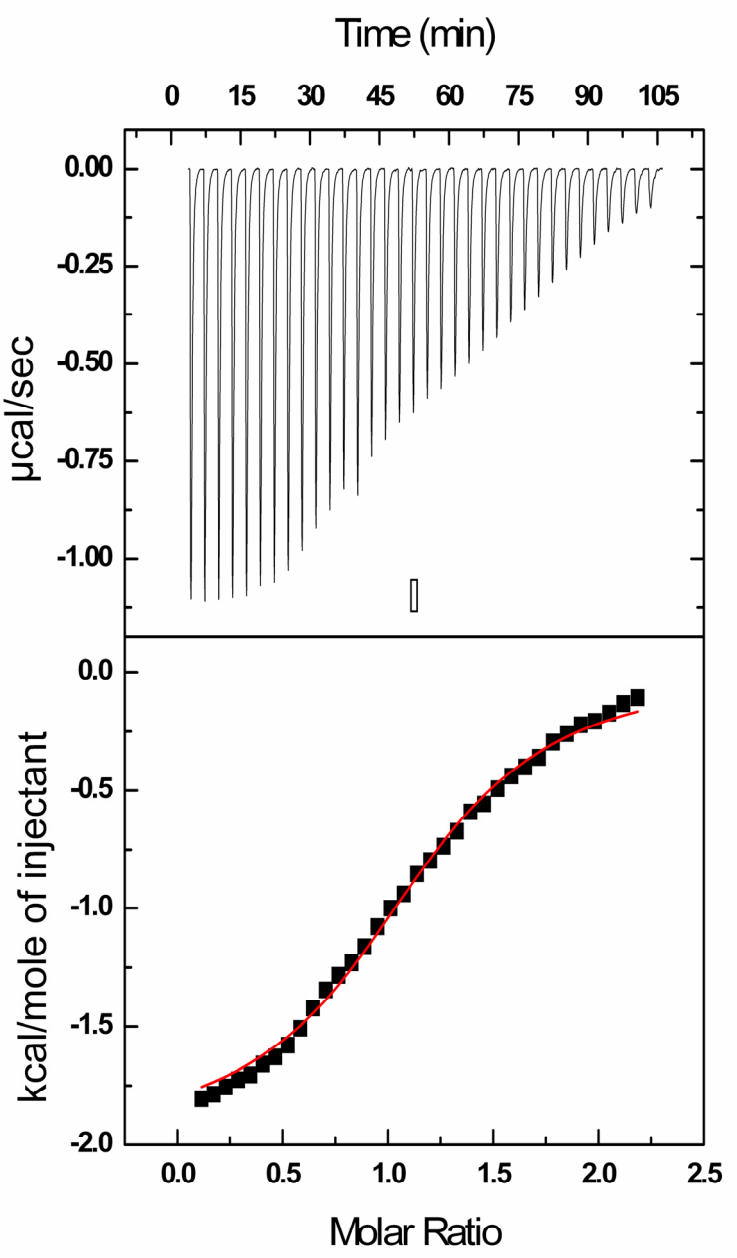

Figure 4.12: ITC data (upper) and fitted binding isotherms (lower) for thermodynamics of wt H-Ras binding to compound 31. Fixed aliquots of compound suspended in ITC buffer were injected into the calorimeter cell containing H-Ras in ITC buffer, and the heats of binding were recorded.

The interaction between compound **31** and H-Ras was then characterized by NMR experiments in solution. In order to achieve information about the Ras-ligand binding interface, a titration of compound **31** into a solution of ^{15}N-enriched H-Ras (1-166), followed by ^{1}H-^{15}N HSQC (Heteronuclear Single-Quantum Correlation) analysis, was performed. A series of spectra was recorded at different Ras: ligand molar ratios and was then compared with ^{15}N-HSQC spectra of H-RasGDP, looking for changes in cross peaks chemical shift (Figure 4.13). The assignment of ^{1}H and ^{15}N cross peaks of H-RasGDP was attributed in accord with literature[90]. On the graph are marked the residues exhibiting statistically significant chemical shift perturbations. The changes in chemical shift were concentration-dependent as shown in Figure 4.13(B-D). Significant chemical shift perturbations were observed in the β-3 strand (residues I55, T58, A59 and Y64) of the central β-sheet and α-2 helix (residues M67, R68, Y71, M72, R73, T74, and G75) as shown in Figure 4.13(E). Residue K5 and V103 are adjacent to the β-3/α-2 region and complete the continuous binding site of the drug lead compound on the catalytic domain of H-RasGDP. The cross peak shifts observed in HSQC experiments are caused by a variation in the electromagnetic environment of the amino acids, due to a variation in chemical background. This may indicate direct binding to the ligand or structural rearrangement of the protein due to the binding. In the case of residues E143 and K147 that do not belong to continuous binding site, the chemical shift variations may be due to a remote or propagated structural change of Ras induced by ligand binding.

90. Kraulis, P. J.; Domaille, P. J.; Campbell-Burk, S. L.; Van Aken, T.; Laue, E. D., Solution Structure and Dynamics of Ras p21.cntdot.GDP Determined by Heteronuclear Three- and Four-Dimensional NMR Spectroscopy. *Biochemistry* **1994,** *33* (12), 3515-3531.

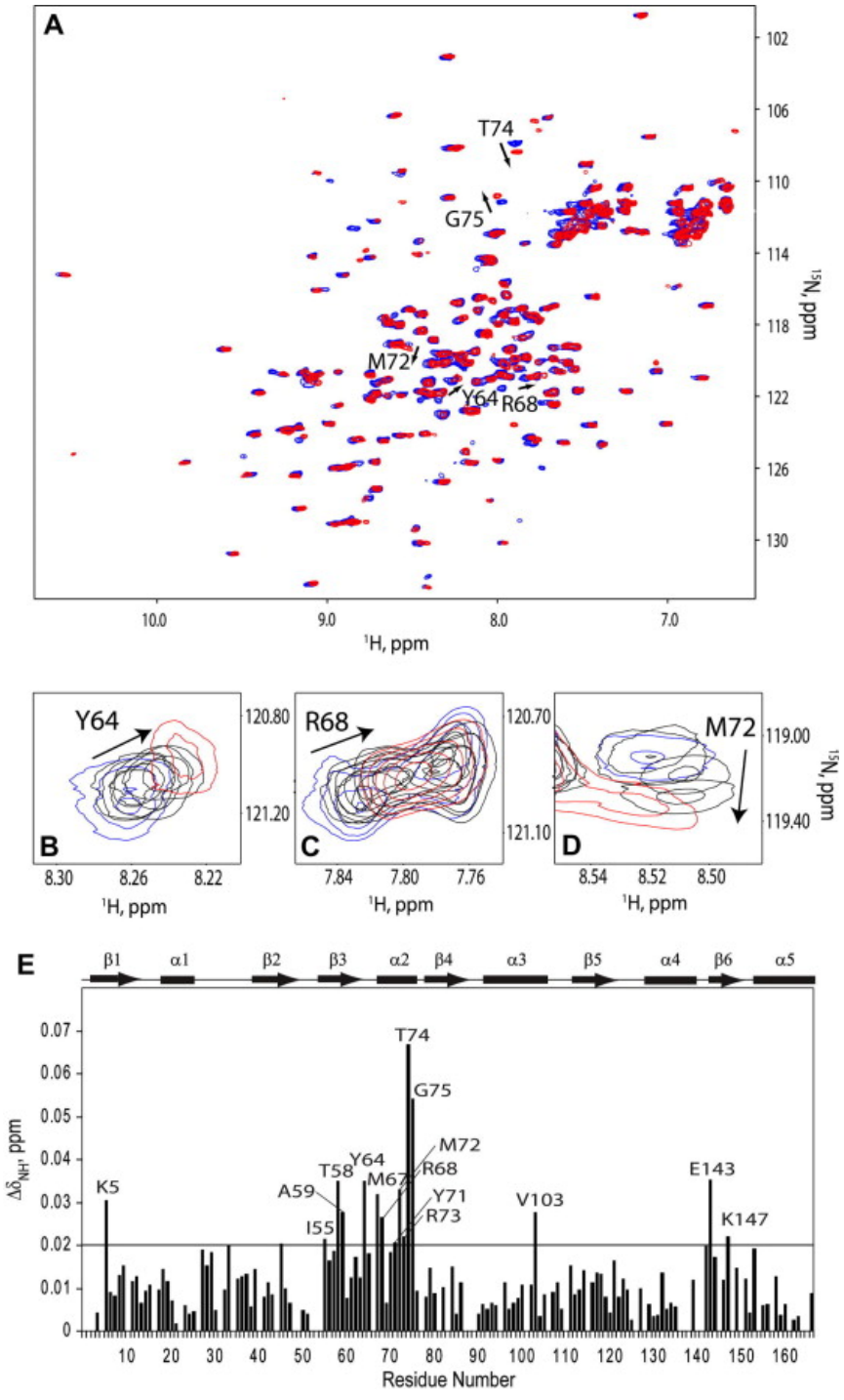

Figure 4.13: NMR titration of H-RasGDP 1–166 with compound 31. (A) ^{15}N HSQC spectra of H-RasGDP 1–166 with 0 (blue) and 20 M equiv of compound **1** (red) are superimposed. Spectral inserts for

Y64 (B), R68 (C), and M72 (D) show addition of 0 (blue), 1, 2, 5, 10, and 20 (red) M equiv of compound **31.** The arrows mark the direction of chemical shift changes. (E) normalized HN chemical shift perturbations. The boxes and arrows above the graph represent helices and sheets in H-RasGDP 1–166. The horizontal line marks the average value of chemical shift perturbations plus one standard deviation.

The NMR binding data were complemented by molecular dynamics (MD) calculations and docking experiments. Using Autodock 4.0, we docked compound **31** into the rigid structure of human H-Ras (PDB code: 4q21), assuming the cleft in the vicinity of the Switch II region as the ligand binding site. Two principal clusters of ligand arrangement were obtained and docking energy of the two lowest energy protein-ligand complexes is -6.41 and -5.91 kcal/mol, respectively. These docking results were then refined with explicit solvent MD simulations (Figure 4.14).

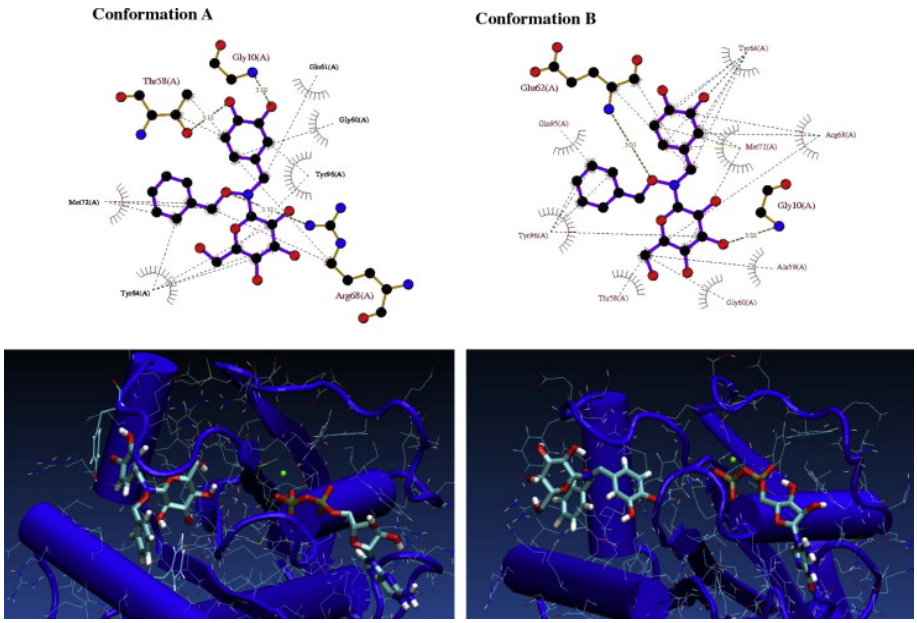

Figure 4.14: Contact maps (upper) and **3D representations** (lower) **of the two most representative lowest-energy protein–ligand complexes** (termed as A and B) as obtained from MD calculations starting from the best docking results of compound **31**.

The MD refined structures were then analysed with the aim of highlight protein residues for which different chemical shift are expected to deviate in consequence of

the ligand binding. In particular, protein residues which dramatically change their chemical environment are listed in Table 4.4. Underlined residues also showed significant chemical shift perturbations in NMR titration experiment.

	Residue		Interaction type
Pose A	Gly	10	H
	Thr	58	*
	Ala	59	*
	Gly	60	*
	Glu	62	H *
	Tyr	64	>> *
	Arg	68	*
	Met	72	*
	Gln	95	*
	Tyr	96	>> *
Pose B	Gly	10	H
	Thr	58	H *
	Gln	61	*
	Tyr	64	H *
	Arg	68	H *
	Met	72	*
	Tyr	96	*

Table 4.4: Residues involved in a chemical environmental changes caused by ligand binding. Interaction type key: H = hydrogen bonds, >> = aromatic-aromatic interactions, * = hydrophobic interactions.

4.4.3. Biological evaluation

4.4.3.1. Biochemical assay on nucleotide exchange

The inhibitory effect of compound **31** on GEF-catalyzed nucleotide exchange on H-RasGDP was tested. The catalytic domain of Ras-specific GEF RasGrf1 was used to promote exchange of bound GDP for mant-GDP as described previously [par. 4.3.4.1]. Exchange assay was performed in the presence of increasing concentrations of compound **31** (0, 50, 100, 250 and 500 μM) (Figure 4.15A). The initial slope, calculated for each reaction, was plotted as a function of compound concentration (dose-response curve, Figure 4.15B). As result evident from the dose-response curve, compound **31** at the concentration of 100 μM induce about fifty percent of

inhibition of the GEF-catalyzed nucleotide exchange rate on H-Ras. Circular Dichroism experiments (data not shown) demonstrated that the binding of compound **31** to Ras does not induce protein denaturation nor damages the protein structure.

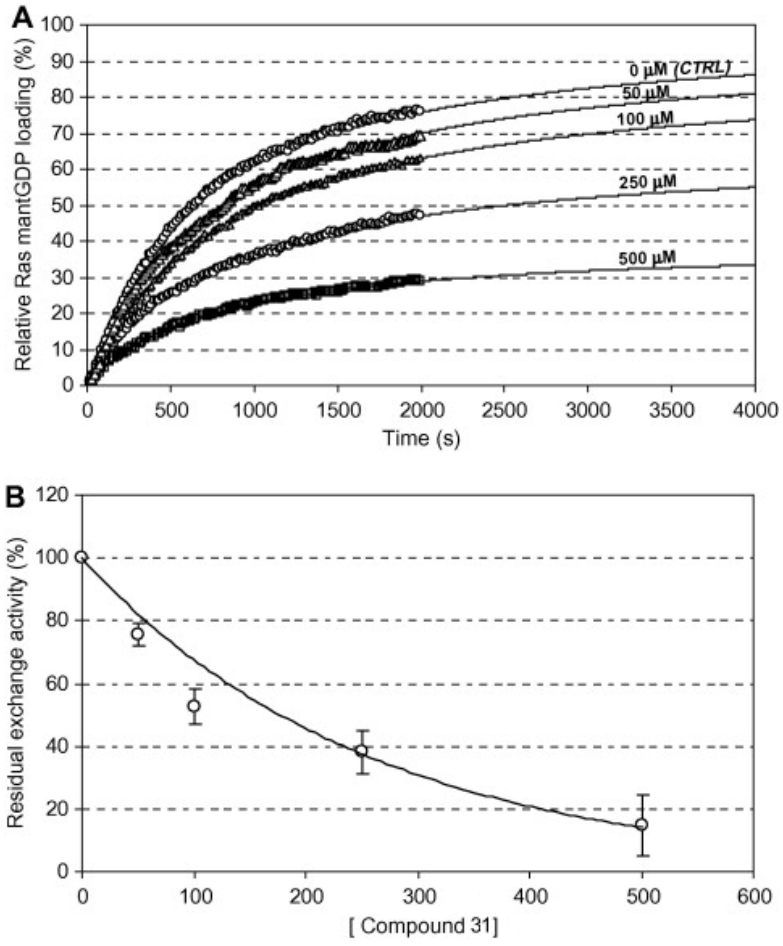

Figure 4.15: (A) **GEF-catalyzed nucleotide exchange reaction of H-Ras in presence of different concentrations of compound 31.** (B) **Dose-response curve.** Mean of at least three independent experiments.

4.4.3.2. *Ex vivo* experiments on mammalian cells

In order to investigate the effect of compound **31** on mammalian cells, the inhibition of the rate of proliferation of mouse fibroblasts NIH3T3 was evaluated. Cells were treated with an increasing concentration of compound **31** (0, 50, 150 and 450 µM)

supplemented in a growth medium, and counted at 24, 48 and 72 h after treatment. The obtained growth curve and morphological analysis (Figure 4.16) of treated cell demonstrated that compound **31** effectively inhibits cell proliferation at 150 μM. In fact the number of cells treated with 150 μM and 450 μM of **31** at 24 h from treatment is lower than control and does not increase later in time. Accordingly, in the culture medium of treated cells it is possible to appreciate many dead cells in suspension (refrangent cells circled in white)[91].

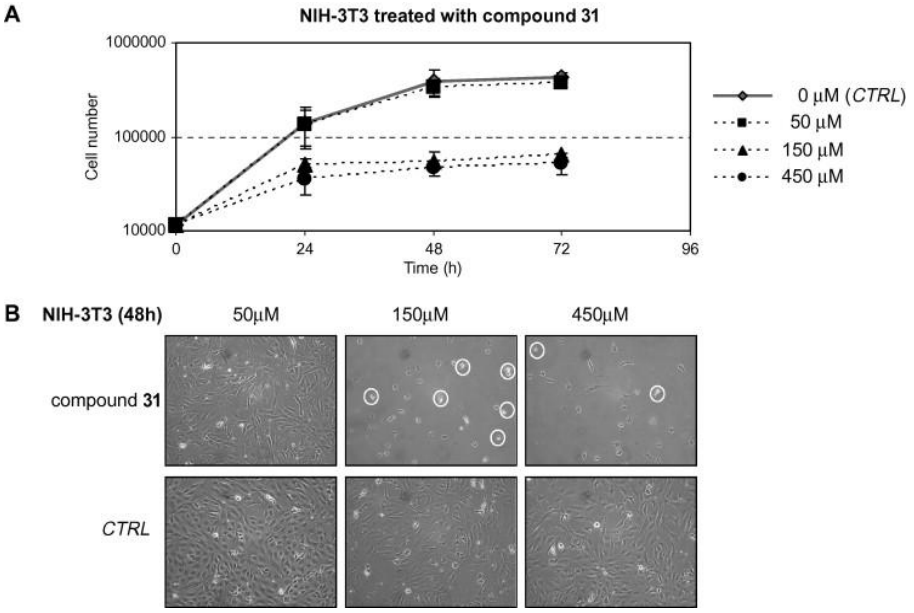

Figure 4.16: (A) **Proliferation curves of NIH3T3 fibroblasts grown in media supplemented with different concentrations of compound 31.** (B) **Morphological analysis of cells treated for 48 hours.**

4.4.4. Discussion

A new class of Ras inhibitors was synthesized using an efficiently and convergent synthetic strategy based on a chemoselective glycosylation approach. In contrast with all Ras inhibitors obtained by our group, compounds **31-34** were clearly soluble in water or aqueous buffer. A complete investigation about the binding mode and the

91. Chiaradonna, F.; Sacco, E.; Manzoni, R.; Giorgio, M.; Vanoni, M.; Alberghina, L., Ras-dependent carbon metabolism and transformation in mouse fibroblasts. *Oncogene* **2006,** *25* (39), 5391-5404.

biological activity is still running. However, compound **31** was able to bind H-RasGDP, and its oncogenic variants, with μM affinity and forming an equimolar ligand-Ras complex. In addition, compound **31** was able to inhibit GEF-mediated nucleotide exchange in *in vitro* biochemical assay and to inhibit cell proliferation of NIH3T3 mouse fibroblast. The binding interface of H-RasGDP-**31** was determined. NMR experimental and MD computed-based converged indicating that certain H-Ras residues are critical for ligand binding. These include amino acids T58, A59 and Y64 belonging to β-3 strand and R68, M72 on the α-2 helix. The observed binding site covers a region that is essential for Ras interaction with Ras-GRF1, homologous to SOS, as described by the crystal structure of the Ras-SOS complex[32]. Therefore it is possible that compound **31** interferes with Ras-GEF interaction. Moreover the binding affinity of **31** is in the same order of magnitude of the GEF-Ras affinity[92], which could suggest that compound **31** could compete efficiently with GEF for Ras binding thus inhibiting Ras activation.

92. Zhang, B.; Zhang, Y.; Shacter, E.; Zheng, Y., Mechanism of the Guanine Nucleotide Exchange Reaction of Ras GTPaseEvidence for a GTP/GDP Displacement Model. *Biochemistry* **2005,** *44* (7), 2566-2576.

4.5. Conclusions and remarks

This PhD thesis allowed to develop new water-soluble Ras inhibitors.

According to the drug discovery process, several data were collected in order to clarify the structure activity relationship in Ras inhibitors. Then, new lead compounds were designed and synthesized following a rational drug design approach.

These original compounds were derived from natural carbohydrates and were obtained with an efficient and convergent synthetic pathway. In these molecules the phenylhydroxylamine group was replaced with a less toxic catechol group and the pharmacophoric portion was then *N*-glycosylated in order to modulate the pharmacokinetics proprieties. In this way, new compound's solubility and stability were markedly improved.

These molecules were demonstrated to be able to prevent the *in vitro* nucleotide exchange, key event for Ras activation, and to inhibit the proliferation of mammalian cells. In addition, the binding to the human Ras were fully characterized, identifying the binding interface. In order to collect this information, a multidisciplinary approach was required, based on the application of different experimental techniques, such as chemical synthesis, binding studies, biological and biochemical evaluation. All these evidences allowed some important considerations about our compound mechanism of action and result to be essential for the design of novel inhibitors with improved affinity and potency.

The major future perspective will consist in the characterization of our compounds biological effect on human tumour cells and in *in vivo* animal models, and a further detailed investigation of their mechanism of action, in order to complete the lead optimization process.

5. Materials and methods

5.1. Organic synthesis

5.1.1. General procedures

5.1.1.1. Dry solvents and reactions

When dry conditions were required, the reactions were performed in oven-dried glassware under argon atmosphere. All solvents were dried over molecular sieves (type 3 Å for acetonitrile, methanol and ethanol and type 4 Å for chloroform, dichloromethane, diethyl ether, dimethylformamide, ethylacetate, pyridine, toluene and tetrahydrofuran, Fluka) for at least 24 h prior to use or purchase by Sigma-Aldrich with a content of water ≤0.005 %. All reagent and solvent were purchased by Sigma-Aldrich and were used without further purification, unless indicated otherwise. The petroleum ether used as eluent in chromatography has boiling range of 40–60°C.

5.1.1.2. Thin-layer chromatography (TLC)

Thin-layer chromatography (TLC) was performed on Silica Gel 60 F254 plates (Merck) with UV detection, or using a developing solution of conc. H_2SO_4/EtOH/H_2O (5:45:45), followed by heating at 180 °C.

5.1.1.3. Flash column chromatography

Flash column chromatography was performed on silica gel 230-400 mesh (Merck), according with the procedure described in literature[93].

93. Still, W. C.; Kahn, M.; Mitra, A., Rapid chromatographic technique for preparative separations with moderate resolution. *The Journal of Organic Chemistry* **1978,** *43* (14), 2923-2925.

5.1.1.4. Mass spectrometry

Mass spectra were recorded on ESI-MS triple quadrupole (model API2000 QTrap™, Applied Biosystems). High resolution mass spectra were recorded on QSTAR Elite® LC/MS/MS system (Applied Biosystems) that is a hybrid quadrupole/TOF instrument, equipped with the Analyst® QS 2.0 software.

5.1.1.5. NMR spectroscopy

^{1}H and ^{13}C spectra were recorded on a Varian 400 MHz MERCURY instrument at 300 K unless otherwise stated. Chemical shift are reported in ppm downfield from TMS as internal standard.

5.1.1.6. Optical rotation

Optical rotations were measured at ambient temperature, using the sodium D line, on ATAGO POLAX-2L polarimeter.

5.1.2. Synthesis of compounds 1-11

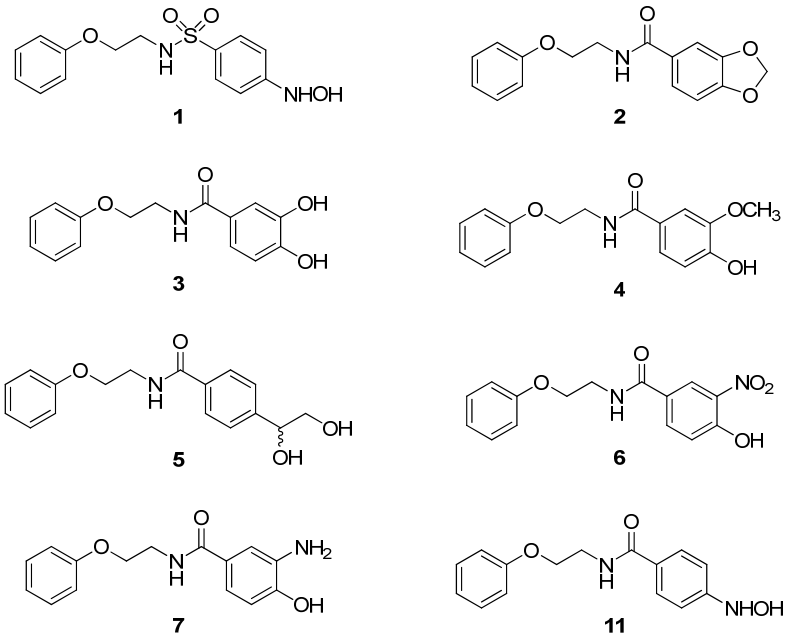

Scheme 5.1: Structure of compounds 1-11.

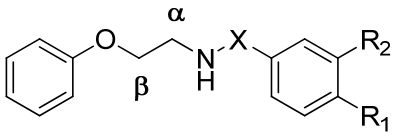

Scheme 5.2: Carbon and hydrogen numbering in compounds 1-11.

Compound 9

8 9

To a solution of 2-phenoxy-ethylamine **8** (1.17 g, 8.53 mmol) in dry DMF (40 mL), triethylamine (1.8 mL, 12.8 mmol) and *p*-nitrobenzensulfonyl chloride (2.84 g, 12.8 mmol) were added under argon atmosphere at 0°C. Then the stirred mixture was allowed to warm at r.t. and after 3h reaction was stopped by evaporate the solvent *in vacuum*. The residue was purified by flash chromatography (8:2 petroleum ether: AcOEt) affording **9** as a yellow powder (2.2 g, 82%).

^{1}H-NMR (400 MHz, CDCl3): δ (ppm) 8.27, 7.93 (AA'XX', 4H, J = 7.0 Hz, benzensulfonamide), 7.29 (t, 2H, J = 8.0 Hz, phenyl), 6.98 (t, 1H, J = 6.7 Hz, phenyl), 6.91 (d, 2H, J = 8.5 Hz, phenyl), 6.77 (bs, 1H, NHCO), 4.17 (t, 2H, J = 5.1 Hz, H-β), 3.90 (q, 2H, J = 5.1 Hz, H-α). ^{13}C-NMR (100 MHz, CDCl3): δ (ppm) 165.7, 158.4, 140.0, 129.9, 128.4, 124.1, 121.7, 114.7, 66.7, 40.3. HRMS (FT-ICR): calcd for $C_{14}H_{14}N_2O_5S$: 322.0623; found: 345.0536 $[M+Na]^+$.

Compound 1

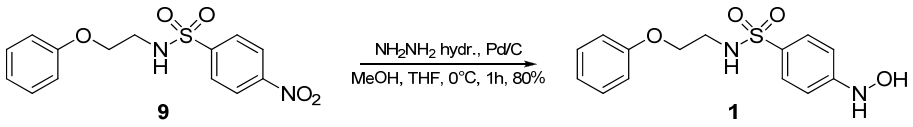

To a solution of **9** (200 mg, 0.62 mmol) in dry MeOH-THF (1:1, 10 mL), Pd/C 10% (catalytic) was added at 0°C under argon atmosphere. After 15 min, the suspension was treated with hydrazine hydrate (32 µL, 0.62 mmol) and stirred at 0°C for 1 h. The reaction was quenched by adding acetone. Then Pd/C was removed by filtering and the solvent was evaporated *in vacuum*. The crude residue was purified by flash column chromatography (7:3 petroleum ether/THF), affording 1 as a white powder (147 mg, 80%).

^{1}H-NMR (400 Mhz, d_6-DMSO): δ (ppm) 7.70, 7.30 (AA'XX', 4H, benzensulfonamide), 6.90-7.30 (m, 5H, phenyl), 4.13 (bt, 2H, J = 5.8 Hz, H-β), 3.73 (bt, 2H, J = 5.8 Hz, H-α). ^{13}C-NMR (100 MHz, d_4-MeOH): δ (ppm) 164.7, 155.0, 140.7, 129.2, 128.1, 125.2, 120.6, 112.2, 66.3, 39.6. HRMS (FT-ICR): calcd for $C_{14}H_{16}N_2O_4S$: 308.0831; found: 331.0701 $[M+Na]^+$.

Compound 2

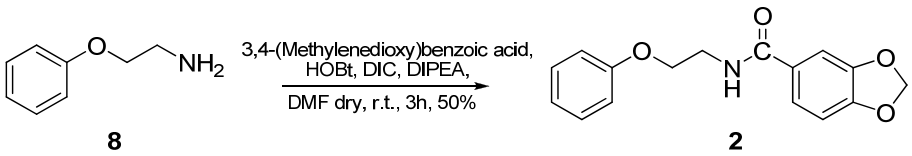

8 **2**

To a solution of 2-phenoxy-ethylamine **8** (100 mg, 0.73 mmol) in dry DMF (4 mL), 3,4-(methylenedioxy)benzoic acid (146 mg, 0.88 mmol), *N*-hydroxybenzotriazole (HOBt, 148 mg, 1.1 mmol), diisopropylcabodiimide (DIC, 170 μL, 1.1 mmol) and diisopropylethylamine (DIPEA, 375 μL, 2.19 mmol) were added under argon atmosphere at 0°C, then the reaction mixture was allowed to warm to r.t. and stirred for 3 h. Solvent was evaporated *in vacuum*, the residue dissolved in AcOEt, and washed with aqueous saturated $NaHCO_3$, the organic layer was dried on anhydrous sodium sulphate, filtered and evaporated. Flash column chromatography (petroleum ether/AcOEt 8:2) of the residue afford **2** (97.3 mg, 47 %) as a white powder.

^{1}H-NMR (400 MHz, d_4-MeOH): δ (ppm) 7.41 (dd, *J*=1.77, 8.14 Hz, 1 H, Harom), 7.30 (d, *J*=1.68 Hz, 1 H, Harom), 7.25 (m, 2 H, Harom), 6.92 (m, 3 H, Harom), 6.87 (d, *J*=8.17 Hz, 1 H, Harom), 6.02 (s, 2 H, OCH_2O), 4.13 (t, *J*=5.74 Hz, 2 H, H-β), 3.73 (t, *J*=5.73 Hz, 2 H, H-α).^{13}C-NMR (100 MHz, d_4-MeOH) δ ppm 169.79, 160.34, 152.04, 149.41, 130.52, 129.56, 123.40, 121.99, 115.73, 108.92, 108.53, 103.22, 67.43, 40.81. HRMS (FT-ICR): calcd for $C_{14}H_{15}NO_4$: 285.1001; found: 308.0898 $[M+Na]^+$.

Compound 3

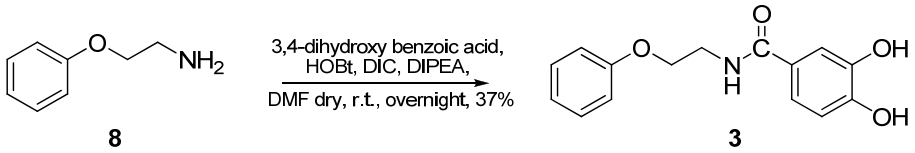

8 **3**

To a solution of 2-Phenoxy-ethylamine **8** (200 mg, 1.46 mmol) in dry DMF (8 mL), 3,4-dihydroxy benzoic acid (270 mg, 1.75 mmol), *N*-hydroxybenzotriazole (HOBt, 296 mg, 2.19 mmol), diisopropylcabodiimide (DIC, 339 μL, 2.19 mmol) and diisopropylethylamine (DIPEA, 750 μL, 4.38 mmol) were added under argon atmosphere at 0°C, then the reaction mixture was allowed to warm to r.t. and stirred overnight. Solvent was evaporated *in vacuum*, the residue dissolved in AcOEt, and washed with HCl 1M, aqueous saturated $NaHCO_3$ and brine; the organic layer was dried on sodium sulphate, filtered and evaporated. Flash column chromatography (chloroform/MeOH/AcOH 9:0.5:0.05) of the residue afford **3** (142 mg, 37 %) as a light green powder.

^{1}H-NMR (400 MHz, d_4-MeOH): δ (ppm) 7.29 (d, *J*=2.09 Hz, 1 H, Harom), 7.25 (m, 2 H, Harom), 7.21 (dd, *J*=2.11, 8.27 Hz, 1 H, Harom), 6.92 (m, 3 H, Harom), 6.78 (d, *J*=8.29 Hz, 1 H, Harom), 4.12 (t, *J*=5.82 Hz, 1 H, H-β), 3.71 (t, *J*=5.82, 5.82 Hz, 1 H, H-α). ^{13}C-NMR (100 MHz, d_4-MeOH) δ ppm 170.60, 160.31, 150.23, 146.34, 130.52, 126.95, 121.93, 120.65, 115.84, 115.80, 115.64, 67.40, 40.63. HRMS (FT-ICR): calcd for $C_{15}H_{15}NO_4$: 273.2839; found: 296.2659 $[M+Na]^+$.

Compound 4

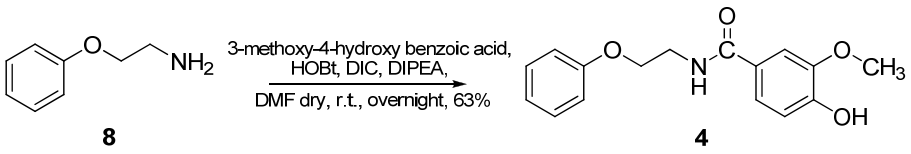

8 **4**

To a solution of 2-Phenoxy-ethylamine **8** (200 mg, 1.46 mmol) in dry DMF (8 mL), 3-Methoxy 4-hydroxy benzoic acid (294 mg, 1.75 mmol), *N*-hydroxybenzotriazole (HOBt, 296 mg, 2.19 mmol), diisopropylcabodiimide (DIC, 339 μL, 2.19 mmol) and diisopropylethylamine (DIPEA, 750 μL, 4.38 mmol) were added under argon atmosphere at 0°C, then the reaction mixture was allowed to warm to r. t. and stirred overnight. Solvent was evaporated *in vacuum*, the residue dissolved in AcOEt and washed with HCl 1M, aqueous saturated $NaHCO_3$ and brine; the organic layer was dried on sodium sulphate, filtered and evaporated. Flash column chromatography (petroleum ether/AcOEt 1:1) of the residue afford **4** (264 mg, 63 %) as a light green powder.

^{1}H-NMR (400 MHz, d_4-MeOH): δ (ppm) 7.44 (d, *J*=2.06 Hz, 1 H, Harom), 7.35 (dd, *J*=2.08, 8.28 Hz, 1 H, Harom), 7.25 (m, 2 H, Harom), 6.93 (m, 3 H, Harom), 6.82 (d, *J*=8.28 Hz, 1 H, Harom), 4.14 (t, *J*=5.78 Hz, 2 H, H-β), 3.89 (s, 3 H, OCH_3), 3.74 (t, *J*=5.77, 2 H, H-α). ^{13}C-NMR (100 MHz, d_4-MeOH) δ ppm 170.33, 160.33, 151.37, 148.82, 130.53, 126.70, 122.12, 121.93, 115.88, 115.63, 111.96, 67.39, 56.44, 40.75. HRMS (FT-ICR): calcd for $C_{16}H_{17}NO_4$: 287.3105; found: 310.2893 $[M+Na]^+$.

Compound 10

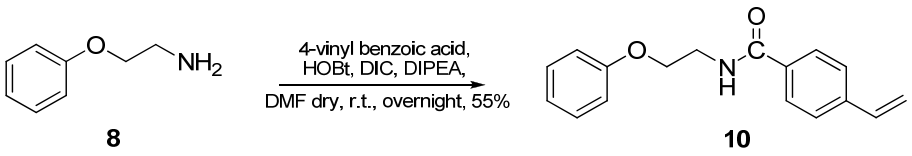

8 10

To a solution of 2-Phenoxy-ethylamine **14** (300 mg, 2.19 mmol) in dry DMF (10 mL), 4-vinyl benzoic acid (397 mg, 2.63 mmol), *N*-hydroxybenzotriazole (HOBt, 443 mg, 3.28 mmol), diisopropylcabodiimide (DIC, 508 µL, 3.28 mmol) and diisopropylethylamine (DIPEA, 1125 µL, 6.57 mmol) were added under argon atmosphere at 0°C, then the reaction mixture was allowed to warm to room temperature and stirred overnight. Solvent was evaporated *in vacuum*, the residue dissolved in AcOEt, and washed with HCl 1M, aqueous saturated $NaHCO_3$ and brine; the organic layer was dried on sodium sulphate, filtered and evaporated. Flash column chromatography (petroleum ether/AcOEt 9:1) of the residue afford **10** (320 mg, 55 %) as a white powder.

^{1}H-NMR (400 MHz, $CDCl_3$): δ (ppm) 7.74, 7.46 (AA'XX', 4H, Harom), 7.30 (m, 2 H, Harom), 6.98 (m, 1 H, Harom), 6.93 (m, 2 H, Harom), 6.73 (dd, *J*=10.92, 17.66 Hz, 1 H, H1'), 6.64 (bs, 1 H, NH), 5.83 (d, *J*=17.66 Hz, 1 H, H2'trans), 5.35 (d, *J*=10.85 Hz, 1 H, H2'cis), 4.15 (t, *J*=5.04 Hz, 2 H, H-β), 3.88 (q, *J*=4.90 Hz, 2 H, H-α). ^{13}C-NMR (100 MHz, $CDCl_3$): δ (ppm) 167.20, 158.40, 140.68, 135.87, 133.31, 129.58, 127.25, 126.29, 121.21, 115.96, 114.44, 66.70, 39.48. HRMS (FT-ICR): calcd for $C_{17}H_{17}NO_2$: 267.3224; found: 290.2882 $[M+Na]^+$.

Compound 5

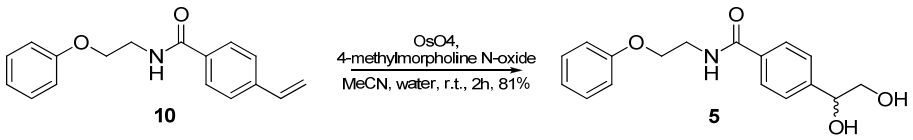

To a solution of 4-vinyl *N*-(2-phenoxy-ethyl)benzamide **10** (50 mg, 0.187 mmol) in 10 ml of MeCN: Water (10:1), 4-methylmorpholine *N*-oxide (32.8 mg, 0.243 mmol), osmium tetroxide (6.17 mg, 0.024 mmol) were added, then the reaction mixture was stirred at room temperature for 2 h. MeCN was evaporated *in vacuum*, the aqueous residue washed with CH_2Cl_2, then the organic layer was dried on sodium sulphate, filtered and evaporated. Flash column chromatography (AcOEt/petroleum ether 9:1) of the residue afford **5** (45.5 mg, 81 %) as a white-yellow powder.

^{1}H-NMR (400 MHz, d_4-MeOH): δ (ppm) 7.80, 7.47 (AA'XX', 4H, Harom), 7.25 (m, 2H, Harom), 6.92 (m, 3H, Harom), 4.73 (dd, *J*=4.82, 6.89 Hz, 1H, H1'), 4.14 (t, *J*=5.73, 2H, H2'), 3.75 (t, *J*=5.72, 2H, H-α), 3.62 (m, 2H, H-β). ^{13}C-NMR (100 MHz, d_4-MeOH) δ ppm 170.41, 160.29, 147.45, 134.60, 130.52, 128.32, 127.58, 121.95, 115.62, 75.48, 68.56, 67.30, 40.75. HRMS (FT-ICR): calcd for $C_{17}H_{19}NO_4$: 301.3371; found: 324.0127 $[M+Na]^+$.

Compound 6

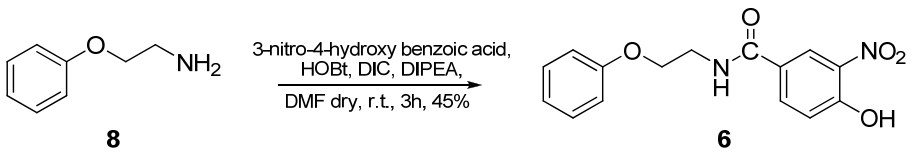

8 **6**

To a solution of 2-phenoxy-ethylamine **8** (300 mg, 2.18 mmol) in dry DMF (8 mL), 3-nitro 4-hydroxy benzoic acid (480 mg, 2.62 mmol), *N*-hydroxybenzotriazole (HOBt, 443 mg, 3.28 mmol), diisopropylcabodiimide (DIC, 508 μL, 3.28 mmol) and diisopropylethylamine (DIPEA, 1125 μL, 6.56 mmol) were added under argon atmosphere at 0°C, then the reaction mixture was allowed to warm to r.t. and stirred for 3 h. Solvent was evaporated *in vacuum*, the residue dissolved in AcOEt, and washed with HCl 1M, aqueous saturated $NaHCO_3$ and brine, the organic layer was dried on sodium sulphate, filtered and evaporated. Flash column chromatography (petroleum ether/AcOEt 6:4) of the residue afford **6** (295 mg, 45 %) as a yellow powder.

^{1}H-NMR (400 MHz, $CDCl_3$): δ (ppm) 8.55 (d, *J*=2.19 Hz, 1H, Harom), 8.05 (dd, *J*=2.20, 8.77 Hz, 1 H, Harom), 7.30 (m, 2 H, Harom), 7.23 (d, *J*=8.78 Hz, 1 H, Harom), 6.98 (m, 1 H, Harom), 6.92 (m, 2 H, Harom), 6.66 (bs, 1 H, NH), 4.16 (t, *J*=5.03, 2 H, H-β), 3.89 (q, *J*=5.54, 2 H, H-α). ^{13}C-NMR (100 MHz, $CDCl_3$): δ (ppm) 164.76, 158.27, 157.13, 135.99, 132.99, 129.62, 126.65, 124.08, 121.35, 120.48, 114.39, 66.43, 39.77. HRMS (FT-ICR): calcd for $C_{15}H_{14}N_2O_5$: 302.2821; found: 325.2675 $[M+Na]^+$.

Compound 7

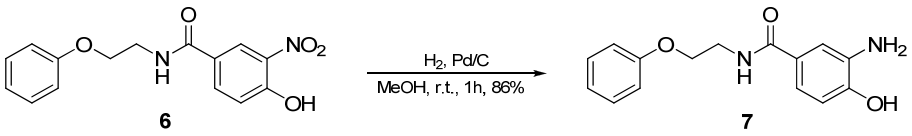

To a solution of **6** (49.3 mg, 0.163 mmol) in dry MeOH (3 mL), palladium on charcoal (catalytic) was added. The reaction was then performed under H_2 atmosphere (vacuum/H_2 cycles). After 1 h, Pd/C was filtered off and solvents evaporated *in vacuum*. The solid residue was dissolved in AcOEt and, after filtration on silica gel pad; pure compound **7** was recovered as a yellow solid (38 mg, 86 %).

^{1}H-NMR (400 MHz, $CDCl_3$): δ (ppm) 7.21 (m, 2H, Hphenyl), 7.08 (d, *J* = 2.0 Hz, 1H, Harom), 6.94 (dd, *J* = 8.2, 2.0 Hz, 1H, Harom), 6.92 – 6.79 (m, 3H, Hphenyl), 6.63 (d, *J* = 8.2 Hz, 1H, Harom), 6.53 (bt, *J* = 5.4 Hz, 1H, NH), 4.04 (d, *J* = 5.0 Hz, 2H, H-β), 3.75 (q, *J* = 5.2 Hz, 2H, H-α). ^{13}C-NMR (100 MHz, d_4-MeOH): δ (ppm) 171.11, 160.42, 149.92, 136.74, 130.60, 127.15, 122.05, 119.63, 116.06, 115.81, 114.95, 67.63, 40.73. HRMS (FT-ICR): calcd for $C_{15}H_{16}N_2O_3$: 272.1161; found: 295.1035 $[M+Na]^+$.

Compound 18

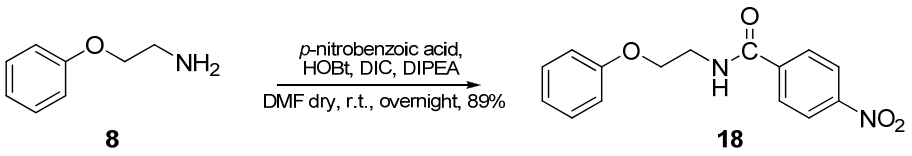

8 **18**

To a solution of 2-phenoxy-ethylamine **8** (580 mg, 4.23 mmol) in dry DMF (12 mL)**,** *p*-nitrobenzoic acid (849 mg, 5.08 mmol), *N*-hydroxybenzotriazole (HOBt, 858 mg, 6.35 mmol), diisopropylcabodiimide (DIC, 983 µL, 6.35 mmol) and diisopropylethylamine (DIPEA, 2.18 mL, 12.7 mmol) were added under argon atmosphere at 0°C, then the reaction mixture was allowed to warm to r.t. and stirred overnight. The solvent was evaporated and the crude was dissolved in AcOEt and washed with aqueous saturated $NaHCO_3$ and brine to eliminate HOBT and diisopropylurea. The product was finally purified by flash chromatography (AcOEt) obtaining compound **18** (89%).

^{1}H-NMR (400 MHz, $CDCl_3$): δ(ppm) 8.27, 7.93 (AA'XX', 4H, *J* = 7.0 Hz, benzamide), 7.29 (t, 2H, *J* = 8.0 Hz, Harom), 6.98 (t, 1H, *J* = 6.7 Hz, Harom), 6.91 (d, 2H, *J* = 8.5 Hz, Harom), 6.77 (bs, 1H, NH), 4.17 (t, 2H, *J* = 5.1 Hz, H-β), 3.90 (q, 2H, *J* = 5.1 Hz, H-α). ^{13}C-NMR (100 MHZ, $CDCl_3$): δ (ppm) 165.7, 158.4, 140.0, 129.9, 128.4, 124.1, 121.7, 114.7, 66.7, 40.3. HRMS(FT-ICR): calcd for $C_{15}H_{14}N_2O_4$: 286.0954; found 309.0853 $[M+Na]^+$.

Compound 11

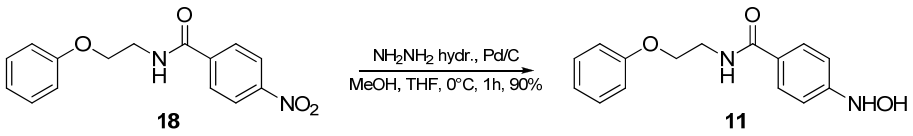

To a solution of **18** (200 mg, 0.7 mmol) in dry MeOH-THF (1:1, 10 mL), Pd/C 10% (3.7 mg) was added at 0°C under argon atmosphere. After 15 min, the suspension was treated with hydrazine hydrate (70 μL, 1.4 mmol) and stirred at 0°C for 45 min. Then Pd/C was removed by filtering and the solvent was evaporated *in vacuum*. The crude residue was purified by flash column chromatography (6:4 petroleum ether/THF) affording **11** as a light yellow powder (180 mg, 90%).

^{1}H-NMR (400 MHz, d_6-DMSO): δ (ppm) 7.70, 7.30 (AA'XX', 4H, benzamide), 7.30-6.90 (m, 5H, Harom), 4.13 (bt, 2H, J = 5.8 Hz, H-β), 3.73 (bt, 2H, J = 5.8 Hz, H-α). ^{13}C-NMR (100 MHz, d_4-MeOH): δ (ppm) 164.7, 155.0, 140.7, 129.2, 128.1, 125.2, 120.6, 112.2, 66.3, 39.6. HRMS (FT-ICR): calcd for $C_{15}H_{16}N_2O_3$: 272.1161, found: 295.1032 $[M+Na]^+$.

5.1.3. Synthesis of compounds 12-14

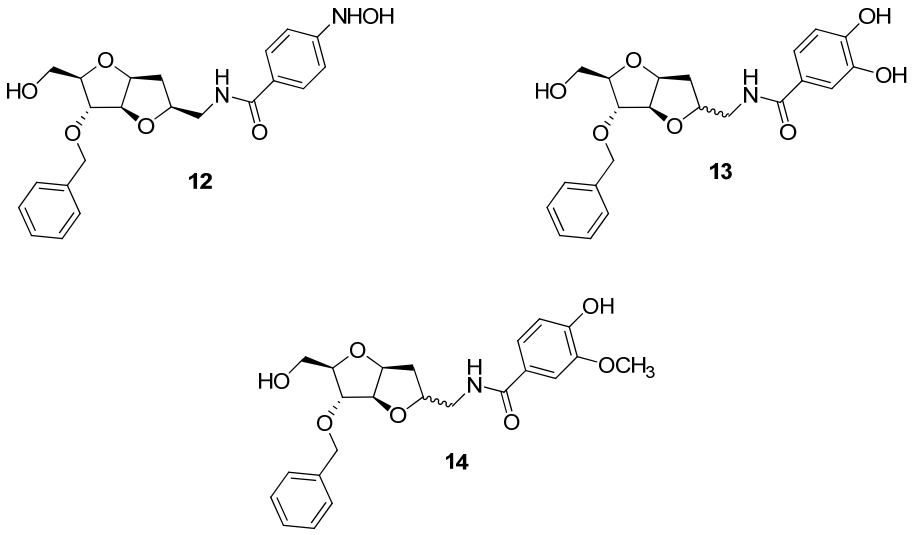

Scheme 5.3: Structure of compounds 12-14.

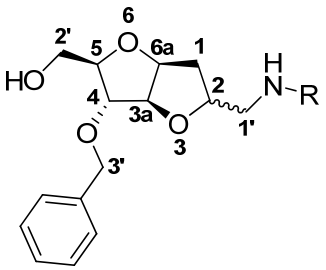

Scheme 5.4: Hydrogen numbering in bicyclic compounds 12-14.

Compound 35

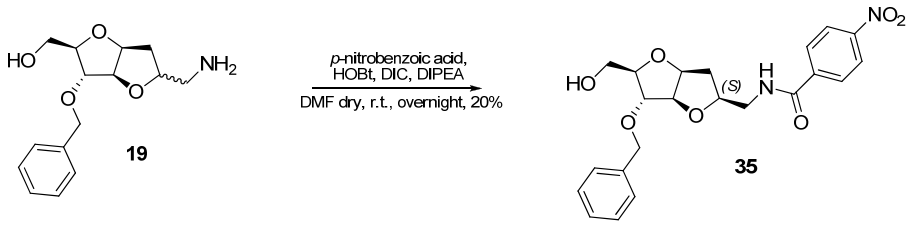

To a solution of amine **19** (mixture of R and S diastereoisomers in C-2 R/S 3:1) (200 mg, 0.716 mmol) in dry DMF (10 ml) HOBt (145 mg, 1.074 mmol), DIPEA (368 μL, 2.148 mmol) and 4-nitrobenzoic acid were added under argon atmosphere; DIC (166 μL, 1.074 mmol) was added at 0°C and the reaction was stirred at room temperature overnight. After this time, the solvent was concentrated *in vacuum* and flash-chromatography (4.5:5.5 toluene/EtOAc) was performed in order to resolve the diastereoisomeric crude mixture. Pure compounds **35** (*S* diastereomer, 59 mg, 20% yield) was obtained as a pale yellow oils.

^{1}H-NMR (400 MHz, $CDCl_3$): δ (ppm) 8.23, 8.01 (AA'XX', 4H, J = 8.9 Hz, Harom), 7.65 (dd, 1H, J = 6.8, 2.8 Hz, NH), 7.35-7.28 (m, 5H, Harom), 4.69 (dd, 1H, J = 5.0, 3.3 Hz, H-6a), 4.66, 4.53 (ABq, 2H, J = 11.7 Hz, benzyl), 4.41 (m, 2H, 2-H, H-3a), 4.09 (d, 1H, J = 5.0 Hz, H-4), 4.02 (m, 1H, H-5), 3.80 (m, 2H, H-1'a, H-2'a), 3.69 (dd, 1H, J = 11.9, 2.9 Hz, H-2'b), 3.53 (td, 1H, J = 14.3, 3.0 Hz, H-1'b), 2.82 (bs, 1H, OH), 2.27 (ddd, 1H, J = 14.4, 9.0, 5.6 Hz, H-1a), 2.07 (dd, 1H, J = 14.4, 4.8 Hz, H-1b); ^{13}C-NMR (100 MHz, $CDCl_3$): δ (ppm) 166.3, 149.1, 140.2, 137.2, 128.514, 128.35, 127.8, 127.5, 123.2, 88.5, 86.8, 83.8, 83.2, 78.6, 72.3, 61.6, 43.4, 33.7. $[\alpha]^{20}_{D}$: -18.4 (c 0.5, $CHCl_3$). HRMS (FT-ICR): calcd for $C_{22}H_{24}N_2O_7Na$: 451.1481; found: 451.1498 $[M+Na]^+$.

Compound 12

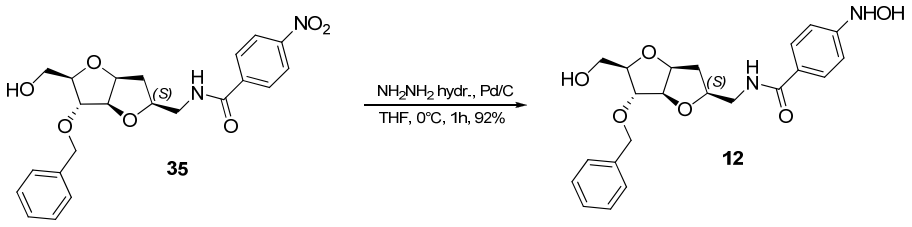

To a solution of **35** (70 mg, 0.163 mmol) in THF (3.7 mL), Pd/C (3.7 mg) was added at 0°C; after 15 min, the suspension was treated with hydrazine hydrate (8.4 μL, 0.172 mmol) and stirred at 0°C for 45 min. The reaction was quenched by adding acetone. Then Pd/C was removed by filtering and the solvents were concentrated *in vacuum*. The product was purified by flash column chromatography (9:1 toluene/MeOH) to give **12** (62 mg, 92%) as a pale yellow oil.

^{1}H-NMR (400 MHz, D_2O: d_4-MeOH 9:1): δ (ppm) 7.60, 6.99 (AA'XX', 4H, J = 8.7 Hz, Harom), 7.28 (m, 5H, Harom), 4.72 (bt, 1H, H-6a), 4.61, 4.48 (ABq, 2H, J = 11.6Hz, benzyl), 4.52 (bd, 1H, J = 4.2Hz, H-3a), 4.27 (m, 1H, 2-H), 3.84 (m, 2H, 4-H, H-5), 3.61 (dd, 1H, J = 12.3, 3.6 Hz, H-2'a), 3.54 (dd, 1H, J = 13.9, 7.1 Hz, H-1'a), 3.51 (m, 1H, H-2'b), 3.38 (dd, 1H, J = 14.0, 3.8 Hz, H-1'b), 2.27 (ddd, 1H, J = 14.5, 8.0, 6.3 Hz, H-1a), 1.86 (dd, 1H, J = 14.6, 4.0 Hz, H-1b). ^{13}C-NMR (100 MHz, d_4-MeOH): δ (ppm) 170.1, 156.0, 139.1, 129.3, 129.2, 128.8, 128.6, 126.4, 113.3, 90.4, 87.9, 85.8, 84.9, 80.7, 73.0, 63.3, 45.3 36.3. $[\alpha]^{20}_{D}$= -3.91 (c 0.7, DMSO). HRMS (FT-ICR): calcd for $C_{22}H_{26}N_2O_6Na$: 437.1689; found: 450.2549 $[M+Na]^+$. Elemental anal calcd for $C_{22}H_{26}N_2O_6$ (437.16): C 63.76%; H 6.32%; N 6.76%; found: C 63.73%; H 6.29%; N 6.81%.

Compound 13

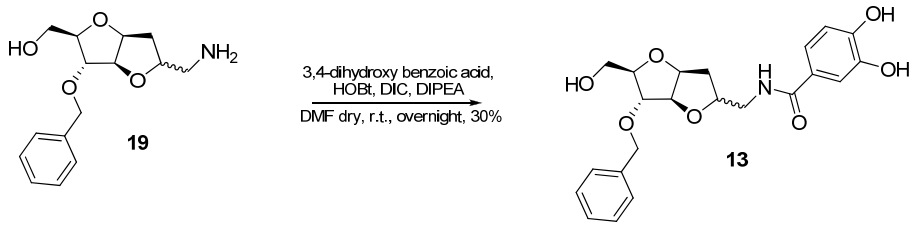

To a solution of amine **19** (mixture of R and S diastereoisomers in C-2 R/S 3:1) (50 mg, 0.179 mmol) in dry DMF (3 mL)**,** 3,4-dihydoxybenzoic acid (33 mg, 0.215 mmol), HOBT (36.3 mg, 0.269 mmol) and DIPEA (92 µL, 0.537 mmol) were added under argon atmosphere. DIC (41 µL, 0.269 mmol) was added at 0 °C, and the reaction mixture was stirred at r.t. overnight. The product was purified by flash chromatography (AcOEt to AcOEt: MeOH 7:3) obtaining compound **13** as an inseparable mixture of R and S diastereoisomers in C-2 (R/S 3:1, 23 mg, 30%).

^{1}H-NMR (the major diastereomer 2R is described, 400 MHz, d_4-MeOH): δ (ppm) 7.35-7.25 (m, 6H), 7.21 (dd, J = 8.1, 2.0 Hz, 1H), 6.80 (dd, J = 8.1, 2.0 Hz, 1H), 4.72 (bt, J = 2.2 Hz, 1H), 4.67-4.52 (ABq, 2 H), 4.61 (bd, J = 4.2 Hz, 1H), 4.23 (m, 1H), 3.80 (m, 2H), 3.68 (dd, J = 12.2, 3.0 Hz, 1H), 3.56 (dd, J = 12.2, 4.5 Hz, 1H), 3.49 (m, 1H), 3.30 (m, 1 H9, 2.13 (dd, J = 13.9, 5.0 Hz, 1H), 1.66 (m, 1H). ^{13}C-NMR (100 MHz, d_4-MeOH): δ (ppm) 173.2, 152.9, 149.1, 149.0, 142.0, 132.1, 131.7, 123.5, 118.7, 92.6, 89.0, 88.9, 87.3, 81.9, 75.7, 65.9, 46.9, 40.3. HRMS (FT-ICR): calcd for $C_{22}H_{25}NO_7$: 415.1631; calcd for $[M+Na]^+$: 438.1529; found 438.1525.

Compound 14

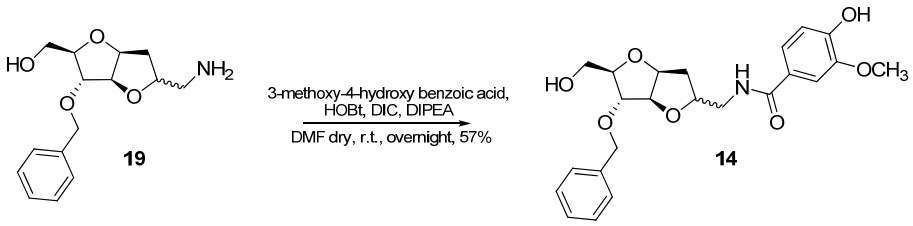

To a solution of amine **19** (mixture of R and S diastereoisomers in C-2 R/S 3:1) (50 mg, 0.179 mmol) in dry DMF (3 mL)**,** 3-methoxy 4-hydroxybenzoic acid (36.1 mg, 0.215 mmol), HOBT (36.3 mg, 0.268 mmol) and DIPEA (92 µL, 0.537 mmol) were added under argon atmosphere. DIC (41 µL, 0.268 mmol) was added at 0 °C, and the reaction mixture was stirred at r.t. overnight. The solvent was evaporated and the crude was dissolved in AcOEt and washed with HCl 1M, aqueous saturated $NaHCO_3$ and brine to eliminate HOBT and diisopropylurea. The product was finally purified by flash chromatography (AcOH) obtaining compound **14** as an inseparable mixture of R and S diastereoisomers in C-2 (R/S 3:1, 43.7 mg, 57 %).

^{1}H-NMR (the major diastereomer 2R is described, 400 MHz, d_4-MeOH): δ (ppm) 7.45 (d, *J* = 1.7 Hz, 1H, Harom), 7.40 – 7.24 (m, 5H, benzyl), 7.20 (dd, *J* = 8.3, 1.8 Hz, 1H, Harom), 6.91 (d, *J* = 8.3 Hz, 1H, Harom), 6.50 (bt, 1H, NH), 6.26 (bs, 1H, OH), 4.73 (t, *J* = 4.6 Hz, 1H, H-6a), 4.69, 4.54 (qAB, 2H, H-3'), 4.62 (m, 1H, H-3a), 4.24 (m, 1H, H-2), 3.91 (s, 3H, OCH_3), 3.90 – 3.78 (m, 3H, H-4, H-5, H-2'a), 3.74 (m, 1H, H-1'a), 3.64 (m, 1H, H-2'b), 3.50 (m, 1H, H-1'b), 2.15 (dd, *J* = 13.6, 4.9 Hz, 1H, H-1a), 1.63 (m, 1H, H-1b). ^{13}C-NMR (100 MHz, $CDCl_3$): δ (ppm) 167.43, 149.05, 146.89, 137.62, 128.68, 128.14, 127.93, 126.53, 119.88, 114.16, 110.79, 88.99, 84.82, 84.33, 83.44, 78.08, 72.43, 62.54, 56.29, 42.68, 36.15. HRMS (FT-ICR): calcd for $C_{23}H_{27}NO_7$: 429.1788; found 452.2019 $[M+Na]^+$.

5.1.4. Synthesis of compounds 15-17

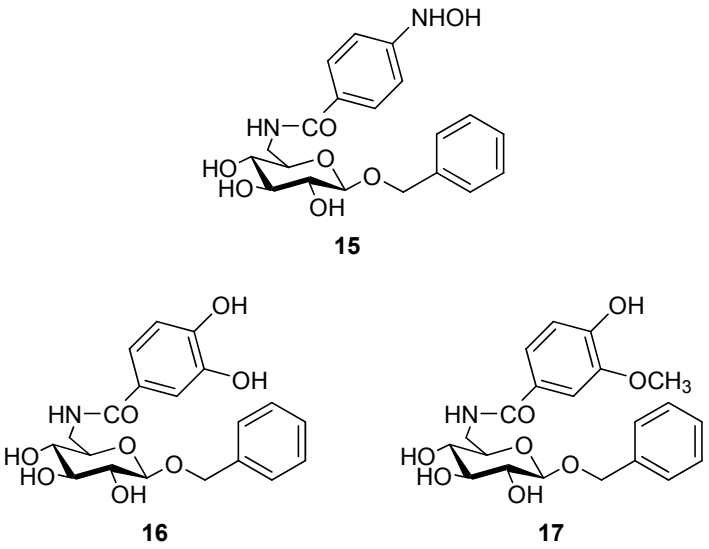

Scheme 5.5: Structure of compounds 15-17.

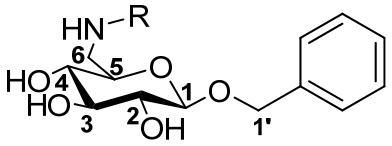

Scheme 5.6: Hydrogens numbering of compounds 15-17.

Compound 21

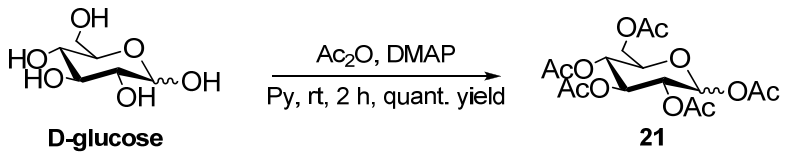

To a solution of D-glucose (5 g, 27.78 mmol) in dry pyridine (40 mL), acetic anhydride (20 mL, 211.76 mmol) and dimethylaminopyridine (catalytic) were added under argon atmosphere. The reaction was heavy stirred at r.t.. After 2h the reaction was quenched by the addition of MeOH (20 mL). The solvent was evaporated and the crude was then dissolved in AcOEt and washed with HCl 0.1 M and brine. After evaporation of the organic layer compound **21** (10.8 g, quant. yield) was recovered as white solid.

Hydrazine acetate

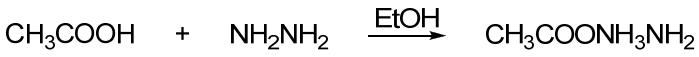

To a solution of hydrazine hydrate (3.4 mL, 70 mmol) in ethanol (30 mL), glacial acetic acid (4 mL, 70 mmol) were added at r.t.. The reaction was heavy stirred for 30 min, and then the solvent was minutely evaporated. The crude was maintained under vacuum until crystallization. Hydrazine acetate (6.45 g, quant. yield) was obtained as white solid.

Compound 22

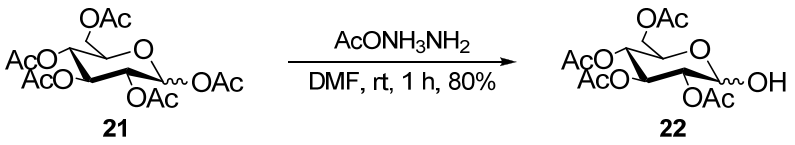

To a solution of compound **21** (10.8 g, 27.8 mmol) in dry DMF (40 mL), hydrazine acetate (5.12 g) was added under argon atmosphere at r.t.. The reaction was stirred and after 3h was stopped by evaporation of the solvent. The residue was dissolved in AcOEt and washed with brine to eliminate the excess of reagent. The crude was purified by flash chromatography (petroleum ether: AcOEt 1:1). Compound **22** (7.73 g, 80 %) was obtained as yellow oil.

Compound 23

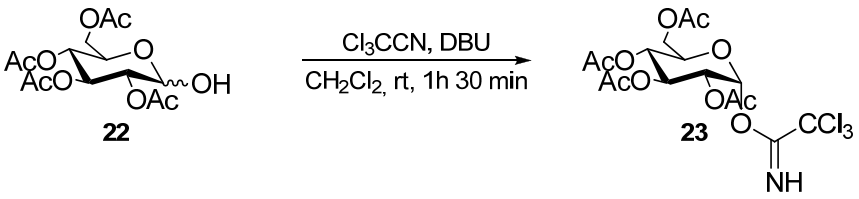

To a solution of compound **22** (6.65 g, 19.11 mmol) in dry dichloromethane, trichloroacetonitrile (9.56 mL, 95.54 mmol) and some drops of DBU were added at r.t. under argon atmosphere. The reaction was stirred for 1h 30', and then was stopped by partial solvent evaporation. Dilution of the residue with a mixture of AcOEt: petroleum ether 3:7 + 1 % Et_3N and a filtration on a pad of silica gel afforded compound **23** (7.2 g) as yellow oil.

Compound 24

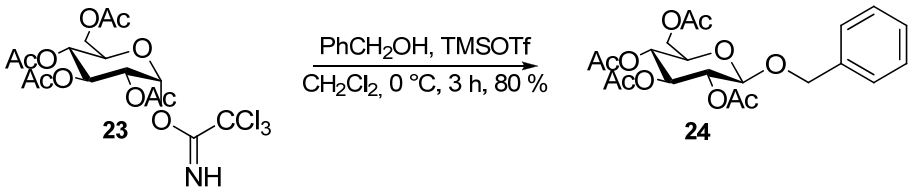

A solution of compound **24** (3.6 g, 7.3 mmol) and benzyl alcohol (1.5 mL, 14.7 mmol) in dichloromethane (30 mL) was treated by trickle addition of a solution of trimethyl trifluoromethanesulphonate (132.5 µL, 0.73 mmol) in dichloromethane (10 mL) under argon atmosphere at 0°C. The reaction was stirred for 2h at 0°C and was then quenched by addition of a saturated solution of $NaHCO_3$ to neutralize the Lewis acid. The organic layer was washed with brine and evaporated *in vacuum*. Flash chromatography (petroleum ether: AcOEt 8:2 to 6:4) afforded pure compound **24** (2.56 g, 80 %) as white solid.

Compound 25

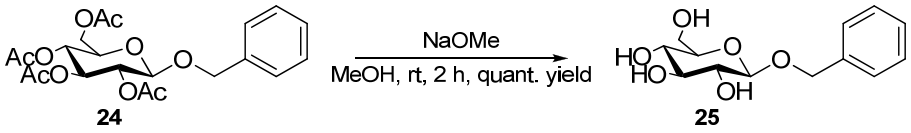

To a solution of compound **24** (2.1 g, 4.82 mmol) in dry methanol (60 mL), a catalytic amount of metallic sodium was added at r.t. under argon atmosphere. The reaction was stirred for 3h afterwards the pH was neutralized by addition of Amberlite IRA-120 (H^+) resin. After 30 min the resin was filtered off and generously washed with methanol. Evaporation of solvents afforded compound **25** (1.3 g, quant. yield) as colourless gel.

Compound 26

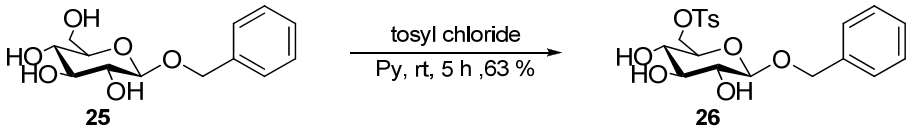

To a solution of benzyl β-D-glucopyranoside **25** (1.3 g, 4.81 mmol) in dry pyridine, tosyl chloride (1.38 g, 7.3 mmol) was added in three portions over 30 min at 0 °C under argon atmosphere. After this time the reaction was allowed to r.t. and stirred for 4 h. The reaction was then quenched by adding of methanol, and the solvent were evaporated *in vacuum*. The product was purified by flash chromatography (CH_2Cl_2: MeOH 10:0.5) obtaining pure compound **26** (1.28 g, 63%).

^{1}H-NMR (400 MHz, d_4-MeOH): δ (ppm) 7.79 (d, *J* = 8.4, 2H), 7.43 – 7.23 (m, 6H), 4.73, 4.52 (q AB, *J* = 12, 2H), 4.34 (dd, *J* = 1.9, 10.8, 1H), 4.24 (d, *J* = 7.7, 1H), 4.16 (dd, *J* = 6.1, 10.8, 1H), 3.41 – 3.34 (m, 1H), 3.28 – 3.13 (m, 3H), 2.38 (s, 3H). ^{13}C-NMR (100 MHz, d_4-MeOH): δ (ppm) 146.61, 139.00, 134.56, 131.18, 129.47, 129.35, 129.26, 128.89, 103.16, 77.97, 75.14, 75.02, 71.80, 71.31, 70.97, 21.71. $[\alpha]^{25}_D$ = -20.8 (*c*=0.96, MeOH). HRMS (FT-ICR): calcd for $C_{20}H_{24}O_8S$: 424.1192; found 447.1294 $[M+Na]^+$.

Compound 27

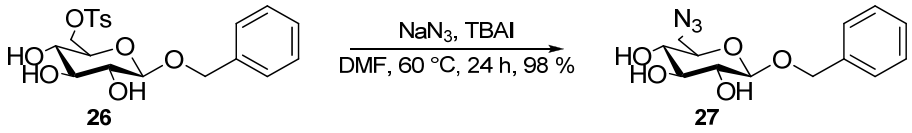

A solution of compound **26** (1 g, 2.35 mmol) in dry DMF (40 mL), sodium azide (460 mg, 7.07 mmol) and catalytic amount of tetrabutylammonium iodide were added under argon atmosphere. The reaction was warmed at 60°C and stirred overnight. After this time the reaction was complete and the solvent was evaporated *in vacuum*. The residue was then suspended in AcOEt and the excess of NaN_3 was filtered off. Flash chromatography (CH_2Cl_2: MeOH 10:1) afforded pure compound **27** (680 mg, 98%) as white solid.

^{1}H-NMR (400 MHz, d_4-MeOH): δ (ppm) 7.51 – 7.13 (m, 5H), 4.88, 4.64 (q AB, J = 12.0, 2H), 4.37 (d, J = 7.6, 1H), 3.57 – 3.14 (m, 6H). ^{13}C-NMR (100 MHz, d_4-MeOH): δ (ppm) 138.97, 129.46, 128.94, 103.22, 77.91, 77.38, 75.21, 72.70, 71.89, 52.97. $[\alpha]^{25}_D$ =-25 (c=0.6, MeOH). HRMS (FT-ICR): calcd for $C_{13}H_{17}N_3O_5$: 295.1168; found 296.3185 $[M+H]^+$.

Compound 28

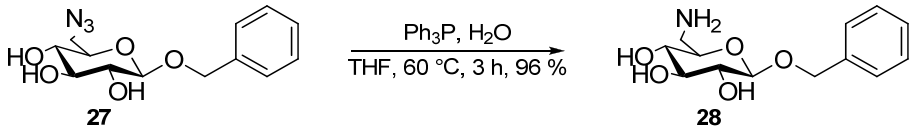

To a solution of compound **27** (380 mg, 1.3 mmol) in tetrahydrofuran (20 mL), triphenylphospine (1.02 g, 3.9 mmol) and water (936 μL, 52 mmol) were added. The reaction was stirred under reflux (60°C) for 3h. The solvents were then evaporated *in vacuum* and the crude was purified by flash chromatography (AcOEt:MeOH:H_2O 7:2:0.5 + 1% Et_3N) obtaining pure compound **28** (360 mg, 96%) as yellow oil.

^{1}H-NMR (400 MHz, d_4-MeOH): δ (ppm) 7.74 – 6.93 (m, 5H), 4.85, 4.68 (q AB, J = 12.0, 2H), 4.35 (d, J = 7.7, 1H), 3.36 – 3.08 (m, 4H), 3.01 (dd, J = 2.5, 13.4, 1H), 2.68 (dd, J = 7.2, 13.3, 1H). ^{13}C-NMR (100 MHz, d_4-MeOH): δ (ppm) 139.40, 129.44, 129.26, 128.87, 103.89, 78.01, 77.27, 75.32, 73.47, 72.38, 43.79. $[\alpha]^{25}_D$ =-31.8 (*c*=1.10, MeOH). HRMS (FT-ICR): calcd for $C_{13}H_{19}NO_5$: 269.1263; found 270.1539 $[M+H]^+$, 292.1366 $[M+Na]^+$.

Compound 29

To a solution of compound **28** (50 mg, 0.18 mmol) in dry DMF (2 mL)**,** *p*-nitrobenzoic acid (36.8 mg, 0.22 mmol), HOBT (36.5 mg, 0.27 mmol) and DIPEA (93 μL, 0.54 mmol) were added under argon atmosphere. DIC (42 μL, 0.27 mmol) was added at 0 °C, and the reaction mixture was stirred at r.t. overnight. The solvent was evaporated, and then the crude was dissolved in AcOEt and washed with aqueous saturated $NaHCO_3$ and brine, to eliminate HOBT and diisopropylurea. The product was finally purified by flash chromatography (AcOEt) obtaining compound **29** (59 mg, 78%) as yellow solid.

^{1}H-NMR (400 MHz, d_4-MeOH): δ (ppm) 8.29, 8.01 (AA'XX', *J* = 8.7, 4H), 7.45 – 7.06 (m, 5H), 4.84, 4.02 (q AB, *J* = 11.9, 2H), 4.32 (d, *J* = 7.8, 1H), 3.83 (dd, *J* = 2.9, 14.0, 1H), 3.62 (dd, *J* = 7.1, 14.1, 1H), 3.45 – 3.38 (m, 1H), 3.38 – 3.14 (m, 3H). ^{13}C-NMR (100 MHz, d_4-MeOH): δ (ppm) 168.81, 151.23, 141.46, 139.06, 129.93, 129.43, 129.24, 128.88, 124.80, 103.44, 77.74, 75.95, 75.36, 73.53, 71.92, 42.75. $[\alpha]^{25}_D$ = -25.8 (*c*=0.58, MeOH). HRMS(FT-ICR): calcd for $C_{20}H_{22}N_2O_8$: 418.1376; found 441.1474 $[M+Na]^+$.

Compound 15

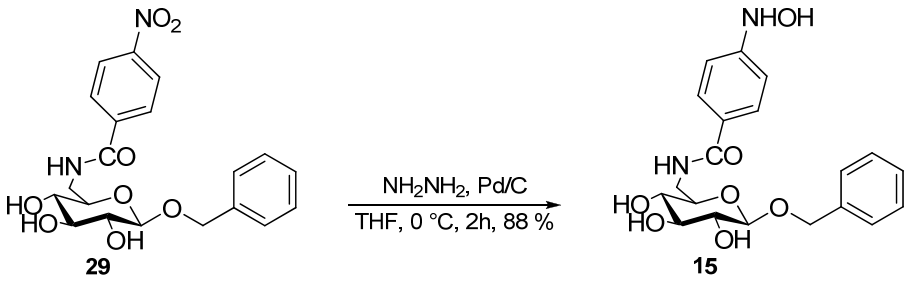

To a stirred solution of compound **29** (30 mg, 0.07 mmol) in a mixture of THF: MeOH (5:1, 3 mL), Pd/C 10% (3 mg) was added at 0 °C. After 15 min, the suspension was treated with hydrazine hydrate (7 µL, 0.14 mmol) and stirred at 0 °C. After 7 h the reaction was complete and was quenched by addition of acetone that reacts with excess of hydrazine. The Pd/C was filtered off, and solvents were evaporated. The product was finally purified by flash chromatography (AcOEt: MeOH 10:1) obtaining compound **15** (25 mg, 88%) as yellow solid.

^{1}H-NMR (400 MHz, d_6-DMSO): δ (ppm) 8.68 (s, 1H), 8.51 (s, 1H), 8.21 (bs, 1H), 7.74, 6.82 (AA'XX', *J* = 8.4, 2H), 7.34 – 7.21 (m, 6H), 5.16 (bs, 2H), 5.00 (bs, 1H), 4.77, 4.52 (q AB, *J* = 12.1, 2H), 4.18 (d, *J* = 7.7, 1H), 3.71 (dd, *J* = 5.3, 11.8, 1H), 3.34 – 2.94 (m, 5H). ^{13}C-NMR (100 MHz, d_6-DMSO): δ (ppm) 146.73, 146.01, 136.85, 130.87, 128.73, 128.12, 127.78, 123.20, 92.51, 78.83, 78.17, 75.58, 70.31, 70.17, 61.39. $[\alpha]^{25}_{D}$ =-29.4 (*c*=0.51, MeOH). HRMS (FT-ICR): calcd for $C_{20}H_{24}N_2O_7$: 404.1584; found 427.1672 $[M+Na]^+$.

Compound 16

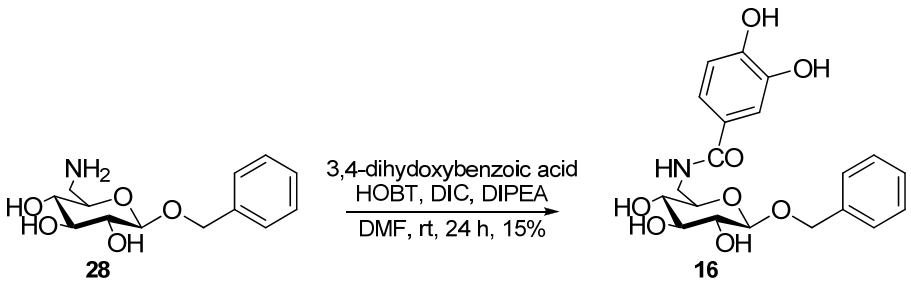

To a stirred solution of compound **28** (50 mg, 0.186 mmol) in dry DMF (2 mL)**,** 3,4-dihydoxybenzoic acid (28.7 mg, 0.186 mmol), HOBT (32.5 mg, 0.24 mmol) and DIPEA (96 μL, 0.56 mmol) were added under argon atmosphere. DIC (37.3 μL, 0.24 mmol) was added at 0 °C, and the reaction mixture was stirred at r.t. overnight. The product was finally purified by repeated flash chromatography (AcOEt:MeOH:H_2O 10:1:0.5) obtaining compound **16** (12 mg, 15%) as light green solid.

^{1}H-NMR (400 MHz, d_4-MeOH): δ (ppm) 7.35 – 7.17 (m, 7H), 6.78 (d, *J* = 8.3, 1H), 4.84, 4.63 (q AB, *J* = 12, 2H), 4.29 (d, *J* = 7.7, 1H), 3.73 (dd, *J* = 2.8, 14.1, 1H), 3.58 (dd, *J* = 6.8, 14.1, 1H), 3.39 – 3.12 (m, 4H). ^{13}C-NMR (100 MHz, d_4-MeOH): δ (ppm) 170.89, 150.42, 146.50, 138.96, 129.44, 129.37, 128.87, 126.90, 120.81, 115.97, 103.22, 77.64, 76.13, 75.41, 73.45, 71.81, 42.39. $[\alpha]^{25}_D$ = -33.3 (*c*=0.60, MeOH). HRMS (FT-ICR): calcd for $C_{20}H_{23}NO_8$: 405.1424; found 428.1523 $[M+Na]^+$.

Compound 17

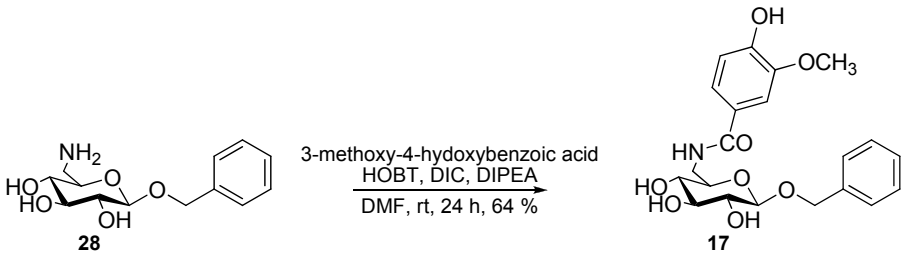

To a stirred solution of compound **28** (50 mg, 0.186 mmol) in dry DMF (2 mL)**,** 3-methoxy-4-hydoxybenzoic acid (37.5 mg, 0.223 mmol), HOBT (37.7 mg, 0.279 mmol) and DIPEA (96 μL, 0.56 mmol) were added under argon atmosphere. DIC (43 μL, 0.28 mmol) was added at 0 °C, and the reaction mixture was stirred at r.t. overnight. The solvent was evaporated and the crude was dissolved in AcOEt and washed with aqueous saturated $NaHCO_3$ and brine, to eliminate HOBT and diisopropylurea. The product was finally purified by flash chromatography ($CHCl_3$: MeOH 9.5:0.5) obtaining compound **17** (50 mg, 64%) as light yellow powder.

^{1}H-NMR (400 MHz, d_4-MeOH): δ (ppm) 7.49 – 7.21 (m, 7H), 6.86 (d, *J* = 8.3, 1H), 4.88, 4.67 (d, *J* = 11.8, 2H), 4.35 (d, *J* = 7.8, 1H), 3.89 (s, 3H), 3.86-3.74 (m, 1H), 3.65 (dd, *J* = 6.9, 14.3, 1H), 3.48 – 3.16 (m, 4H). ^{13}C-NMR (100 MHz, d_4-MeOH): δ (ppm) 170.68, 151.57, 148.99, 138.98, 129.44, 129.34, 128.89, 126.74, 122.28, 116.04, 112.20, 103.31, 77.67, 76.15, 75.42, 73.51, 71.84, 56.59, 42.50. $[\alpha]^{25}_D$ = -38.1 (*c*=1.05, MeOH). HRMS (FT-ICR): calcd for $C_{21}H_{25}NO_8$: 419.1580; found 420.2025 $[M+H]^+$.

5.1.5. Synthesis of compounds 30-34

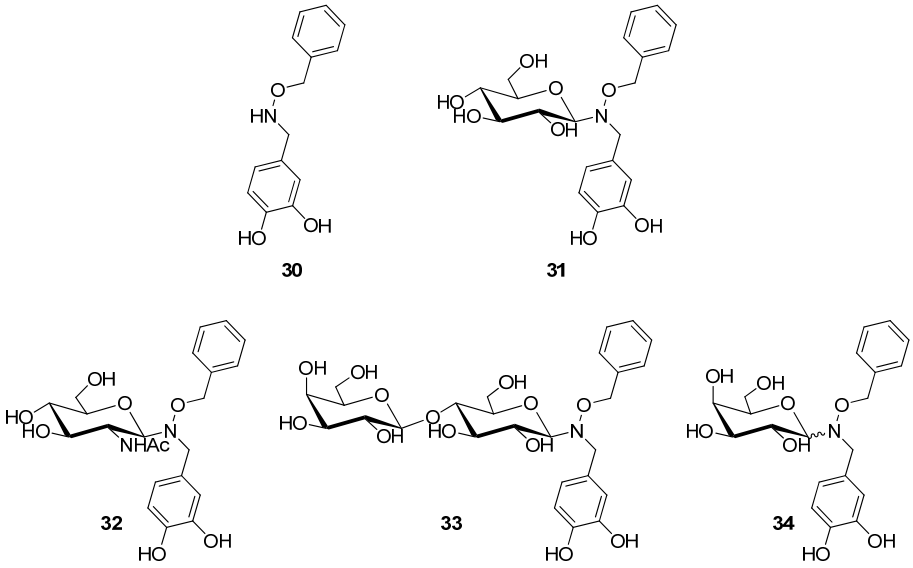

Scheme 5.7: Structure of compounds 30-34.

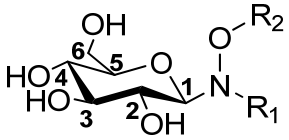

Scheme 5.8: Hydrogen numbering of compounds 31-34.

Compound 35

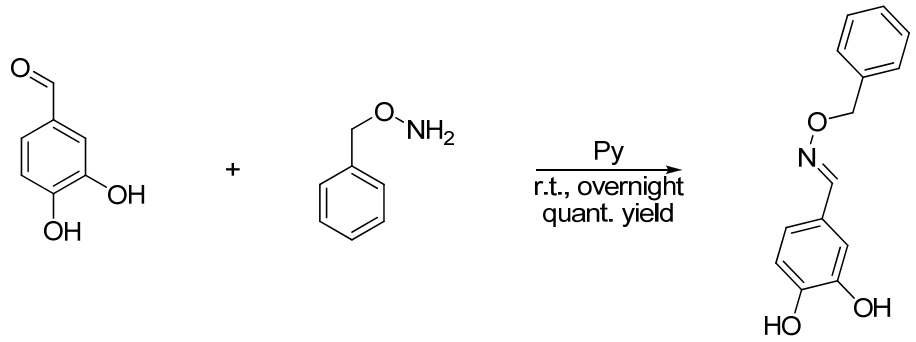

35

A solution of *O*-benzylhydroxylamine hydrochloride (1,15 g, 7.24 mmol) and 3,4-dihydroxybenzaldehyde (1 g, 7.24 mmol) in anhydrous pyridine (10 mL) was stirred at room temperature overnight. The solvent was concentrated and the residue was dissolved in AcOEt (200 mL), washed with saturated $NaHCO_3$ (50 mL) and brine (50 mL), dried over sodium sulphate and evaporated to give compound **35** (1.8 g, quant. yield) as dark yellow oil.

^{1}H-NMR (400 MHz, d_4-MeOH): δ (ppm) 7.95 (s, 1H), 7.39 – 7.21 (m, 5H), 7.05 (d, *J* = 1.8, 1H), 6.83 (dd, *J* = 1.8, 8.2, 1H), 6.71 (d, *J* = 8.1, 1H), 5.07 (s, 2H). ^{13}C-NMR (100 MHz, d_4-MeOH): δ (ppm) 150.66, 148.94, 146.83, 139.52, 129.46, 129.43, 128.92, 125.58, 121.66, 116.34, 113.99, 77.02. HRMS (FT-ICR): calcd for $C_{14}H_{14}NO_3$: 244.0974; found 245.2125 $[M+H]^+$.

Compound 30

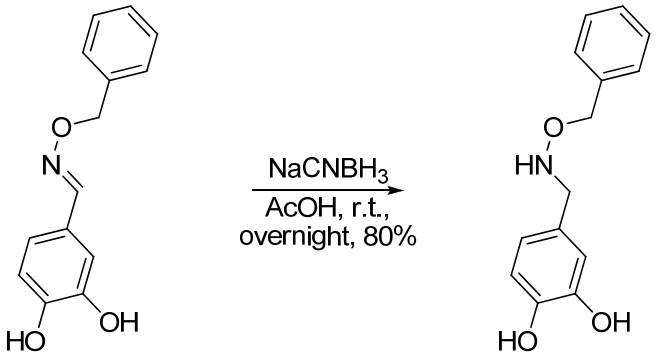

35 **30**

To a stirred solution of compound **35** (1.8 g, 7.24 mmol) in glacial acetic acid (15 mL) was added slowly $NaCNBH_3$ (910 mg, 14.48 mmol). The reaction mixture was stirred at room temperature overnight until the reaction was complete. The solvent was evaporated and the residue was dissolved in AcOEt (250 mL), washed with saturated $NaHCO_3$ (30 mL) and brine (30 mL), dried over sodium sulphate and evaporated. The crude was finally purified by flash chromatography (ETP: AcOEt: MeOH: AcOH 10: 2: 1: 0.1) obtaining compound **30 (**1.4 g, 80%) as green oil.

^{1}H-NMR (400 MHz, d_4-MeOH): δ (ppm) 7.32 – 7.16 (m, 5H), 6.77 (d, J = 1.7, 1H), 6.68 (d, J = 8.0, 1H), 6.62 (dd, J = 1.8, 8.0, 1H), 4.57 (s, 2H), 3.80 (s, 2H).^{13}C-NMR (100 MHz, d_4-MeOH): δ (ppm) 146.27, 145.93, 139.24, 130.29, 129.63, 129.41, 128.91, 121.99, 117.68, 116.24, 77.00, 56.91. HRMS (FT-ICR): calcd for $C_{14}H_{15}NO_3$: 245.1052; found 246.3042 $[M+H]^+$.

Compound 31

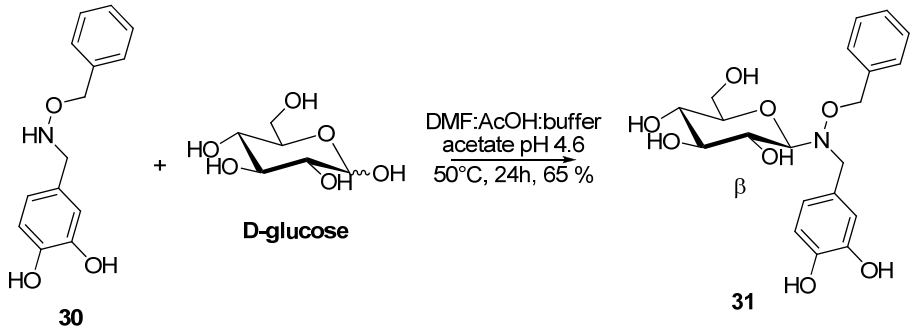

A solution of compound **30** (80 mg, 0.32 mmol) and **D-glucose** (40 mg, 0.22 mmol) in a mixture of DMF/AcOH/buffer acetate pH 4.5 (1:1:1, 3 mL) was stirred at 50°C for 24 h. The solvent was evaporated and the crude was purified by flash chromatography (AcOEt:MeOH:H_2O 11:1:0.3) obtaining compound **31** (58 mg, 65%) as light green powder.

^{1}H-NMR (400 MHz, d_4-MeOH): δ (ppm) 7.34 – 7.19 (m, 5H), 6.93 – 6.69 (m, 3H), 4.65, 4.48 (qAB, 2H), 4.03, 3.92 (qAB, 2H), 3.97 (d, *J* = 9.0, 1H), 3.84 (dd, *J* = 1.9, 12.1, 1H), 3.68 (dd, *J* = 5.0, 12.2, 1H), 3.62 (m, 1H), 3.40 – 3.22 (m, 2H), 3.13 (m, 1H). ^{13}C-NMR (100 MHz, d_4-MeOH): δ (ppm) 146.29, 146.10, 137.88, 130.96, 129.80, 129.52, 129.48, 123.04, 118.59, 116.22, 93.12, 79.72, 79.63, 78.20, 71.73, 71.17, 62.76, 57.95. HRMS (FT-ICR): calcd for $C_{20}H_{25}NO_8$: 407.1580; found 408.2781 $[M+H]^+$.

Compound 32

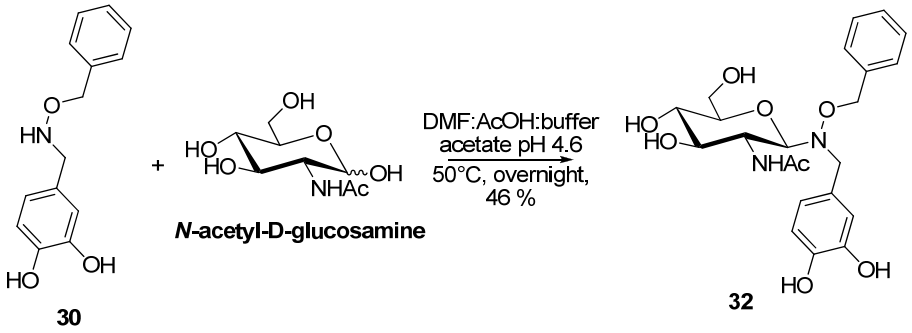

A solution of compound **30** (71 mg, 0.29 mmol) and ***N*-acetyl-D-glucosamine** (50 mg, 0.23 mmol) in a mixture of DMF/AcOH/buffer acetate pH 4.5 (1:1:1, 3 mL) was stirred at 50°C for 24 h. The solvent was evaporated and the crude was purified by flash chromatography (AcOEt:MeOH:H_2O 11:1:0.3) obtaining compound **32** (48 mg, 46%) as light green powder.

^{1}H-NMR (400 MHz, D_2O): δ (ppm) 7.35 – 7.25 (m, 3H, Hbenzyl), 7.17 – 7.08 (m, 2H, Hbenzyl), 6.82 (d, *J* = 8.1 Hz, 1H, Harom), 6.79 (d, *J* = 1.4 Hz, 1H, Harom), 6.73 (dd, *J* = 8.1, 1.6 Hz, 1H, Harom), 4.33, 4.27 (qAB,2H, CH_2O), 4.23 (d, *J* = 9.7 Hz, 1H, H-1), 4.00 (m, 1H, H-2), 3.95, 3.81 (qAB, 2H, CH_2N), 3.87 (dd, *J* = 12.3, 1.6 Hz, 1H, H-4), 3.71 (dd, *J* = 12.4, 5.3 Hz, 1H, H-3), 3.48 – 3.34 (m, 2H, H-5, H-6a), 3.30 (m, 1H, H-6b), 2.05 (s, 3H, $COCH_3$). ^{13}C-NMR (100 MHz, d_4-MeOH): δ (ppm) 173.58, 146.30, 146.07, 137.73, 131.16, 130.01, 129.44, 129.42, 122.98, 118.54, 116.18, 79.73, 78.13, 77.49, 71.61, 71.60, 62.90, 53.95, 23.24. HRMS (FT-ICR): calcd for $C_{22}H_{28}N_2O_8$: 448.4663; found 449.3925 $[M+H]^+$.

Compound 33

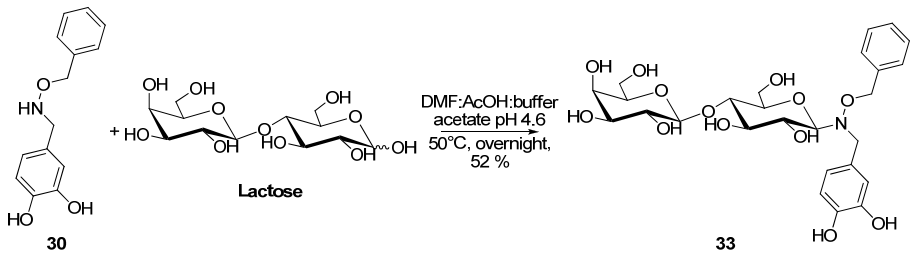

A solution of compound **30** (87.3 mg, 0.36 mmol) and **lactose** (156 mg, 0.43 mmol) in a mixture of DMF/AcOH/buffer acetate pH 4.5 (1:1:1, 4 mL) was stirred at 50°C for 24 h. The solvent was evaporated and the crude was purified by flash chromatography (AcOEt:MeOH:H_2O 8:2:0.5 to 8:2:1) obtaining compound **33** (105 mg, 52%) as light brown powder.

^{1}H-NMR (400 MHz, D_2O): δ (ppm) 7.35 (m, 3H, Hbenzyl), 7.18 (m, 2H, Hbenzyl), 6.95 (d, *J* = 1.2 Hz, 1H, Harom), 6.90 (d, *J* = 8.0 Hz, 1H, Harom), 6.86 (dd, *J* = 8.3, 1.2 Hz, 1H, Harom), 4.57, 4.38 (qAB, 2H, CH_2O), 4.41 (d, *J* = 7.8 Hz, 1H, H-1'), 4.15 (d, *J* = 8.9 Hz, 1H, H-1), 4.09, 3.92(qAB, 2H, CH_2N), 3.93 (m, 1H), 3.84 – 3.39 (m, 11H). ^{13}C NMR (100 MHz, D_2O): δ (ppm) 143.86, 143.71, 135.46, 129.75, 129.10, 128.85, 128.73, 123.00, 118.20, 116.08, 103.01, 91.33, 78.16, 77.02, 76.15, 75.84, 75.46, 72.60, 71.05, 69.74, 68.68, 61.19, 60.26, 56.53. HRMS (FT-ICR): calcd for $C_{26}H_{35}NO_{13}$: 569.5550; found 570.6317 $[M+H]^+$, 592.3824 $[M+Na]^+$.

Compound 34

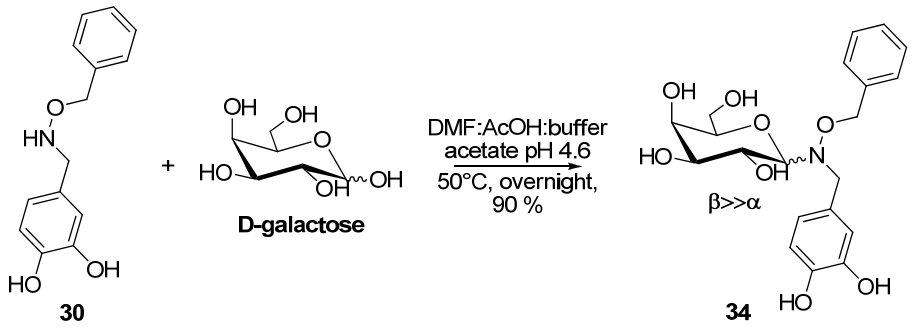

A solution of compound **30** (98 mg, 0.40 mmol) and **D-galactose** (60 mg, 0.33 mmol) in a mixture of DMF/AcOH/buffer acetate pH 4.5 (1:1:1, 4 mL) was stirred at 50°C for 24 h. The solvent was evaporated and the crude was purified by flash chromatography (AcOEt:MeOH:H_2O 8:2:0.5 to 8:2:1) obtaining compound **34** (121 mg, 90 %) as light brown powder.

^{1}H-NMR (the major β anomer is described, 400 MHz, d_4-MeOH): δ (ppm) 7.26 (m, 5H, Hbenzyl), 6.90 (d, *J* = 1.5 Hz, 1H, Harom), 6.78 (dd, *J* = 8.1, 1.6 Hz, 1H, Harom), 6.74 (d, *J* = 7.9 Hz, 1H, Harom), 4.64, 4.55 (qAB, 2H, CH_2O), 4.04, 3.97 (qAB, 2H, CH_2N), 3.97 (d, *J* = 9.4 Hz, 1H, H-1), 3.90 (m, 1H, H-3), 3.86 – 3.76 (m, 2H, H-2, H-6a), 3.70 (dd, *J* = 11.6, 4.9 Hz, 1H, H-6b), 3.44 (dd, *J* = 9.1, 3.3 Hz, 1H, H-4), 3.41 (m, 1H, H-5). ^{13}C-NMR (100 MHz, d_4-MeOH): δ (ppm) 146.22, 145.98, 138.13, 130.77, 130.09, 129.42, 129.30, 123.01, 118.56, 116.20, 93.86, 78.61, 77.94, 76.65, 70.91, 69.26, 62.94, 57.31. HRMS (FT-ICR): calcd for $C_{20}H_{25}NO_8$: 407.1580; found 408.3491 $[M+H]^+$, 430.8846 $[M+Na]^+$.

5.2. Biological procedures

5.2.1. Expression and isolation of proteins

The C-Cdc25^{Mm} (GEF from mouse; portion of CDC25^{Mm} that contains the catalytic domain of the protein)[94, 95]was expressed in *Escherichia coli* using the pGEX-2T expression vector and then purified by affinity chromatography using a Glutathione Sepharose 4B resin. The p21 h-Ras (1-166) was expressed in *E. coli* using the pQE-30 expression vector and then purified by affinity as a 6xHis-tagged protein using a Ni-NTA resin[95]. The Bio-Rad protein assay[96] (Bradford, 1976) was used to determine protein concentrations using bovine serum albumin (BSA, Sigma) as the standard.

5.2.2. Measurement of C-Cdc25^{Mm}-stimulated guanine nucleotide exchange on p21 h-Ras

To investigate the ability of putative Ras inhibitors to inhibits or reduce the C-Cdc25^{Mm}-stimulated nucleotide exchange on purified human Ras proteins, we used a technique described by Lenzen and co-worker[84] with some modification. This approach utilises guanine nucleotide carrying an *N*-methylanthranoyl fluorophore (mant-GDP or mant-GTP). p21 h-Ras (100 nM) and mant-GTP (0.5 μM) were incubated in buffer A (50 mM Tris/HCl, pH 7.5, 1 mM $MgCl_2$, 100 mM NH_4Cl, and 1 mM DTE) in the absence and in presence of tested compound (100 μM). The exchange reaction was started by addition of 25 nM C-Cdc25^{mM}. The reaction was monitored at an excitation wavelength of 370 nm and emission wavelength of 450

94. Coccetti, P.; Mauri, I.; Alberghina, L.; Martegani, E.; Parmeggiani, A., The Minimal Active Domain of the Mouse Ras Exchange Factor CDC25Mm. *Biochemical and Biophysical Research Communications* **1995,** *206* (1), 253-259.

95. Martegani, E.; Vanoni, M.; Zippel, R.; Coccetti, P.; Brambilla, R.; Ferrari, C.; Sturani, E.; Alberghina, L., Cloning by functional complementation of cDNA encoding homologue of CDC25, Saccharomyces cerevisiae RAS activator. *The EMBO Journal* **1992,** *11* (6), 2151-2157.

96. Bradford, M., A rapid and sensitive method for the quantitation of microgram quantities of protein utilizing the principle of protein-dye binding. *Analytical biochemistry* **1976,** *72* (1-2), 248-254.

nm using a Perkin-Elmer Luminescence Spectrometer LS-45. Measurements have been taken every second at least for 1500 s. Each experimental curve was fitted to a sigmoidal Hill curve with OriginPro 8.0 software (Origin Lab Corporation, MA USA) and the exchange rate of control reaction (performed without compound) was normalized to 100. The normalized curve was reported on the graph as thin line.

5.2.1. Measurement of RasGRF1-stimulated guanine nucleotide exchange on p21 h-Ras

RasGRF1-stimulated guanine nucleotide exchange was performed as previously described[97,98]. RasGRF1 Ras-GEF domain (residues 976-1262 of the mature protein) was used to catalyze the nucleotide exchange reaction. The fluorescence measurements were carried out at 25°C in 40 mM Hepes pH 7.5, 5 mM DTE, 10 mM $MgCl_2$ buffer using a Perkin-Elmer LS45 luminescence spectrometer with an excitation wavelength of 366 nm and emission wavelength of 442 nm. Stimulation of the GDP to mant-GDP exchange reaction on H-Ras was performed by adding to 0.25 μM H-RasGDP, a 5-fold excess of mant-GDP (1.25 μM) in presence of catalytic amounts of exchange factor (0.0625 μM). The exchange reaction was monitored for 1500 s. Data were fitted to a non linear "growth-sigmoidal Hill" curve, (Hill coefficient=1) using the OriginPro 8 software. The initial exchange rate for each reaction (initial slope) was determined computing the first derivative at time zero of the corresponding Hill-fitted curve.

97. Lenzen, C.; Cool, R. H.; Prinz, H.; Kuhlmann, J.; Wittinghofer, A., Kinetic Analysis by Fluorescence of the Interaction between Ras and the Catalytic Domain of the Guanine Nucleotide Exchange Factor Cdc25Mm â€ *Biochemistry* **1998,** *37* (20), 7420-7430.

98. Sacco, E.; Metalli, D.; Busti, S.; Fantinato, S.; D'Urzo, A.; Mapelli, V.; Alberghina, L.; Vanoni, M., Catalytic competence of the Ras-GEF domain of hSos1 requires intra-REM domain interactions mediated by Phenylalanine 577. *FEBS Letters* **2006,** *580* (27), 6322-6328.

Papers

1. Airoldi, C.; Palmioli, A.; D'Urzo, A.; Colombo, S.; Vanoni, M.; Martegani, E.; Peri, F., Glucose-derived Ras pathway inhibitors: evidence of Ras-ligand binding and Ras-GEF (Cdc25) interaction inhibition. *Chembiochem* **2007,** *8* (12), 1376-1379.

2. Palmioli, A.; Sacco, E.; Airoldi, C.; Di Nicolantonio, F.; D'Urzo, A.; Shirasawa, S.; Sasazuki, T.; Di Domizio, A.; De Gioia, L.; Martegani, E.; Bardelli, A.; Peri, F.; Vanoni, M., Selective cytotoxicity of a bicyclic Ras inhibitor in cancer cells expressing K-RasG13D. *Biochemical and Biophysical Research Communications* **2009,** *386* (4), 593-597.

3. Palmioli, A.; Sacco, E.; Abraham, S.; Thomas, C. J.; Domizio, A. D.; Gioia, L. D.; Gaponenko, V.; Vanoni, M.; Peri, F., First experimental identification of Ras-inhibitor binding interface using a water-soluble Ras ligand. *Bioorganic & Medicinal Chemistry Letters* **2009,** *19* (15), 4217-4222.

4. S. Colombo, A. Palmioli, C. Airoldi, R. Tisi, S. Fantinato, S. Olivieri, L. De Gioia, E. Martegani, F. Peri, Structure-Activity Studies on Arylamides and Arysulfonamides Ras Inhibitors, *Curr. Cancer Drug Target,* accepted **2009.**

Communications

1. Palmioli A., Airoldi C., Colombo S., Peri F., Structure activity relationship in low molecular weight Ras inhibitors, International Symposium on Advances in Synthetic and Medicinal Chemistry ASMC 07, 27/08-01/09 2007, Saint Petersburg (Russia), Poster.

2. Airoldi C., Palmioli A., Peri F., Barbero J. J., Molinari H., Nicotra F., New sugar-derived Ras protein inhibitors: design, synthesis, biological activity and elucidation of their interaction with the protein target, International Symposium on Advances in Synthetic and Medicinal Chemistry, ASMC 07, 27/08-01/09 2007, St. Petersburg (Russia), Poster.

3. Palmioli A., Airoldi C., Sacco E., Vanoni M., Nicotra F., Peri F., Carbohydrates as a tool for anticancer drugs, XI Convegno sulla Chimica dei Carboidrati, 22 - 26 giugno 2008, Pontignano (Siena), Poster.

4. Airoldi C., Palmioli A., Di Domizio A., De Gioia L., Peri F., A combined NMR/molecular modelling approach as tool to elucidate the binding modes of new Ras protein inhibitors, Gordon Research Conference in Computational Aspects – Biomolecular NMR, 18-23 Maggio 2008, Barga (LU), Poster.

5. Palmioli A., Airoldi C., Di Domizio A., Sacco E., Peri F., Small Ras inhibitors and their binding to the proteins, Italian Meeting on Organic Chemistry and Biotechnology (Biotech.Org), 20-23 Maggio 2009, Forte dei marmi (LU), Poster.

6. Palmioli A., Airoldi C., Di Domizio A., Sacco E., Peri F., Small Ras inhibitors from carbohydrates, Gordon Research Conference on Carbohydrate Chemistry, 14 – 19 Giugno 2009, Tilton (NH), USA, Poster.

Bibliography

1. Bourne, H. R.; Sanders, D. A.; McCormick, F., The GTPase superfamily: a conserved switch for diverse cell functions. *Nature* **1990,** *348* (6297), 125-132.
2. Bourne, H. R.; Sanders, D. A.; McCormick, F., The GTPase superfamily: conserved structure and molecular mechanism. *Nature* **1991,** *349* (6305), 117-127.
3. Goody, R. S.; Frech, M.; Wittinghofer, A., Affinity of guanine nucleotide binding proteins for their ligands: facts and artefacts. *Trends in biochemical sciences* **1991,** *16* (9), 327.
4. van Blesen, T.; Hawes, B. E.; Luttrell, D. K.; Krueger, K. M.; Touhara, K.; Porfflri, E.; Sakaue, M.; Luttrell, L. M.; Lefkowitz, R. J., Receptor-tyrosine-kinase- and G -mediated MAP kinase activation by a common signalling pathway. **1995**.
5. Lowenstein, E. J.; Daly, R. J.; Batzer, A. G.; Li, W.; Margolis, B.; Lammers, R.; Ullrich, A.; Skolnik, E. Y.; Bar-Sagi, D.; Schlessinger, J., The SH2 and SH3 domain-containing protein GRB2 links receptor tyrosine kinases to ras signaling. *Cell* **1992,** *70* (3), 431-442.
6. Lodish, H. F., *Molecular cell biology*. 6th ed.; W.H. Freeman: New York, 2008.
7. Robinson, L. C.; Gibbs, J. B.; Marshall, M. S.; Sigal, I. S.; Tatchell, K., CDC25: a component of the RAS-adenylate cyclase pathway in Saccharomyces cerevisiae. *Science* **1987,** *235* (4793), 1218-1221.
8. Sondermann, H.; Nagar, B.; Bar-Sagi, D.; Kuriyan, J., Computational docking and solution x-ray scattering predict a membrane-interacting role for the histone domain of the Ras activator son of sevenless. *Proceedings of the National Academy of Sciences* **2005,** *102* (46), 16632-16637.
9. Sondermann, H.; Soisson, S. M.; Boykevisch, S.; Yang, S. S.; Bar-Sagi, D.; Kuriyan, J., Structural analysis of autoinhibition in the Ras activator Son of sevenless. *Cell* **2004,** *119* (3), 393-405.
10. Donovan, S.; Shannon, K. M.; Bollag, G., GTPase activating proteins: critical regulators of intracellular signaling. *BBA-Reviews on Cancer* **2002,** *1602* (1), 23-45.
11. Marais, R.; Light, Y.; Paterson, H. F.; Marshall, C. J., Ras recruits Raf-1 to the plasma membrane for activation by tyrosine phosphorylation. *Embo Journal* **1995,** *14*, 3136-3136.
12. Yordy, J. S.; Muise-Helmericks, R. C., Signal transduction and the Ets family of transcription factors. *Oncogene* **2000,** *19* (55), 6503.
13. Rodriguez-Viciana, P.; Warne, P. H.; Dhand, R.; Vanhaesebroeck, B.; Gout, I.; Fry, M. J.; Waterfield, M. D.; Downward, J., Phosphatidylinositol-3-OH kinase direct target of Ras. **1994**.

14. Datta, S. R.; Brunet, A.; Greenberg, M. E., Cellular survival: a play in three Akts. *Genes & Development* **1999,** *13* (22), 2905-2927.
15. Hall, A., Rho GTPases and the actin cytoskeleton. *Science* **1998,** *279* (5350), 509.
16. Kikuchi, A.; Demo, S. D.; Ye, Z. H.; Chen, Y. W.; Williams, L. T., ralGDS family members interact with the effector loop of ras p21. *Molecular and Cellular Biology* **1994,** *14* (11), 7483-7491.
17. Song, C.; Hu, C. D.; Masago, M.; Kariya, K.; Yamawaki-Kataoka, Y.; Shibatohge, M.; Wu, D.; Satoh, T.; Kataoka, T., Regulation of a novel human phospholipase C, PLC , through membrane targeting by Ras. *Journal of Biological Chemistry* **2001,** *276* (4), 2752-2757.
18. Kelley, G. G.; Reks, S. E.; Ondrako, J. M.; Smrcka, A. V., Phospholipase C : a novel Ras effector. *EMBO journal(Print)* **2001,** *20* (4), 743-754.
19. Schubbert, S.; Shannon, K.; Bollag, G., Hyperactive Ras in developmental disorders and cancer. *Nature Reviews Cancer* **2007,** *7* (4), 295-308.
20. John, J.; Schlichting, I.; Schiltz, E.; Rosch, P.; Wittinghofer, A., C-terminal truncation of p21H preserves crucial kinetic and structural properties. *Journal of Biological Chemistry* **1989,** *264* (22), 13086-13092.
21. Casey, P. J.; Solski, P. A.; Der, C. J.; Buss, J. E., p21ras is modified by a farnesyl isoprenoid. *Proceedings of the National Academy of Sciences* **1989,** *86* (21), 8323-8327.
22. Hancock, J. F.; Paterson, H.; Marshall, C. J., A polybasic domain or palmitoylation is required for the addition of the CAAX motif to localize p21 to the plasma membrane. *Cell* **1990,** *63* (1), 133-139.
23. Omerovic, J.; Prior, A., Compartmentalized signalling: Ras proteins and signalling nanoclusters. *FEBS Journal* **2009,** *276* (7), 1817-1825.
24. Omerovic, J.; Laude, A. J.; Prior, I. A., Ras proteins: paradigms for compartmentalised and isoform-specific signalling. *Cellular and Molecular Life Sciences (CMLS)* **2007,** *64* (19-20), 2575-2589.
25. Esteban, L. M.; Vicario-Abejon, C.; Fernandez-Salguero, P.; Fernandez-Medarde, A.; Swaminathan, N.; Yienger, K.; Lopez, E.; Malumbres, M.; McKay, R.; Ward, J. M., Targeted genomic disruption of H-ras and N-ras, individually or in combination, reveals the dispensability of both loci for mouse growth and development. *Molecular and cellular biology* **2001,** *21* (5), 1444-1452.
26. Vetter, I. R.; Wittinghofer, A., The guanine nucleotide-binding switch in three dimensions. *Science* **2001,** *294* (5545), 1299-1304.
27. Pai, E. F.; Krengel, U.; Petsko, G. A.; Goody, R. S.; Kabsch, W.; Wittinghofer, A., Refined crystal structure of the triphosphate conformation of H-ras p21 at 1.35 A resolution: implications for the mechanism of GTP hydrolysis. *EMBO J* **1990,** *9* (8), 2351-2359.
28. Maegley, K. A.; Admiraal, S. J.; Herschlag, D., Ras-catalyzed hydrolysis of GTP: a new perspective from model studies. *Proceedings of the National Academy of Sciences* **1996,** *93* (16), 8160-8166.

29. Wittinghofer, A.; Waldmann, H., Ras - A molecular switch involved in tumor formation. *Angew Chem Int Edit* **2000,** *39* (23), 4193-4214.
30. Neal, S. E.; Eccleston, J. F.; Hall, A.; Webb, M. R., Kinetic analysis of the hydrolysis of GTP by p21N-ras. The basal GTPase mechanism. *Journal of Biological Chemistry* **1988,** *263* (36), 19718-19722.
31. Scheffzek, K.; Ahmadian, M. R.; Kabsch, W.; Wiesmuller, L.; Lautwein, A.; Schmitz, F.; Wittinghofer, A., The Ras-RasGAP complex: structural basis for GTPase activation and its loss in oncogenic Ras mutants. *Science* **1997,** *277* (5324), 333.
32. Boriack-Sjodin, P. A.; Margarit, S. M.; Bar-Sagi, D.; Kuriyan, J., The structural basis of the activation of Ras by Sos. *Nature* **1998,** *394* (6691), 337.
33. Herrmann, C., Ras-effector interactions: after one decade. *Current Opinion in Structural Biology* **2003,** *13* (1), 122-129.
34. Rensland, H.; John, J.; Linke, R.; Simon, I.; Schlichting, I.; Wittinghofer, A.; Goody, R. S., Substrate and Product Structural Requirements for Binding of Nucleotides to H-ras p21: The Mechanism of Discrimination between Guanosine and Adenosine Nucleotides. *Biochemistry* **2002,** *34* (2), 593-599.
35. John, J.; Rensland, H.; Schlichting, I.; Vetter, I.; Borasio, G. D.; Goody, R. S.; Wittinghofer, A., Kinetic and structural analysis of the Mg(2+)-binding site of the guanine nucleotide-binding protein p21H-ras. *J. Biol. Chem.* **1993,** *268* (2), 923-929.
36. Harvey, J. J.; Harvey, An unidentified virus which causes the rapid production of tumours in mice. *Nature* **1964,** *204* (4963), 1104.
37. Chang, E. H.; Gonda, M. A.; Ellis, R. W.; Scolnick, E. M.; Lowy, D. R., Human genome contains four genes homologous to transforming genes of Harvey and Kirsten murine sarcoma viruses. *Proceedings of the National Academy of Sciences of the United States of America* **1982,** *79* (16), 4848-4852.
38. Franken, S. M.; Scheidig, A. J.; Krengel, U.; Rensland, H.; Lautwein, A.; Geyer, M.; Scheffzek, K.; Goody, R. S.; Kalbitzer, H. R., Three-dimensional structures and properties of a transforming and a nontransforming glycine-12 mutant of p21H-ras. *Biochemistry* **1993,** *32* (33), 8411-8420.
39. Bentires-Alj, M.; Kontaridis, M. I.; Neel, B. G., Stops along the RAS pathway in human genetic disease. *Nature medicine* **2006,** *12* (3), 283-285.
40. Friday, B. B.; Adjei, A. A., K-ras as a target for cancer therapy. *Biochimica et biophysica acta* **2005,** *1756* (2), 127-44.
41. Kloog, Y.; Cox, A. D., RAS inhibitors: potential for cancer therapeutics. *Molecular Medicine Today* **2000,** *6* (10), 398-402.
42. Cox, A. D.; Der, C. J., Farnesyltransferase inhibitors: promises and realities. *Current Opinion in Pharmacology* **2002,** *2* (4), 388-393.
43. Lobell, R. B.; Omer, C. A.; Abrams, M. T.; Bhimnathwala, H. G.; Brucker, M. J.; Buser, C. A.; Davide, J. P.; deSolms, S. J.; Dinsmore, C. J.; Ellis-Hutchings, M. S.; Kral, A. M.; Liu, D.; Lumma, W. C.; Machotka, S. V.; Rands, E.; Williams, T. M.; Graham, S. L.; Hartman, G. D.; Oliff, A. I.; Heimbrook, D. C.; Kohl, N. E.,

Evaluation of Farnesyl:Protein Transferase and Geranylgeranyl:Protein Transferase Inhibitor Combinations in Preclinical Models. *Cancer Res* **2001,** *61* (24), 8758-8768.
44. Prendergast, G. C., Actin'up: RhoB in cancer and apoptosis. *Nature Reviews Cancer* **2001,** *1* (2), 162-168.
45. Marom, M.; Haklai, R.; Ben-Baruch, G.; Marciano, D.; Egozi, Y.; Kloog, Y., Selective inhibition of Ras-dependent cell growth by farnesylthiosalisylic acid. *Journal of Biological Chemistry* **1995,** *270* (38), 22263.
46. Jansen, B.; Schlagbauer-Wadl, H.; Kahr, H.; Heere-Ress, E.; Mayer, B. X.; Eichler, H. G.; Pehamberger, H.; Gana-Weisz, M.; Ben-David, E.; Kloog, Y.; Wolff, K., Novel Ras antagonist blocks human melanoma growth. *Proceedings of the National Academy of Sciences of the United States of America* **1999,** *96* (24), 14019-14024.
47. Haklai, R.; Weisz, M. G.; Elad, G.; Paz, A.; Marciano, D.; Egozi, Y.; Ben-Baruch, G.; Kloog, Y., Dislodgment and Accelerated Degradation of Ras. *Biochemistry* **1998,** *37* (5), 1306-1314.
48. Gana-Weisz, M.; Halaschek-Wiener, J.; Jansen, B.; Elad, G.; Haklai, R.; Kloog, Y., The Ras Inhibitor S-trans,trans-Farnesylthiosalicylic Acid Chemosensitizes Human Tumor Cells Without Causing Resistance. *Clin Cancer Res* **2002,** *8* (2), 555-565.
49. Barkan, B.; Starinsky, S.; Friedman, E.; Stein, R.; Kloog, Y., The Ras Inhibitor Farnesylthiosalicylic Acid as a Potential Therapy for Neurofibromatosis Type 1. *Clin Cancer Res* **2006,** *12* (18), 5533-5542.
50. Crooke, S. T., Potential roles of antisense technology in cancer chemotherapy. *Oncogene* **2000,** *19* (56), 6651.
51. Ross, P. J.; George, M.; Cunningham, D.; DiStefano, F.; Andreyev, H. J. N.; Workman, P.; Clarke, P. A., Inhibition of Kirsten-ras Expression in Human Colorectal Cancer Using Rationally Selected Kirsten-ras Antisense Oligonucleotides1. *Molecular Cancer Therapeutics* **2001,** *1* (1), 29-41.
52. Clark, G. J.; Drugan, J. K.; Terrell, R. S.; Bradham, C.; Der, C. J.; Bell, R. M.; Campbell, S., Peptides containing a consensus Ras binding sequence from Raf-1 and theGTPase activating protein NF1 inhibit Ras function. *Proceedings of the National Academy of Sciences of the United States of America* **1996,** *93* (4), 1577-1581.
53. Herrmann, C.; Block, C.; Geisen, C.; Haas, K.; Weber, C.; Winde, G.; Möröy, T.; Müller, O., Sulindac sulfide inhibits Ras signaling. *Oncogene* **1998,** *17* (14), 1769.
54. Herbert, W.; Ioanna-Maria, K.; Mercedes, C.; Eleni, G.; Christian, H.; Christoph, B.; Hartmut, O.; Oliver, M., Sulindac-Derived Ras Pathway Inhibitors Target the Ras-Raf Interaction and Downstream Effectors in the Ras Pathway13. *Angewandte Chemie International Edition* **2004,** *43* (4), 454-458.
55. Ahmadian, M. R.; Zor, T.; Vogt, D.; Kabsch, W.; Selinger, Z.; Wittinghofer, A.; Scheffzek, K., Guanosine triphosphatase stimulation of oncogenic

Ras mutants. *Proceedings of the National Academy of Sciences of the United States of America* **1999,** *96* (12), 7065-7070.
56. Taveras, A. G.; Remiszewski, S. W.; et al., Ras oncoprotein inhibitors: the discovery of potent, ras nucleotide exchange inhibitors and the structural determination of a drug-protein complex. *Bioorganic & medicinal chemistry* **1997,** *5* (1), 125-33.
57. Ganguly, A. K.; Pramanik, B. N.; Huang, E. C.; Liberles, S.; Heimark, L.; Liu, Y. H.; Tsarbopoulos, A.; Doll, R. J.; Taveras, A. G.; Remiszewski, S.; Snow, M. E.; Wang, Y. S.; Vibulbhan, B.; Cesarz, D.; Brown, J. E.; del Rosario, J.; James, L.; Kirschmeier, P.; Girijavallabhan, V., Detection and structural characterization of ras oncoprotein-inhibitors complexes by electrospray mass spectrometry. *Bioorganic & medicinal chemistry* **1997,** *5* (5), 817-820.
58. Ganguly, A. K.; Wang, Y. S.; Pramanik, B. N.; Doll, R. J.; Snow, M. E.; Taveras, A. G.; Remiszewski, S.; Cesarz, D.; Del Rosario, J.; Vibulbhan, B., Interaction of a novel GDP exchange inhibitor with the Ras protein. *Biochemistry* **1998,** *37* (45), 15631-15637.
59. Colombo, S.; Peri, F.; Tisi, R.; Nicotra, F.; Martegani, E. In *Design and characterization of a new class of inhibitors of Ras activation*, Diederich, M., Ed. New York Acad Sciences: 2004; pp 52-61.
60. Peri, F.; Airoldi, C.; Colombo, S.; Martegani, E.; van Neuren, A. S.; Stein, M.; Marinzi, C.; Nicotra, F., Design, synthesis and biological evaluation of sugar-derived Ras inhibitors. *Chembiochem* **2005,** *6* (10), 1839-1848.
61. Bernd Meyer; Thomas Peters, NMR Spectroscopy Techniques for Screening and Identifying Ligand Binding to Protein Receptors. *Angewandte Chemie International Edition* **2003,** *42* (8), 864-890.
62. Peri, F.; Airoldi, C.; Colombo, S.; Mari, S.; Jimenez-Barbero, J.; Martegani, E.; Nicotra, F., Sugar-derived Ras inhibitors: Group epitope mapping by NMR spectroscopy and biological evaluation. *Eur J Org Chem* **2006,** (16), 3707-3720.
63. Airoldi, C.; Palmioli, A.; D'Urzo, A.; Colombo, S.; Vanoni, M.; Martegani, E.; Peri, F., Glucose-derived Ras pathway inhibitors: Evidence of Ras-ligand binding and Ras-GEF (Cdc25) 14 interaction inhibition. *Chembiochem* **2007,** *8* (12), 1376-1379.
64. Kazanis, S.; McClelland, R. A., Electrophilic intermediate in the reaction of glutathione and nitroso arenes. *Journal of the American Chemical Society* **2002,** *114* (8), 3052-3059.
65. Wang, C. Y.; Zheng, D.; Hughes, J. B., Stability of hydroxylamino-and amino-intermediates from reduction of 2, 4, 6-trinitrotoluene, 2, 4-dinitrotoluene, and 2, 6-dinitrotoluene. *Biotechnology Letters* **2000,** *22* (1), 15-19.
66. Meutermans, W.; Le, G. T.; Becker, B., Carbohydrates as scaffolds in drug discovery. *Chemmedchem* **2006,** *1* (11), 1164-1194.
67. Peri, F.; Cipolla, L.; Forni, E.; Nicotra, F., Carbohydrate-based scaffolds for the generation of sortiments of bioactive compounds. *Monatshefte für Chemie/Chemical Monthly* **2002,** *133* (4), 369-382.

68. Gruner, S. A. W.; Locardi, E.; Lohof, E.; Kessler, H., Carbohydrate-Based Mimetics in Drug Design: Sugar Amino Acids and Carbohydrate Scaffoldsâ€ *Chemical Reviews* **2002,** *102* (2), 491-514.
69. Hirschmann, R.; Nicolaou, K. C.; Pietranico, S.; Salvino, J.; Leahy, E. M.; Sprengeler, P. A.; Furst, G.; Strader, C. D.; Smith, A. B., Nonpeptidal peptidomimetics with .beta.-D-glucose scaffolding. A partial somatostatin agonist bearing a close structural relationship to a potent, selective substance P antagonist. *Journal of the American Chemical Society* **2002,** *114* (23), 9217-9218.
70. Velter, I.; La Ferla, B.; Nicotra, F., Carbohydrate-Based Molecular Scaffolding. *Journal of Carbohydrate Chemistry* **2006,** *25* (2), 97-138.
71. Forni, E.; Cipolla, L.; Caneva, E.; La Ferla, B.; Peri, F.; Nicotra, F., Polycyclic scaffolds from fructose. *Tetrahedron Letters* **2002,** *43* (7), 1355-1357.
72. Peri, F.; Bassetti, R.; Caneva, E.; Gioia, L. d.; Ferla, B. L.; Presta, M.; Tanghetti, E.; Nicotra, F., Arabinose-derived bicyclic amino acids: synthesis, conformational analysis and construction of an alpha, beta 3-selective RGD peptide. *Journal of the Chemical Society, Perkin Transactions 1* **2002,** (5), 638-644.
73. Griffith, B. R.; Langenhan, J. M.; Thorson, J. S., `Sweetening' natural products via glycorandomization. *Current Opinion in Biotechnology* **2005,** *16* (6), 622-630.
74. Ahmed, A.; Peters, N. R.; Fitzgerald, M. K.; Watson, J. A.; Hoffmann, F. M.; Thorson, J. S., Colchicine Glycorandomization Influences Cytotoxicity and Mechanism of Action. *Journal of the American Chemical Society* **2006,** *128* (44), 14224-14225.
75. Griffith, B. R.; Krepel, C.; Fu, X.; Blanchard, S.; Ahmed, A.; Edmiston, C. E.; Thorson, J. S., Model for Antibiotic Optimization via Neoglycosylation: Synthesis of Liponeoglycopeptides Active against VRE. *Journal of the American Chemical Society* **2007,** *129* (26), 8150-8155.
76. Langenhan, J. M.; Griffith, B. R.; Thorson, J. S., Neoglycorandomization and Chemoenzymatic Glycorandomization: Two Complementary Tools for Natural Product Diversification. *Journal of Natural Products* **2005,** *68* (11), 1696-1711.
77. Fu, X.; Albermann, C.; Zhang, C.; Thorson, J. S., Diversifying Vancomycin via Chemoenzymatic Strategies. *Organic Letters* **2005,** *7* (8), 1513-1515.
78. Thorson, J. S., *Glycorandomization and production of novel vancomycin analogs*. US Patent References 7259141: 2004.
79. Peri, F.; Dumy, P.; Mutter, M., Chemo- and stereoselective glycosylation of hydroxylamino derivatives: A versatile approach to glycoconjugates. *Tetrahedron* **1998,** *54* (40), 12269-12278.
80. Peri, F.; Nicotra, F., Chemoselective Ligation in Glycochemistry. *ChemInform* **2004,** *35* (27).
81. Peri, F.; Jiménez-Barbero, J.; García-Aparicio, V.; Tvaroscaronka, I.; Nicotra, F., Synthesis and Conformational Analysis of Novel N(OCH3)-linked Disaccharide Analogues. *Chemistry - A European Journal* **2004,** *10* (6), 1433-1444.

82. Gudmundsdottir, A. V.; Paul, C. E.; Nitz, M., Stability studies of hydrazide and hydroxylamine-based glycoconjugates in aqueous solution. *Carbohydrate Research* **2009,** *344* (3), 278-284.
83. Langenhan, J. M.; Peters, N. l. R.; Guzei, I. A.; Hoffmann, F. M.; Thorson, J. S., Enhancing the anticancer properties of cardiac glycosides by neoglycorandomization. *Proceedings of the National Academy of Sciences of the United States of America* **2005,** *102* (35), 12305-12310.
84. Lenzen, C.; Cool, R.; Wittinghofer, A., Analysis of intrinsic and CDC25-stimulated guanine nucleotide exchange of p21ras-nucleotide complexes by fluorescence measurements. *Methods in enzymology* **1995,** *255*, 95.
85. Palmioli, A.; Sacco, E.; Airoldi, C.; Di Nicolantonio, F.; D'Urzo, A.; Shirasawa, S.; Sasazuki, T.; Di Domizio, A.; De Gioia, L.; Martegani, E.; Bardelli, A.; Peri, F.; Vanoni, M., Selective cytotoxicity of a bicyclic Ras inhibitor in cancer cells expressing K-RasG13D. *Biochemical and Biophysical Research Communications* **2009,** *386* (4), 593-597.
86. Morris, G.; Goodsell, D.; Halliday, R.; Huey, R.; Hart, W.; Belew, R.; Olson, A., Automated docking using a Lamarckian genetic algorithm and an empirical binding free energy function. *Journal of Computational Chemistry* **1998,** *19* (14), 1639-1662.
87. Mayer, M.; Meyer, B., Group Epitope Mapping by Saturation Transfer Difference NMR To Identify Segments of a Ligand in Direct Contact with a Protein Receptor. *Journal of the American Chemical Society* **2001,** *123* (25), 6108-6117.
88. Shirasawa, S.; Furuse, M.; Yokoyama, N.; Sasazuki, T., Altered growth of human colon cancer cell lines disrupted at activated Ki-ras. *Science* **1993,** *260* (5104), 85-88.
89. Palmioli, A.; Sacco, E.; Abraham, S.; Thomas, C. J.; Domizio, A. D.; Gioia, L. D.; Gaponenko, V.; Vanoni, M.; Peri, F., First experimental identification of Ras-inhibitor binding interface using a water-soluble Ras ligand. *Bioorganic & Medicinal Chemistry Letters* **2009,** *19* (15), 4217-4222.
90. Kraulis, P. J.; Domaille, P. J.; Campbell-Burk, S. L.; Van Aken, T.; Laue, E. D., Solution Structure and Dynamics of Ras p21.cntdot.GDP Determined by Heteronuclear Three- and Four-Dimensional NMR Spectroscopy. *Biochemistry* **1994,** *33* (12), 3515-3531.
91. Chiaradonna, F.; Sacco, E.; Manzoni, R.; Giorgio, M.; Vanoni, M.; Alberghina, L., Ras-dependent carbon metabolism and transformation in mouse fibroblasts. *Oncogene* **2006,** *25* (39), 5391-5404.
92. Zhang, B.; Zhang, Y.; Shacter, E.; Zheng, Y., Mechanism of the Guanine Nucleotide Exchange Reaction of Ras GTPaseEvidence for a GTP/GDP Displacement Model. *Biochemistry* **2005,** *44* (7), 2566-2576.
93. Still, W. C.; Kahn, M.; Mitra, A., Rapid chromatographic technique for preparative separations with moderate resolution. *The Journal of Organic Chemistry* **1978,** *43* (14), 2923-2925.

94. Coccetti, P.; Mauri, I.; Alberghina, L.; Martegani, E.; Parmeggiani, A., The Minimal Active Domain of the Mouse Ras Exchange Factor CDC25Mm. *Biochemical and Biophysical Research Communications* **1995,** *206* (1), 253-259.
95. Martegani, E.; Vanoni, M.; Zippel, R.; Coccetti, P.; Brambilla, R.; Ferrari, C.; Sturani, E.; Alberghina, L., Cloning by functional complementation of cDNA encoding homologue of CDC25, Saccharomyces cerevisiae RAS activator. *The EMBO Journal* **1992,** *11* (6), 2151-2157.
96. Bradford, M., A rapid and sensitive method for the quantitation of microgram quantities of protein utilizing the principle of protein-dye binding. *Analytical biochemistry* **1976,** *72* (1-2), 248-254.
97. Lenzen, C.; Cool, R. H.; Prinz, H.; Kuhlmann, J.; Wittinghofer, A., Kinetic Analysis by Fluorescence of the Interaction between Ras and the Catalytic Domain of the Guanine Nucleotide Exchange Factor Cdc25Mm â€ *Biochemistry* **1998,** *37* (20), 7420-7430.
98. Sacco, E.; Metalli, D.; Busti, S.; Fantinato, S.; D'Urzo, A.; Mapelli, V.; Alberghina, L.; Vanoni, M., Catalytic competence of the Ras-GEF domain of hSos1 requires intra-REM domain interactions mediated by Phenylalanine 577. *FEBS Letters* **2006,** *580* (27), 6322-6328.
99. Palmioli, A.; Airoldi, C.; Colombo, S.; Peri, F., Structure activity relationship in low molecular weight Ras inhibitors. In *International Symposium on Advances in Synthetic and Medicinal Chemistry ASMC 07*, Saint Petersburg (Russia), 2007.